# Assessing Tidal Current Power Resources

Astrid Marlene Suzanne Lorange

a thesis submitted for the degree of

Master of Science

at the University of Otago, Dunedin,

New Zealand.

26 June 2014

# Contents

# List of Tables

# List of Figures

# Abstract

Tidal current energy is looked upon worldwide as a largely untapped, potentially significant and reliable source of energy. Countries, such as the United Kingdom and Canada, are working towards the implantation of tidal turbine farms in order to exploit this promising form of renewable energy. One of the barriers to further developing tidal energy extraction is the difficulty of accurately assessing the extractable energy or realisable tidal current output of a given site. Various numerical models for site assessments currently exist. Three of them, the Kinetic Energy Flux and two models, named GC05 and V10, which take into account the effect on the flow of the introduction of turbines are described, discussed and used throughout this work. Data regarding 239 channels worldwide have been collected. These data are used to investigate the possible existence of patterns between channel characteristics or parameters and channel potential estimates. New upper limits for the tidal current potentials of the UK and Ireland are calculated using the collected data and the most advanced model - V10, and compared to previous values. Finally, resource assessments, based on realisable power, are produced using the V10 model and the Seagen turbine characteristics. For these resource assessments, limits of up to 20% with regards to the blockage ratio and the reduction in flow speed for a given channel are put in place. These results show that a substantial fraction of the upper tidal current potential limit can be realised with only a 20% blockage ratio and a 20% reduction in flow speed for most channels.

# Nomenclature

### Notation

Flow Reduction: ratio of a volume transport over the volume transport in the undisturbed channel.

Lagoon Channel: channel connecting a large body of water to a lagoon.

Ocean Channel: channel connecting two large bodies of water. The bodies of water are large enough not to be considered to form lagoons at either end.

Peak Power Potential: see Upper Tidal Current Potential Limit.

Potential: see Upper Tidal Current Potential Limit.

Power Efficiency: ratio of power potential over a relevant peak power potential value.

Realisable Ouput or Realisable Power: refers to the tidal current power that can veritably be extracted after taking into account background bottom friction, the effect of power extraction on the flow, as well as a combination of the following specifications: losses due to drag from support structures, mixing in the turbulent wake behind the turbines, between the rotor and grid connection and constraints regarding the allowed blockage ratio for a given channel. The more specifications taken into account, the more accurate the realisable potential value produced.

Upper Tidal Current Potential Limit: refers to the maximum potential available at a given site attained through optimisation of the resistance to the flow with regards to both background and farm drags. It takes into account background bottom friction and the effect of power extraction on the flow, but without taking into account losses due to drag from support structures, mixing in the turbulent wake behind the turbines, or between the rotor and grid connection, as well as ignoring constraints regarding the allowed blockage ratio for a given channel. Such a potential equates with the upper

bound for the available potential at a given site. It is also referred to as potential or peak power potential of a channel.

**Abbreviations**

GC05: refers to a model or assessment method developed to produce upper tidal current potential limits of ocean channels [23].

GC07: refers to a model or assessment method developed to produce upper tidal current potential limits of ocean channels when only partially filling a channel's cross-section [24].

Is: island(s)

KE Flux: refers to the Kinetic Energy Flux method or assessment model used to produce what was believed to be equivalent to upper tidal current potential limits.

Lagoon-GC05: refers to a model or assessment method developed to produce upper tidal current potential limits of lagoon channels [7].

Lagoon-V11: refers to a model or assessment method developed to produce upper tidal current potential limits of lagoon channels [54].

MHWN: mean high water neap

MHWS: mean high water spring

MLWN: mean low water neap

MLWS: mean low water spring

N: South

S: South

V10: refers to the model or assessment method developed to produce realisable potentials for ocean and lagoon channels [52]. The version used in this study applies to ocean channels only.

V10: refers to the model or assessment method developed to produce realisable potentials for ocean and lagoon channels [52]. The version used in this study applies to ocean channels only.

V11: refers to a model or assessment method developed to produce upper tidal current potential limits of ocean channels [54].

**Symbols**

$\alpha^*$ dimensionless variable relating to lagoon channels

$\alpha$ dimensionless constant representing the dynamical balance within the channel

$\beta_L$ dimensionless lagoon parameter

$\eta_{01}$ amplitude of the tidal elevation in the ocean

$\gamma$ represents the range of possible channel dynamics and it varies between 0.21 and 0.24 for ocean channels and between 0.19 and 0.26 for lagoon channels

$\lambda_0$ resistance to the flow of water originating from bottom friction defined differently for ocean and lagoon channels

$\lambda_{peak}$ resistance to the flow of water at optimal farm and bottom friction drag coefficients defined differently for ocean and lagoon channels

$\omega$ tide's angular frequency, $\omega = 1.4 \times 10^{-4}\, radians\, s^{-1}$
(M2 tidal angular frequency)

$\overline{P}_{max}$ peak power potential available over a tidal cycle, or upper limit of the tidal current potential

$\rho$ density of seawater, $\rho = 1025\, kg\, m^{-3}$

$\zeta_0$ amplitude of the head loss between the two ends of the channel

$A_C$ average cross-sectional area of the channel

$A_L$ average surface area of the lagoon

$A$ cross-sectional area of the channel

$C_D$ drag coefficient for background bottom friction based on the channel's horizontal area

$C_F^{peak}$ farm's optimal drag coefficient defined differently for ocean and lagoon channels

$KE_{Flux}$ kinetic energy flux

$U_{0UD}$ peak volume transport in the undisturbed channel

$U_0^{peak}$ volume transport in a channel fitted with turbines at peak farm's drag coefficient defined differently for ocean and lagoon channels

$U_1$ volume transport in the channel in the absence of bottom friction or turbines

D represents the channel's dynamical balance

h average depth of channel

L channel length

v mean peak velocity

w average width of the channel

**Country Codes**

CA Canada

CH Chile

IR Ireland

IT Ireland

JP Japan

NW Norway

NZ New Zealand

OZ Australia

SG Singapore

UK United Kingdom

US United States of America

# Acknowledgements

There are several people whom I would like to sincerely thank, as they have played important roles in the successful completion of this thesis.

Thank you to my lab co-workers: Cerys Bailey, Hamish Bowman, Dr. Tim Divett, Dr. Pete Russel, Malcolm Smeaton, Rob Smith and Lara Wilcocks for your help and encouragement all throughout the working process.

Thank you to Dr. Mårten Grabbe, whose act of generosity will not be forgotten.

Thank you to my supervisors: Associate Professor Ross Vennell and Dr. Alice Harang for your guidance, support, wisdom and your remarkable patience.

# Chapter 1

# Introduction

In this introduction, the role of tidal energy on the global energy production scale will be discussed. Its modes of exploitation will then be introduced. Finally, the aims and structure of the thesis will be discussed.

## 1.1 Background

**Global Electricity Trends: Issues & Responses** Projections from the International Energy Agency show a significant increase in electricity demand worldwide over the next 20 years [33]. At present, fossil fuels are regarded as an unreliable response to the new energy needs mainly because the supply is expected to dry out possibly as early as 50 years from now [34, 15]. Increasing the number of nuclear power plants worldwide could also offer a solution, but the Fukushima nuclear accident led to a widespread fear of the ill-effects resulting from such incidents [34, 55, 50]. Therefore, a compensation for the rise in electricity needs emanating solely from traditional energy sources appears an unlikely solution.

The most commonly agreed-upon answer to the future electricity-supply issue consists in expanding the quantity of electricity produced from renewable energy sources, or renewables, and in increasing their share in the global electricity generation [33, 16, 50]. Renewables consist of hydropower, biomass, wind, solar, marine (mainly waves and tides) and geothermal sources. They hold the advantage of being virtually inexhaustible and contain sufficient potential worldwide to cover global needs in electricity supply [31, 50]. Numerous countries around the world have put forward plans to establish substantial electricity generation from renewables, including the United States and China [50]. The European Union has set a binding target of 20% of energy consumption to be provided by renewables by 2020 for its members [12, 50]. Some countries, such as Germany, decided to partly base their

economical recovery plans on the development of renewable energy production strategies [50, 39].

However, renewables such as wind, solar and tidal energies are currently limited by their intermittency and variability, because the storage of large quantities of electricity is, at present, technologically impossible [16, 15]. The compensation adopted for wind-produced electricity, consisting in using one or more balancing energies to counteract times of low electricity generation, could be extended to solar and tidal sources [16]. The larger the number of energy-source options to choose from, the easier the realisation of this balancing act. In addition, the availability of renewables vary from region to region. The most productive approach would thus be based on harnessing efficiently as many of the local resources as possible. Diversification is therefore a key strategy to achieve successful electricity production through renewables [33, 16]. Consequently, the renewable nature of tidal energy makes it a valuable component of global renewable energy development.

**Tidal Energy: Source & Modes of Exploitation** Tides, which originate mainly from the gravitational pull of the Moon, produce raised and depressed water levels leading to the formation of long waves and associated tidal currents. Tidal energy is intermittent, but as opposed to wind energy, it has the advantage of being highly predictable [1]. The average tidal power that can be extracted from a given device at a given site is positively correlated to the velocity of the flow through the device [9]. Channels, i.e. narrow bodies of water, represent the most suitable locations for tidal power extraction because they cause spatial restrictions for the flow and therefore increased flow speeds [53, 40]. Most channels connect two bodies of water. In this study, two types of channels are considered. Channels of the first type, referred to here as ocean channels, connect two large bodies of water. Channels of the second type, referred to here as lagoon channels, connect a large body of water to a smaller lagoon. Tidal flows in channels can be exploited using two types of devices: barrages or in-stream turbines [37].

A tidal barrage is a dam-like structure built across a body of water. It is therefore mostly applicable to lagoon channels. A tidal barrage uses large tidal ranges, i.e. contrasts in water levels between low and high tides, to create a potential difference via a variation in heights between the two sides of the barrage. Its operating principle is similar to that of a hydro-electric power station with the flow of water from high to low height inducing the rotation of turbines as it passes through the dam [37, 43]. Tidal barrages have raised a mild interest over the last 50 years, mainly because of their significant environmental impact. Indeed, water levels reached in the inner basin, in the case of a lagoon-type channel, are higher than

(a) Horizontal-axis turbine (adapted from [47, fig 1])

(b) Vertical-axis turbine (adapted from [47, fig 1])

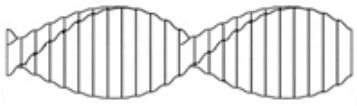

(c) Helical turbine

Figure 1.1: Three designs of turbines currently being developed.

natural levels and cause the destruction of local habitats. Moreover, the blockage of the body of water is responsible for sediment transport regime alterations and the obstruction of navigational or migratory pathways for shipping vessels and marine organisms [43, 62].

The principles guiding the production of power through in-stream turbines are similar to that of wind turbines [48]. In-stream turbines are most commonly anchored on the sea-floor and are designed so that the flow of the current generates a pressure difference across them, making them turn. Their configuration needs to be such that they offer the optimum resistance to tidal currents in order to yield the best power possible [24]. Most tidal turbine designs are based on the use of horizontal-axis turbines (Figure 1.1a), which correspond to the concept adopted for wind turbines. However, other possibilities are being investigated including vertical-axis or helical turbines (Figures 1.1b and 1.1c) amongst others. Only a handful of designs of in-stream turbines have been deployed and are currently connected to the power grid. At present, the one with the largest generating capacity is the Seagen turbine installed in 2008 in Strangford Lough, UK, with $1.2\,MW$ [37, 8]. The vast majority of tidal turbine projects are still undergoing testing [37].

Although we are yet to see the implementation of a tidal turbine farm, the energy from wind farms has been exploited for more than 30 years. The success of a wind farm in producing electricity relates to the combination of a location with sufficient potential and the appropriate wind turbine design for that location. The poor performances associated with some of the wind farms deployed in the past have increased awareness for the need to make better wind-power site assessments. Site assessments are usually done by determining the typical wind behaviour at a location through data collection over long periods of time,

which can be up to several years. Potential yields are then calculated for a given turbine design using the data collected. When choosing the appropriate turbine design for a given site, cut-in speed, rated speed and cut-out speed are taken into account and compared to the wind patterns at the site. This thesis follows a similar approach to site potential assessment by combining channel physical characteristics, including current velocity, with the Seagen turbine parameters, which do not include a cut-out speed. The major difference between wind and tidal site assessments pertains to the type of flow that is observed. Wind flows are unbounded whereas tidal flows have boundaries formed by the ocean floor and the sides of the flow channel. The boundaries affect the flow and the resulting differences must be taken into account when calculating the potential of a tidal site or the optimal arrangement of turbines [35, 11, 14].

## 1.2 Thesis Aims

This thesis is based on the use of a large database of naturally occurring channels including 206 and 33 ocean and lagoon ones respectively. A large number of channels from a given country or a sample of the most promising sites enable the production of representative tidal resource assessments. A broad database also allows the investigation of potentially existing trends within groups of channels. The aims of this thesis are as follows:

- Produce and compare the potentials calculated using the KE Flux, GC05 and V11 models for ocean channels and KE Flux, Lagoon-GC05 and Lagoon-V11 models for lagoon channels.

- Produce resource estimations based on the upper tidal current potential limits of the channels for each of the country represented here. Compare the results obtained with other existing appropriate resource studies.

- Research the existence of patterns between channels' potential assessments and relevant dimensionless parameters to be determined.

- Determine, for each channel, the flow reduction required to reach peak power potential and investigate the effects of flow reduction limitations on available potential results.

- Produce a sensitivity study in relation to the input variables and parameters used for V11 and Lagoon-V11 potential calculations.

- Compare, for ocean channels, the realisable outputs obtained from two different farm configurations with a blockage ratio of a maximum of 20% for each of their rows and investigate the particulars of the best farm configuration.
- Produce, based solely on ocean channels, realisable power estimations for each of the country represented here. Compare the results obtained with other existing resource studies and the upper tidal current potential limits as appropriate.

## 1.3 Thesis Structure

This thesis begins by discussing the various site assessment methods, which will be used throughout its chapters. Then the sources and methods chosen to build the required database of channels are examined. The ranges of channels obtained are then reviewed against the input variables. The potentials of all the channels are calculated using the KE Flux, GC05 and V11 models and the KE Flux, Lagoon-GC05 and Lagoon-V11 for ocean and lagoon channels respectively. The results obtained are compared to verify the validity of the V11 and Lagoon-V11 models and establish the lack of validity of the KE Flux model. Potential resource estimations are generated per country and compared to existing resource studies. In Chapter 4, a series of discriminatory quantities are derived from the V11 and Lagoon-V11 equations and investigated in relation to the V11 potential results as well as the quality of the KE Flux estimates. The ranges of flow reductions at peak power potentials as well as the power potentials for a series of acceptable flow reductions are then produced, discussed and tested against the discriminatory quantities. Subsequently, a sensitivity study relative to the input variables and parameters is conducted. Chapter 5 begins with discussing the changes in the method. Two possible farm configurations, with a blockage ratio of a maximum of 20% for each of their rows, are then compared and the particulars from the best one examined. Finally, realisable power estimations are generated per country and compared to existing resource studies as well as the potentials produced in Chapter 3.

# Chapter 2

# Site Assessment Methods

In order to extract the largest possible amount of power from a given location, tidal turbines must be organised in arrays forming tidal farms [40, 38]. Building a tidal farm requires a substantial initial financial investment. Before the deployment of tidal turbines, an evaluation of the tidal current power resource extractable is therefore necessary to determine if the project is to be cost-effective. In the absence of existing farms, the only sensible solution for the evaluation is the use of mathematical models [41, 42]. Historically, one model, the Kinetic Energy Flux (KE Flux) model, has extensively been used to produce site assessments [9, 54]. However, new models have recently been developed and their designers have strongly criticised the validity of the KE Flux model as an assessment method. These newer models take into account the effect on the flow of the introduction of turbines, which is ignored in the KE Flux model [27]. The GC05 model [25] for ocean channels and its adaptation for lagoon channels, the Lagoon-GC05 model [6], are such models. Most of the more recent site assessments have been based on these newer models [28, 3, 30]. Another model, the V11 model [57], has been devised base on the GC05 model in order to make it more accessible by simplifying the input data acquisition. It allows site assessments of ocean channels to be conducted without having to measure the tidal water levels at the ends of the channel. The V11 model has also been adapted to lagoon-type channels, via its Lagoon-V11 version [57].

All of the models aforementioned are focused on establishing a preliminary gauge of the upper tidal current potential limit, or potential of a channel at given sites of interest, i.e. without taking into account limitations regarding mixing and electro-mechanical losses or acceptable blockage ratio. The potential values they produce represent therefore upper thresholds for the extractable power [57]. Some models have been and are currently being developed to refine power potentials beyond their upper-bound values by taking into account partial cross-section fillings, hydrodynamic interactions between turbines and/or electro-

mechanical losses of energy [26, 56, 61]. These models give a better indication of what may be the realisable output for a given channel. The V10 model [58, 60] is such a model. It has been designed as a combination of both the GC05 [25] and GC07 [26] models, the latest of the two meant to allow for partial cross-section fillings.

## 2.1 KE Flux

The KE Flux model has been used since the 1970's, following the onset of interest in in-stream tidal current energy generation, to assess site potentials [6]. The upper tidal current potential limit, or potential of a channel, averaged over a tidal cycle is calculated using the following equation derived from the basic physics equation for kinetic energy:

$$KE_{Flux} = \frac{\rho}{2A^2}\frac{4}{3\pi}U_{0UD}^3 \tag{2.1}$$

where $KE_{Flux}$ is the kinetic energy flux (assumed in earlier studies to be equivalent to the upper tidal current potential limit), the coefficient $\frac{4}{3\pi}$ gives the average over a tidal cycle, $\rho$ is the density of seawater, $A$ is the cross-sectional area of the channel and $U_{0UD}$ is the peak volume transport in the undisturbed channel, i.e. without any turbine installed [57].

**Advantages**

- Few, easy-to-measure input data required.

**Disadvantages [26, 27]**

- Varies greatly, as $A^{-2}$, with the cross-sectional area used.
- Does not take into account the flow reduction due to the power extracted.
- Established not to be representative of the upper tidal current potential limit.

## 2.2 GC05 & Lagoon-GC05

### 2.2.1 GC05

In a paper published in 2005, Chris Garrett and Patrick Cummins proposed a new assessment method to determine the tidal potentials of ocean channels [25]. They described the flow state in a channel using the momentum equation, which they had simplified through a series of

assumptions described hereafter. Considerations were reduced to the one along-channel dimension with a flow velocity and friction term, introduced to represent both the background and turbine drags, assumed to be independent from the across-channel position. The introduction of a turbine friction term meant that the back effect on the flow of the installation of in-stream devices was taken into account in the channel's potential calculation. Considering that the turbine drag was uniform across the channel's cross-section meant that turbines were expected to occupy the full cross-section of the channel. The expected negligible length of a given channel in comparison to the large wavelengths of tides enabled them to use a volume transport independent from the along-channel position and thus varying solely with time. The changes in depth related to the tides were considered to be negligible compared to the channel's depth, thus not significantly affecting the channel's cross-section. The two bodies of water linked by the channel were also considered large enough not to be affected by the flow within the channel.

They examined the cases of negligible background friction and dominating background friction. In the first case considered, they investigated multiple turbine drag laws by pairing the velocity term of the friction with a range of different exponents. This led them to uncover a series of interesting findings. They determined that for all channels, there exists an ideal value of the resistance to the flow brought about by the turbines, at which the power potential of the channel peaks. Any less of a value would lead to under-exploitation of the channel's maximum potential and any more of a value to a diminution in the channel's available potential due to excessive reduction in the flow velocity within. They also established that the potential of a channel is independent of the position of the turbines in the along-flow direction. Finally, they produced a comparison with the KE Flux model and showed that the results it generates had no correlation with the potentials as they calculated them.

The case of dominating background friction enabled them to unify their theory across all ranges of flow dynamics, from regimes dominated by flow inertia to the ones dominated by background friction. Indeed, they obtained a potential defined by the same group of variables affected of a different coefficient, varying from 0.21 to 0.24. As a result, using a mid-range coefficient from the existing bracket of possible values enables the production of channel potentials within 10% of their true values, without any flow regime considerations. Additional losses related to the electro-mechanical efficiency of the turbines or hydrodynamic interactions between the turbines were ignored.

Upper tidal current potential limits of ocean channels averaged over a tidal cycle can be calculated using the GC05 model through the following equation:

$$\overline{P}_{max} = \gamma \rho g \, \zeta_0 \, U_{0UD} \tag{2.2}$$

where $\overline{P}_{max}$ is the upper tidal current potential limit over a tidal cycle. The coefficient $\gamma$, which can be varied from 0.21 to 0.24 over the full range of possible channel dynamics, represents the flow regime of the channel, $g$ is the acceleration due to gravity and $\zeta_0$ is the amplitude of the head loss between the two ends of the channel [25].

### 2.2.2 Lagoon-GC05

Justin Blanchfield presented a thesis in 2007, in which he extended the potential results obtained for ocean channels in GC05 to channels connecting a lagoon to a large body of water, i.e. lagoon channels [7]. He used the same initial equation, based on the momentum balance, and the same assumptions with the addition of having the surface area of the channel significantly smaller than that of the lagoon. When developing the GC05 solution, the tidal regimes in the two large bodies of water were considered unaffected by the flow within the channel. Contrastingly, the solution worked out for lagoon channels was derived on the assumption that the tidal regime inside the lagoon is dependent on the rate of the flow inside the channel.

Similarly to the work done towards solving the equation for the GC05 model, a range of scenarios were investigated. The bottom drag and exit flow separation were first considered to be negligible. Whilst maintaining these requisites, both a linear and a quadratic law for the turbine drag with regards to the flowrate were examined. The third and last scenario included considerations made for non-negligible exit flow separation as well as bottom drag and turbine drag, both deemed quadratic in the flowrate. The solutions adapted to each of the scenarios gave a similar expression with only a variation in the multiplicative coefficient, varying from 0.19 to 0.26. Consequently, using a mid-range coefficient from the possible range enables one to obtain a channel's potential within 15% of its true value without any knowledge of its flow regime.

Upper tidal current potential limits of lagoon channels can be calculated using the Lagoon-GC05 model through the following equation:

$$\overline{P}_{max} = \gamma \rho g \, \eta_{01} \, U_{0UD} \tag{2.3}$$

where $\eta_{01}$ is the amplitude of the tidal elevation in the ocean. The coefficient $\gamma$ can be varied from 0.19 to 0.26 over the full range of possible channel dynamics [6].

**Advantages [25, 6, 57]**

- Only requires calculation from one equation.
- Takes into account the flow reduction due to the power extracted.
- Allows for the consideration of a range of flow regimes: from flow dominated by bottom friction to flow dominated by inertia.
- Allows for a channel of varying cross-section.

**Disadvantages [25, 6, 57]**

- [GC05 only] The amplitude of the head loss, $\zeta_0$, may be difficult to obtain, especially to the accuracy required.
- Assumes the turbines occupy the whole cross-section of the channel.
- Ignores hydrodynamic interactions between the turbines, i.e. mixing losses.
- Ignores electro-mechanical losses of energy.
- The flow velocity is considered uniform across the channel.

## 2.3 V11 & Lagoon-V11

In 2010, Ross Vennell developed a new model, V10, discussed in the subsequent subsection [56]. As part of this model, he derived an approximate analytical solution to the GC05's momentum equation, which differs from the numerical solution by at most 5%. He later used this approximate analytical solution to produce a new model, V11, for the purpose of simplifying the calculation of the potential of an ocean channel [57]. The simplification stems from the elimination of the need to obtain the amplitude of the head loss between the two ends of the channel, which is a requirement when applying the GC05 model.

He subsequently introduced the same supplementary assumption that had been included by Justin Blanchfield [7], with regards to the relationship between the tidal regime inside the lagoon and the flowrate within the channel, for the equation to also be applicable to lagoon channels. He then used an approximate analytical solution derived by [36] to produce another model, named Lagoon-V11 in this thesis, enabling one to calculate the upper limit of the tidal current potential of a lagoon channel [57].

The resulting expression of potential averaged over a tidal cycle for both ocean and lagoon channels calculated via V11 or Lagoon-V11 is given by the following equation:

$$\overline{P}_{max} = \frac{4}{3\pi} \frac{\rho C_F^{peak}}{A_C^2} (U_0^{peak})^3 \tag{2.4}$$

where $A_C$ corresponds to the average cross-sectional area of the channel. $C_F^{peak}$ represents the farm's optimal drag coefficient and $U_0^{peak}$ corresponds to the volume transport in a channel fitted with turbines at peak farm drag coefficient. These variables have different expressions depending on the channel type they are associated with. For ocean channels, they are defined as follows:

$$C_F^{peak} = 2\frac{L}{h} C_D + \frac{3\pi\sqrt{2}}{8\alpha} \tag{2.5}$$

$$U_0^{peak} = U_1 \sqrt{\frac{\sqrt{4\lambda_{peak}^2 + 1} - 1}{2\lambda_{peak}^2}} \tag{2.6}$$

where $L$ is the length of the channel, $h$ is its average depth and $C_D$ is the drag coefficient for background bottom friction based on the channel's horizontal area. The dimensionless variable $\alpha$ gives an indication of the dynamical balance within the channel, $U_1$ represents the volume transport in the channel in the absence of bottom friction or turbines and the dimensionless $\lambda_{peak}$ corresponds to the resistance to the flow of water at optimal farm and bottom friction drag coefficients. They are defined as described below:

$$\alpha = \frac{U_1}{\omega L A_C} \tag{2.7}$$

$$U_1 = U_{0UD} \sqrt{D^2 U_{0UD}^2 + 1} \tag{2.8}$$

$$\lambda_{peak} = \frac{8\alpha}{3\pi} \left(\frac{L}{h} C_D + C_F^{peak}\right) \tag{2.9}$$

where $\omega$ is the tide's angular frequency. The variable $D$ indicates the channel's dynamical balance and is defined by the following equation:

$$D = \frac{8 C_D}{3\pi\, \omega A_C h} \tag{2.10}$$

For lagoon channels, $C_F^{peak}$ and $U_0^{peak}$ are expressed by the following equations:

$$C_F^{peak} = 2\frac{L}{h} C_D + \frac{3\pi\sqrt{2}}{8\alpha^*} (1 - \beta_L)^2 \tag{2.11}$$

$$U_0^{peak} = \frac{g A_C \eta_{01}}{\omega L} \sqrt{\frac{\sqrt{4\lambda_{peak}^2 + (1-\beta_L)^4} - (1-\beta_L)^2}{2\lambda_{peak}^2}} \tag{2.12}$$

where $\eta_{01}$ represents the amplitude of the tidal elevation in the ocean. The definition of $\lambda_{peak}$ for lagoon channels corresponds to the one used for ocean channels, but its expression differs from it and is detailed below:

$$\lambda_{peak} = \frac{8\alpha^*}{3\pi}\left(\frac{L}{h} C_D + C_F^{peak}\right) \tag{2.13}$$

The dimensionless variable $\alpha^*$ and dimensionless lagoon parameter $\beta_L$ are defined as follows:

$$\alpha^* = \frac{g \eta_{01}}{\omega^2 L^2} \tag{2.14}$$

$$\beta_L = \frac{g A_C}{L \omega^2 A_L} \tag{2.15}$$

where $A_L$ represents the average surface area of the lagoon.

**Advantages [57]**

- Does not require the measurement of the amplitude of the head loss.
- Takes into account the back effect of turbines on the flow.
- Allows for the consideration of a range of flow regimes: from flow dominated by bottom friction to flow dominated by inertia.
- Allows for a channel of varying cross-section.

**Disadvantages [57]**

- Large number of calculations required.
- More sensitive than GC05 or Lagoon-GC05 to the cross-sectional area of the channel.
- Assumes the turbines occupy the whole cross-section of the channel.
- Ignores hydrodynamic interactions between the turbines.
- Ignores electro-mechanical losses of energy.
- The flow velocity is considered uniform across the channel.

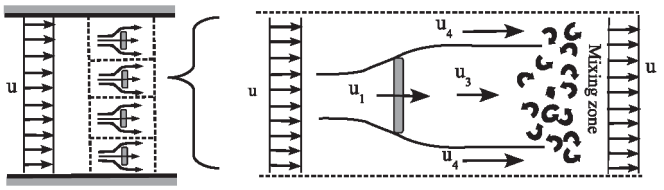


Figure 2.1: Diagram representing the flow upstream of a row of turbines placed in a channel and the details of the flows around a single turbine from the row (from [59]).

## 2.4 V10

According to Lanchester-Betz theory, based on turbines modelled as actuator disks, turbine efficiency[1] is limited to $16/27$. The corresponding maximum conversion efficiency[2] of a turbine is $2/3$. The portion of the energy which is not converted into power, $1/3$, is lost due to mixing in the turbine's wake. The tuning required to reach maximum conversion efficiency coincides with having a ratio of the flow velocity just downstream of the turbine — $u_3$ on Figure 2.1 — over the flow velocity of the free-stream flow — $u$ on Figure 2.1 — equal to $1/3$, i.e. $u_3/u = 1/3$ [59].

In 2007, Chris Garrett and Patrick Cummins applied the Lanchester-Betz theory to a row of turbines filling a given ratio of a channel's cross-section [26]. They established that the same tuning of $u_3/u = 1/3$ (see Figure 2.1) was required to reach maximum conversion efficiency and introduced a new model, the GC07 model. However, in their work, the free-stream flow velocity was considered independent of the presence or absence of turbines, a fact they had shown to be untrue in their previous work leading to the GC05 model [25].

In 2010, Ross Vennell combined the Lanchester-Betz actuator disc theory applied to a row of turbines in GC07 with the retardation effect on the flow stemming from the implantation of the turbines introduced in GC05 [56]. This new model — the V10 model — established that the optimum tuning for a given channel varies with regards to its geometry, dynamical balance, as well as the characteristics of the farm to be implanted. The corresponding $u_3/u$ ratio (see Figure 2.1) ranges between $1/3$ for smaller farms and 1 for larger farms, as the main energy source shifts from the loss of momentum by the flow to the head loss across the farm [59]. Results from the V10 model also show that maximising the realisable power can ensue exceeding the Betz limit of $2/3$ of a channel's potential through optimal

[1] Turbine efficiency is defined as the ratio of the power produced by a turbine over the kinetic energy flux of the upstream flow passing by an area equal to the turbine cross-section.

[2] The conversion efficiency of a turbine is defined as the fraction of the energy lost by the flow to the turbine which contributes to power production.

tuning of its farm configuration [59]. A numerical version of this model adapted to ocean channels was made available to use in this study.

**Advantages [57, 56, 61]**

- Does not require the measurement of the amplitude of the head loss.
- Takes into account the back effect of turbines on the flow.
- Allows for the consideration of a range of flow regimes: from flow dominated by bottom friction to flow dominated by inertia.
- Allows for a channel of varying cross-section.
- Allows for varying blockage ratios on a row by row basis for a given farm.
- Takes into account hydrodynamic interactions between the turbines, i.e. mixing losses.
- Allows to take into account electro-mechanical losses of energy.

**Disadvantages [57]**

- More sensitive than GC05 or Lagoon-GC05 to the cross-sectional area of the channel.
- Not publicly available.

# Chapter 3

# Upper Limits of the Tidal Current Potentials

The upper tidal current potential limit of a given channel corresponds to the maximum tidal current power that can be lost by the flow at the site. It is also referred to as the potential of the channel. When calculated using the KE Flux model, it is only a measure of the kinetic energy of the flow passing through the channel. On the other hand, when it is calculated using the GC05 and V11 models or their lagoon versions, it takes into account background bottom friction and the effect of power extraction on the flow. It does not take into account, however, additional losses or constraints such as mixing and electro-mechanical losses or rows of turbines only partially filling the channel's cross-section. It then represents an upper bound for the potential output of a channel [57].

In this Chapter, the method used to collect the required data will be discussed first. Then, the ranges of ocean and lagoon channels comprised in this study with regards to their respective input variables will be examined. The potentials of the channels will be produced via each of the relevant three models associated with either ocean or lagoon channels. The results will be compared for validity assertion purposes. The ranges of potentials for the channels grouped according to their country of origin and their type will then be examined to verify that no major inconsistencies exist. Finally, tidal current potential resource estimations will be produced per country and compared to results from existing studies when available. The method used to collect the data required to produce the ocean and lagoon channels' potentials is now discussed.

## 3.1 Method

This section describes the procedures used to collect the input data used for the 206 ocean channels and 33 lagoon channels included in this study. Will be discussed: the origins of the collected data, the values assigned to the input parameters and the definitions of the input variables. A series of tables regrouping the information pertaining to each channel including their physical characteristics (Appendix A) and geographical location (Appendix E) can be found in the Appendices. The specific input variables needed for ocean and lagoon channels and the sources used for each of the countries represented in this study are considered next.

### 3.1.1 Data Sources

The work for this thesis depends upon the assemblage of a broad database of channels accompanied by their respective physical characteristics. The required physical characteristics vary with the model used and the channel type (ocean or lagoon). To be able to calculate the potentials using the KE Flux model for all channels as well as the GC05 and V10 models and their lagoon-type versions for ocean and lagoon channels respectively, the data that must be collected for each channel include:

- for both channel types
  - its average width ($w$),
  - its average depth ($h$),
  - its length ($L$);
- for ocean channels
  - the mean peak velocity of the flow within ($v$);
- for lagoon channels
  - the average surface area of the lagoon ($A_L$),
  - the amplitude of the tidal elevation in the ocean ($\eta_{01}$).

The sites included in this study were initially selected from existing resource assessments published in reports [13, 54, 20, 52, 4, 19, 3, 5, 28] or papers [18, 57, 45, 51, 30] and then completed by additional sites found through a thorough examination of the nautical charts of the UK and Ireland. The UK and Ireland were chosen because they both display a notable

cluster of potentially promising lagoon sites with regards to tidal power extraction. Very few of these lagoon channels were identified in the commissioned surveys of these areas as these were mainly focused on ocean sites [3, 9, 52, 44]. Required pieces of data that were missing from the aforementioned publications were gathered using the appropriate nautical charts or tide tables. The sites for which data could only be partially collected were discarded. The values assigned to the required parameters and the definitions and values of the physical characteristics used as input variables are now examined.

### 3.1.2 Data Definitions & Data Tables

**Parameters** Calculations for both ocean and lagoon channels require three input parameters: the acceleration due to gravity, $g$, the volumetric mass density, $\rho$, and the tidal frequency, $\omega$ . These parameters were fixed at $g = 9.81\,ms^{-2}$, $\rho = 1025\,kgm^{-3}$ and $\omega = 1.4 \times 10^{-4}\,radians\,s^{-1}$ (M2 tidal angular frequency) respectively. One of the required physical characteristics of the channels, the drag coefficient for background bottom friction based on the channel's horizontal area, $C_D$, could not be determined from the available data sources. This variable was thus used as a parameter with a fixed value of $C_D = 0.0025$ for all channels [57].

**Physical Characteristics of the Channels** The boundaries for all the channels in this study were characterised by the physical barriers, land or underwater rise, which restrict the flow of seawater. These can be found delineated on the pertinent nautical charts. Channel selection was limited to the ones with physical barriers causing the velocity of the flow within to peak above a threshold of $1\,ms^{-1}$ on average. The physical characteristics of the channels used as variables for calculations were defined as described below.[1]

- The average width for a given channel ($w$) was determined by measuring the average distance in the direction perpendicular to the flow within the channel boundaries on the relevant nautical charts. This method was applied to all the channels except the ones located in Canada and Norway, for which width values were given in the reports used. The widths for the Canadian sites were described as representative of the locations at which maximum currents occur [54]. The widths for the Norwegian sites were depicted as estimated from digital sea charts made available by the Norwegian Coastal Administration[2] [30].

[1] All the required data for Cook Strait and Kaipara Harbour (New Zealand) following the specific definitions given thereafter were found directly in [57].

[2] http://kart2.kystverket.no/

- The average depth for a given channel ($h$) was determined by averaging the depth values displayed on the appropriate nautical charts within the channel boundaries. This approach was followed for all the channels except the ones located in Canada and Norway, for which depth values were provided in the reports used. The depths for the Canadian and Norwegian sites were described in a similar manner to the widths mentioned above [54, 30].

- The length of a given channel ($L$) was determined by measuring the distance in the along-flow direction within the channel boundaries on the relevant nautical charts.

- The mean peak velocity ($v$) of the flow within an ocean channel was determined by calculating the average of the maximum drift values for neap and spring tides. These were found either on nautical charts directly in the relevant area or in tidal stream tables via tidal diamonds, or in appropriate tide tables. This method was applied to all channels except the ones located in Canada, Chile, Norway, the USA and the *Strait of Messina* in Italy, for which velocity values were given in the reports and research papers used. The velocities for the Canadian sites were calculated as the average of the given maximum current speeds for the ebb and the flood tides [54]. The velocities for the Chilean sites were evaluated from Figure 8 in [20], which is a representation of the average tidal current velocities around the island of Chiloé. The velocities for the Norwegian sites were interpreted as representing the mean maximum spring speeds, although it was sometimes unclear whether the values from the sources were peak or mean values [30]. The velocities for the American sites were determined using the national database built by Georgia Tech Research Corporation[3] [28]. The velocity for the *Strait of Messina* is given as a mean of the maximum velocities recorded in the region [18].

- The average surface area of the lagoon ($A_L$) of a given lagoon channel was calculated as the average of the measured surface areas of the body of water behind the channel at low tide, i.e. excluding the mudflats, and at high tide, i.e. including the mudflats, using the information displayed on relevant nautical charts.

- The amplitude of the tidal elevation in the ocean ($\eta_{01}$) for a given lagoon channel was determined by calculating the average of the Mean High Water Spring (MHWS), Mean High Water Neap (MHWN), Mean Low Water Spring (MLWS) and Mean Low Water

[3]The database has been made available at the following url http://www.tidalstreampower.gatech.edu/

Neap (MLWN) values found at the closest appropriate location on the relevant nautical charts.

Some of the collected data gathered to represent given physical characteristics of the channels have slightly disparate definitions based on the source used. This diversity in the input data may have an impact on the results found here. However, because consistency exists across channels from a given country, possible effects on the outcomes of this study should be identifiable (3.4). One benefit from using a large database of channels is the resulting clear separation of the outliers, for which it can be reasonable to assume there exist data issues.

**Data Tables** The physical characteristics of the channels required for potential calculations and derived from the data gathered are displayed in the two tables presented in Appendix A. The data are organised by country listed in alphabetical order and represented by their country code[4]. Within each country, the data are sorted in alphabetical order according to the site name used. The first table, Table A.1, includes information regarding the ocean channels and the second one , Table A.2, information pertaining to the lagoon channels. The number of ocean and lagoon channels included in this study for each of the countries represented is shown in Table 3.1, in which countries are listed in alphabetical order. The geographical coordinates of all the channels included here can be found in Appendix E. The ranges of ocean and lagoon channels comprised in this study with regards to their respective input variables are introduced next.

[4] A list of countries and corresponding country codes can be found in the Nomenclature.

Table 3.1: Number of ocean and lagoon channels for each of the countries included in this study listed in alphabetical order. Country codes can be found in the Nomenclature.

| Country Code | Number of Ocean Channels | Number of Lagoon Channels |
|---|---|---|
| OZ | 2 | 2 |
| CA | 64 | 1 |
| CH | 3 | 0 |
| IR | 13 | 8 |
| IT | 1 | 0 |
| JP | 2 | 0 |
| NW | 50 | 0 |
| NZ | 4 | 1 |
| SG | 1 | 0 |
| UK | 42 | 12 |
| US | 24 | 9 |
| TOTAL | 206 | 33 |

## 3.2 Ranges of Channels

The study includes a total of 206 ocean channels and 33 lagoon channels originating from 11 and 6 different countries respectively. This section examines the ranges of ocean and lagoon channels grouped on several figures according to the values of four of their respective input variables. It is interesting to consider the spread of naturally occurring physical characteristics of ocean and lagoon channels and how closely it matches existing turbine design applicabilities.

**Ocean Channels** Figure 3.1 presents the ranges of ocean channels grouped according to the velocity $v$, depth $h$, length $L$ and width $w$.

Figure 3.1a presents the 206 ocean channels distributed according to their mean peak velocity. As expected, due to high flow speed being the main criterion used for inclusion in the study, a majority of ocean channels have a mean peak velocity over $2.5\,ms^{-1}$. Such a velocity threshold was earlier on deemed ideal for economically viable electricity production using in-stream turbines [23]. 58% of the ocean channels display mean peak velocities above $2\,ms^{-1}$. The $2\,ms^{-1}$ mark has been more recently referred to as the minimum flow speed value necessary to produce electricity on a commercial scale [49, 21]. Some of the latest

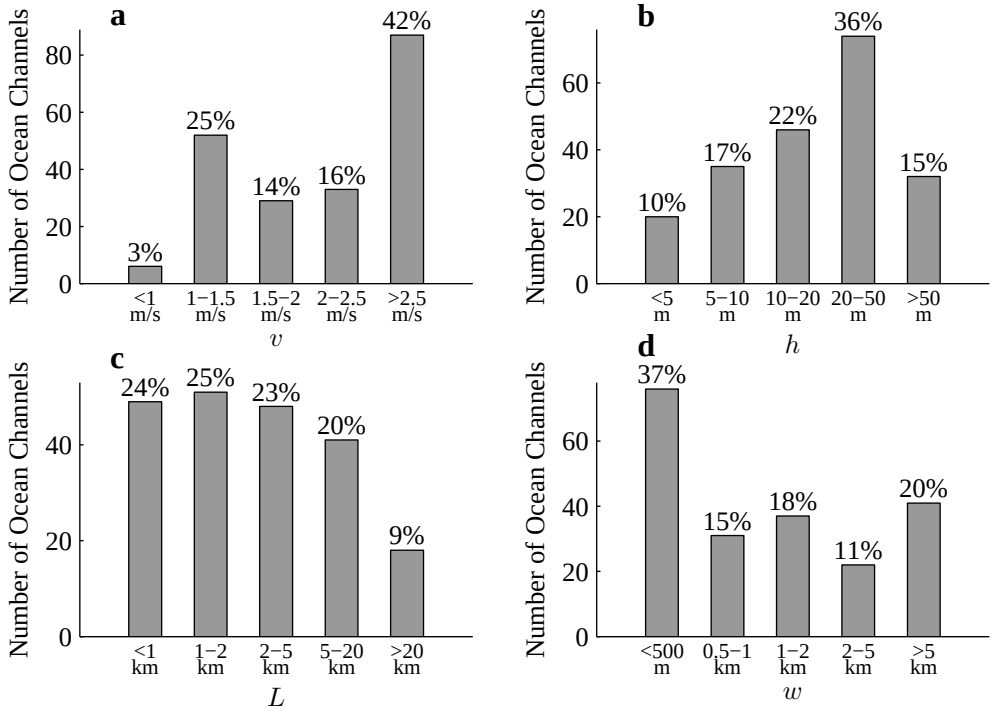


Figure 3.1: Ocean channels included in this study distributed in series of ranges of values according to mean peak velocity ($v$), average depth ($h$), length ($L$) and average width ($w$).

publications indicate that the minimum threshold to achieve economically viable electricity production, considering technological improvements, could be as low as $1\,m\,s^{-1}$ [2]. Such a mean peak velocity value applies to more than 97% of the sites included here. The 6 sites with mean peak velocities below $1\,m\,s^{-1}$ have been kept in the study because of the high uncertainty pertaining to the velocity data collected.

Figure 3.1b presents the 206 ocean channels distributed according to their average depth. Approximately one third of the ocean channels included in the study have average depths between $20\,m$ and $50\,m$. This depth range corresponds to the largest domain of turbine designs currently in development [46, 49, 29]. For the purpose of tidal farm implementations, sites shallower than $20\,m$ tends to be considered 'shallow' and deeper than $50\,m$ 'deep' [49]. Present-day devices require a minimum water depth of about $5\,m$ [28]. 12 ocean channels from this study present average depths shallower than $5\,m$, but these sites have been kept as part of the research data in order to account for both the uncertainties on the depth-average measurements and the future technological improvements, which may include smaller designs for small-scale applications. Most of the ocean channels in the study, 49% or 39% when excluding the sites shallower than $5\,m$, are located in 'shallow' waters. Alternatively, 15% of them are found in 'deep' areas, including 10 sites with depths exceeding

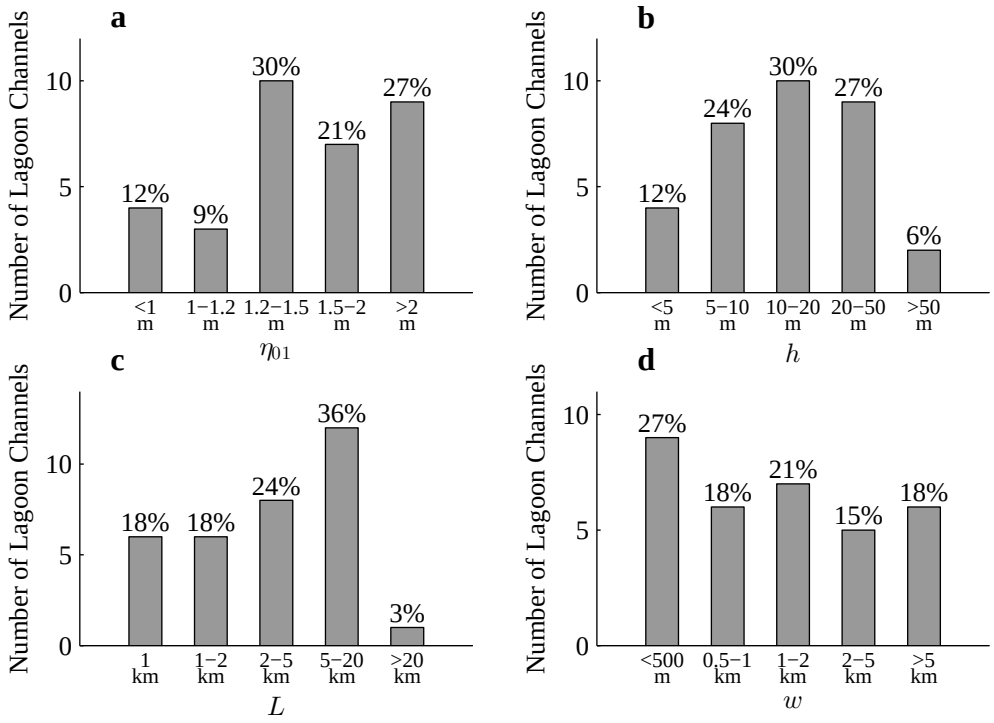


Figure 3.2: Lagoon channels included in this study distributed in series of ranges of values according to average tidal elevation in the ocean ($\eta_{01}$), average depth ($h$), length ($L$) and average width ($w$).

100 $m$ and for which a few technologies are being currently developed [46].

Figures 3.1c and 3.1d present the 206 ocean channels distributed according to their length and average width respectively. Their arrangements show notable diversities with lengths varying from less than 1 $km$ to more than 50 $km$ and average widths ranging from less than 200 $m$ to more than 10 $km$. These physical properties of the channels affect possible tidal farm configurations, which will be discussed in Chapter 5.

**Lagoon Channels** Figure 3.2 presents the ranges of lagoon channels grouped according to the tidal elevation $\eta_{01}$, average depth $h$, length $L$ and width $w$.

Figure 3.2a presents the 33 lagoon channels distributed according to their average oceanic tidal elevation. All but 4 of the lagoon channels have average oceanic tidal elevation exceeding 1 $m$. Larger oceanic tidal elevations assure sizeable tidal prisms and therefore substantial flow velocities during the flood and ebb tides. The existing high uncertainty on the collected average oceanic tidal elevation data explains why the 4 channels with lower tidal elevation values were not discarded.

Figure 3.2b presents the 33 lagoon channels distributed according to their average depth.

All but 2 of the lagoon channels are located in 'shallow' waters, which is to be expected from estuary-type channels offering sufficient tidal range around their mouth areas. Four of them have depth-averages below the technological $5\,m$ threshold. For the same reasons as the depth-equivalent ocean channels, these very shallow sites have been kept in this study.

Figures 3.2c and 3.2d present the 33 lagoon channels distributed according to their length and average width respectively. Their arrangements show some diversities with lengths varying from less than $500\,m$ to more than $5\,km$ and average widths ranging from less than $200\,m$ to more than $2\,km$. As per the ocean channels, these physical properties affect possible tidal farm configurations, but these will not be discussed for lagoon channels in this thesis. Tidal current potential estimates are now produced using three different models for each channel-type and compared for validity assertion purposes.

## 3.3 Tidal Current Potential Estimation Methods

There exists a range of models designed to produce tidal current potential estimations. The KE Flux model has been historically used to produce such figures. However, its validity has since been put into question, as it does not take into account the back effect on the flow of the deployment of turbines [26, 27]. The latest models, GC05 and Lagoon GC05, are usually found to be the ones applied in more recently produced resource estimates [25, 7, 28, 3]. Other similarly built models, which address some of the issues associated with the GC05 model, namely the V11 and Lagoon-V11 models, are also useful to produce preliminary assessments [57]. In this section, firstly, the V11 and GC05 models as well as their lagoon versions are compared to ensure reliability. The V11 and Lagoon-V11 models are then compared to the KE Flux model to examine the quality of the estimates produced by the latest. All the values correspond to the upper limits of the tidal current potentials of the channels and do not take into account mixing losses in the wake of the turbines, electro-mechanical losses or partial blockage of the cross-sections of the channels by the turbines.

### 3.3.1 V11 vs GC05 & Lagoon-V11 vs Lagoon-GC05

The GC05 and Lagoon-GC05 models, which take into account background friction and the effect on the flow of power extraction, have become the methods of choice to generate reliable tidal current potential estimates [28, 3, 30]. The V11 and Lagoon-V11 models have been derived from the GC05 and Lagoon-GC05 models respectively. Tidal current potential estimations used for site preliminary assessments or country-wide potential assessments

benefit from relatively easily accessible data and inexpensive costs. The main advantage of the V11 model over the GC05 model relies on data acquisition made simpler and cheaper by eliminating the need for measurements pertaining to the amplitude of the head loss [57].

**Ocean Channel** The amplitude of the head loss ($\zeta_0$) is a required piece of data for the purpose of GC05 potential calculations. It could not be accessed or measured, therefore it was calculated for all the ocean channels included here using the following equation [57]:

$$\zeta_0 = \frac{\omega U_1 L}{g A_C} \tag{3.1}$$

Figure 3.3 shows how the potentials calculated via the V11 and GC05 models compare for every ocean channel included in this thesis. Each one of the ocean channels has been assigned a unique symbol formed by the combination of a coloured circle, representing its potential range, and filled with a number, representing its rank within its range. The key for the ocean channel identification can be found in Appendix B. The colour code is based on the potential results calculated via the V11 model. Channels with potentials above $10\,GW$ are represented in brown; channels with potentials between $1\,GW$ and $10\,GW$ in red; channels with potentials between $100\,MW$ and $1\,GW$ in orange; channels with potentials between $50\,MW$ and $100\,GMW$ in yellow; channels with potentials between $20\,MW$ and $50\,MW$ in green; channels with potentials between $10\,MW$ and $20\,MW$ in turquoise; channels with potentials between $1\,MW$ and $10\,MW$ in blue; channels with potentials less than $1\,MW$ in violet.

Figure 3.3 effectively verifies that the deviation in the values of the potential for a given ocean channel calculated via the V11 and GC05 models remain within the expected range of +/-15%, with +/-10% originating from the use of a $\gamma$ coefficient value of 0.22 in the GC05 model [25] and the additional +/-5% inherent to the V11 model from the use of the approximate analytic solution instead of the numerical one [57]. The largest and mean separations reach 12.5% and 10.4% respectively. Considering the uncertainties pertaining to the data collected, evaluations of the potentials of ocean channels determined within 15% of their true potentials are sufficient. The V11 model produces estimations lower than the ones from the GC05 model for the vast majority, 95%, of the ocean channels.

**Lagoon Channels** Figure 3.4 shows how the potentials calculated via the Lagoon-V11 and Lagoon-GC05 models compare for every lagoon channel included in this research. Each one of the lagoon channels has been assigned a unique symbol formed by the combination of a coloured circle, representing its potential range, filled with a letter, representing its rank

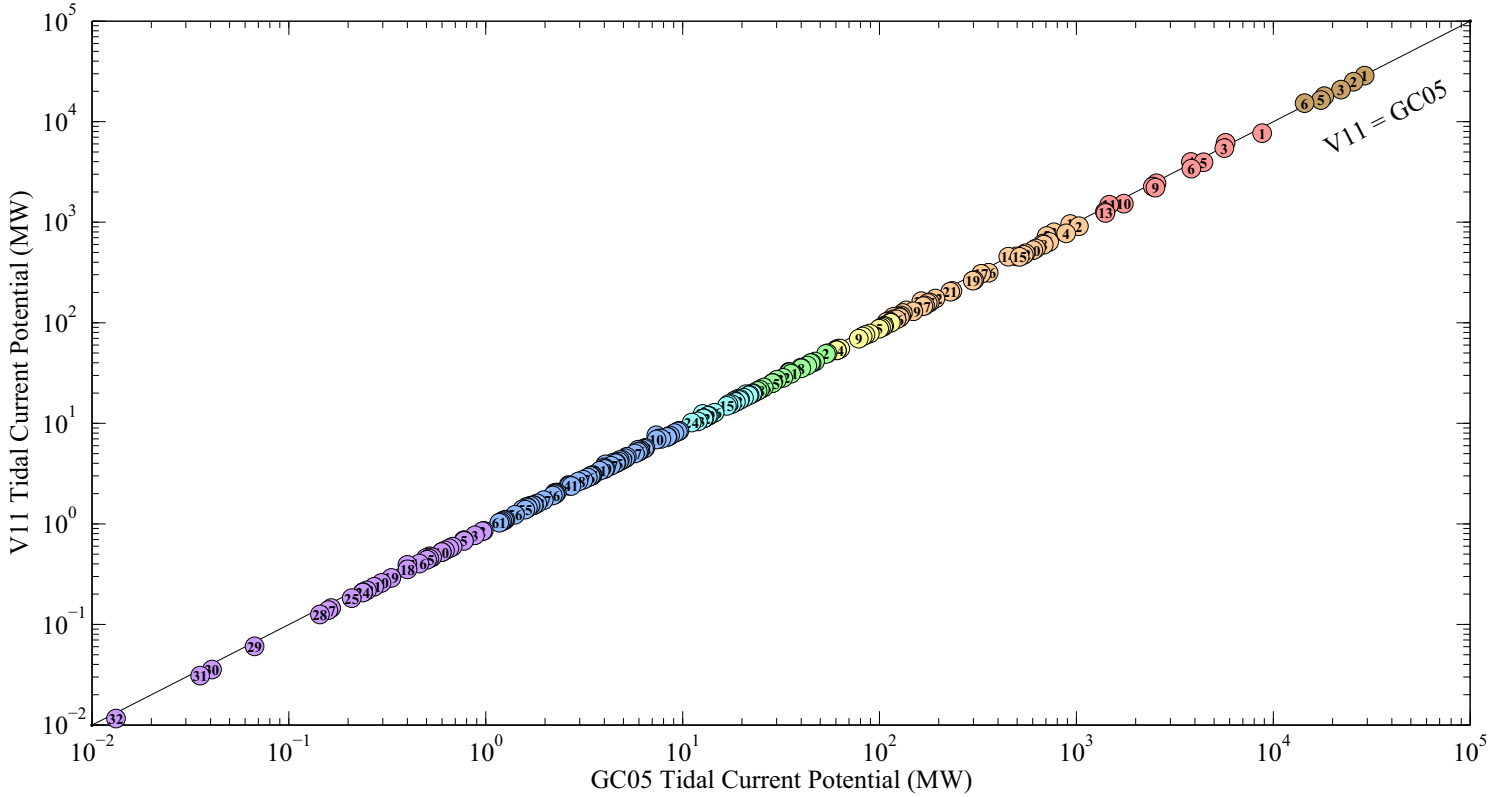


Figure 3.3: Comparison between the upper tidal current potential limits obtained using the V11 and GC05 models for all the ocean channels in the study. The black line represents the values for which both models give equal potentials. The key for the ocean channel identification can be found in Appendix B.

within its range. The key for the lagoon channel identification can be found in Appendix B. The colour code is based on the potential results calculated via the Lagoon-V11 model. Channels with potentials above $10\,GW$ are represented in brown; channels with potentials between $1\,GW$ and $10\,GW$ in red; channels with potentials between $100\,MW$ and $1\,GW$ in orange; channels with potentials between $50\,MW$ and $100\,GMW$ in yellow; channels with potentials between $20\,MW$ and $50\,MW$ in green; channels with potentials between $10\,MW$ and $20\,MW$ in turquoise; channels with potentials between $1\,MW$ and $10\,MW$ in blue. There are no lagoon channels with potentials less than $1\,MW$.

Figure 3.4 effectively verifies that the deviation in the values of the potential for a given lagoon channel calculated via the Lagoon-V11 and Lagoon-GC05 models remain within the expected range of approximately +/-15% [6], resulting from a choice of value of 0.21 for the $\gamma$ coefficient. The largest and mean separations reach 16.0% and 11.0% respectively. Evaluations of the potentials of lagoon channels within approximately 15% of their true potentials are satisfactory for this study, considering the uncertainties in the collected data. The Lagoon-V11 model produces estimations higher than the ones from the Lagoon-GC05 model for a large majority, 73%, of the lagoon channels.

For the purpose of preliminary site assessments, the V11 and Lagoon-V11 models produce results of sufficient accuracy. Bypassing the need for the measurement of the amplitude of the head loss is a significant benefit with regards to simplicity and cost in relation to the data acquisition process. Therefore, with site assessments planned for a database of 206 ocean channels, the V11 model is preferred in this thesis. For consistency reasons, the Lagoon-V11 model will be used in association with the V11 one, but for lagoon channels. The quality of site assessments produced using the KE Flux model for both ocean and lagoon channels is examined next.

### 3.3.2 V11 vs KE Flux & Lagoon-V11 vs KE Flux

The quality of resource assessments produced based on the KE Flux model has been put into disrepute [26, 27]. Simply calculating the kinetic energy of the flow passing through a given cross-sectional area of a channel as a mean of assessing its potential is no longer considered a valid approach. Indeed, it has now been shown that considerations must be made for the effect on the flow of the implantation of turbines within in a channel [25]. Although the KE Flux model ignores such effect, it is interesting to examine the differences observed in the figures produced using the KE Flux model as opposed to acceptable methods such as the V11 and Lagoon-V11 models as is done below.

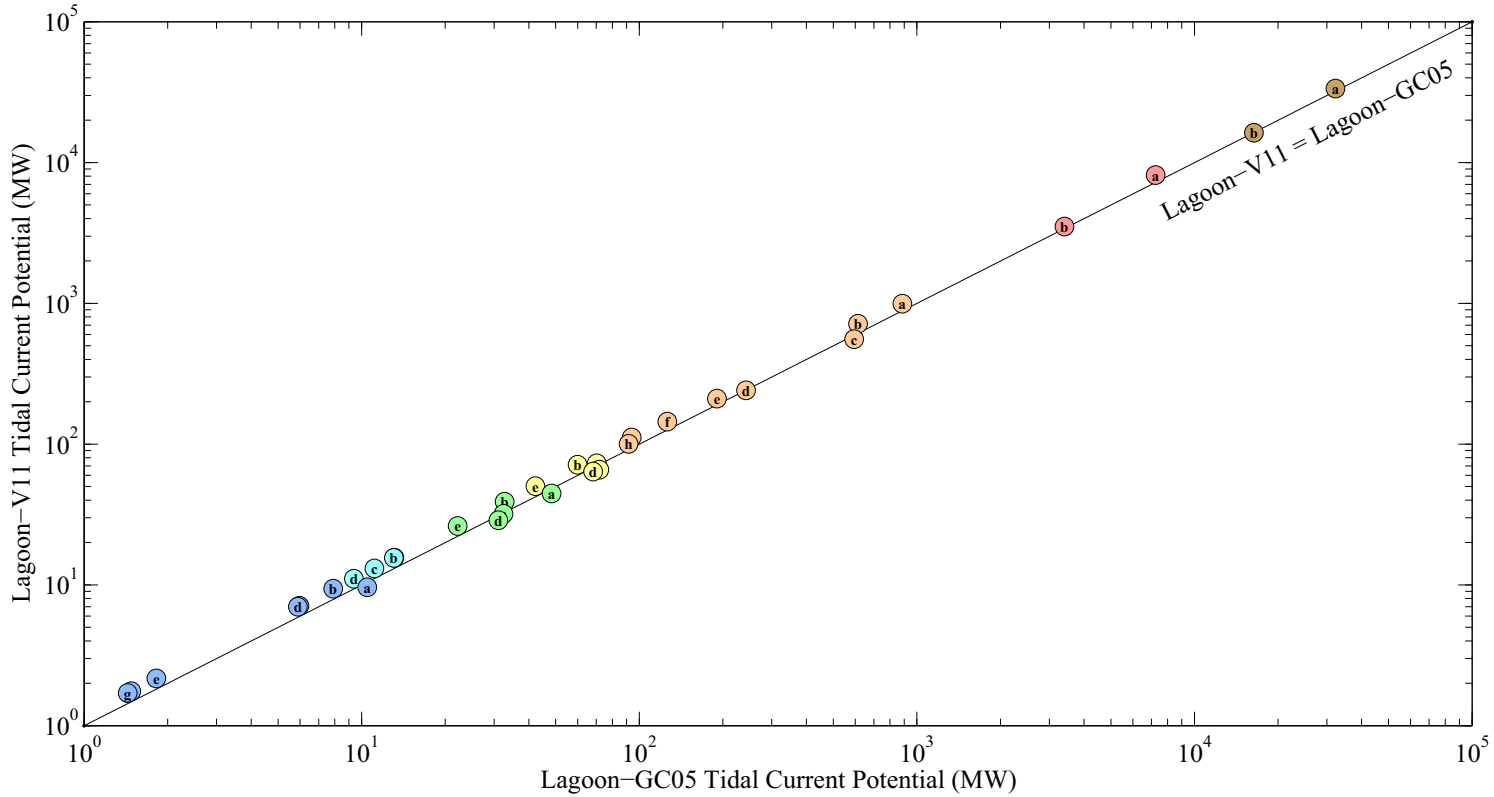


Figure 3.4: Comparison between the upper tidal current potential limits obtained using the Lagoon-V11 and Lagoon-GC05 models for all the lagoon channels in the study. The black line represents the values for which both models give equal potentials. The key for the lagoon channel identification can be found in Appendix B.

**Ocean Channels** Figure 3.5 presents how the potentials calculated via the V11 and KE Flux models compare for every ocean channel included in this research. The results show that the KE Flux model is unreliable as a measure of the potential for a given ocean channel, as was previously highlighted [27]. Calculations of potentials via the KE Flux model produce in majority, 78%, values which are higher than the ones obtained through the V11 model. However, the potential for a given ocean channel, when calculated using the KE Flux model, can be either overestimated or underestimated. Here, the overestimations range between 3.0% and 8,800%, averaging at 540%, whilst the underestimations range between 1.3% and 97%, averaging at 49%. Since there exists at present no medium through which one might be able to determine if the potential of a given channel has been overestimated or underestimated by the KE Flux assessment method and the extent of the misestimation, values produced via the KE Flux model cannot carry any relevance or usefulness in terms of resource estimations. Figure 3.5 shows no obvious relationship between the potential estimates from the two models. Further investigations of possible latent relationships relative to relevant discriminatory quantities are carried out in Subsection 4.1.2.

**Lagoon Channels** Figure 3.6 presents how the potentials calculated via the Lagoon-V11 and KE Flux models compare for every lagoon channel included in this research. The results show that the KE Flux model is also unreliable as a measure of the potential for a given lagoon channel. For the vast majority of the lagoon channels in this study, 94%, the KE Flux model underestimates their potentials. However, the potential is overestimated for 2 of the channels. The overestimations are of 9.5% and 420%, whilst the underestimations range between 2.8% and 100%, averaging at 83%. With the possibility of both over and under estimations over a wide range of proportions, the usefulness of resource assessments produced using the KE Flux model in the context of lagoon channels can be put into question. Figure 3.6 shows no obvious relationship between the potentials from the two models. Further investigations of possible latent relationships relative to relevant discriminatory quantities are carried out in Subsection 4.1.1.

The KE Flux model offers no obvious connection with the potentials of ocean or lagoon channels. There appears to be little clue as to whether it produces over or under estimations and as to how bad or how good of an estimation it generates. This model is thus unreliable when used to determine the potential of a given site. The ranges of potentials of the channels included here grouped according to their country of origin and their type is examined next to ensure there exists no data issue.

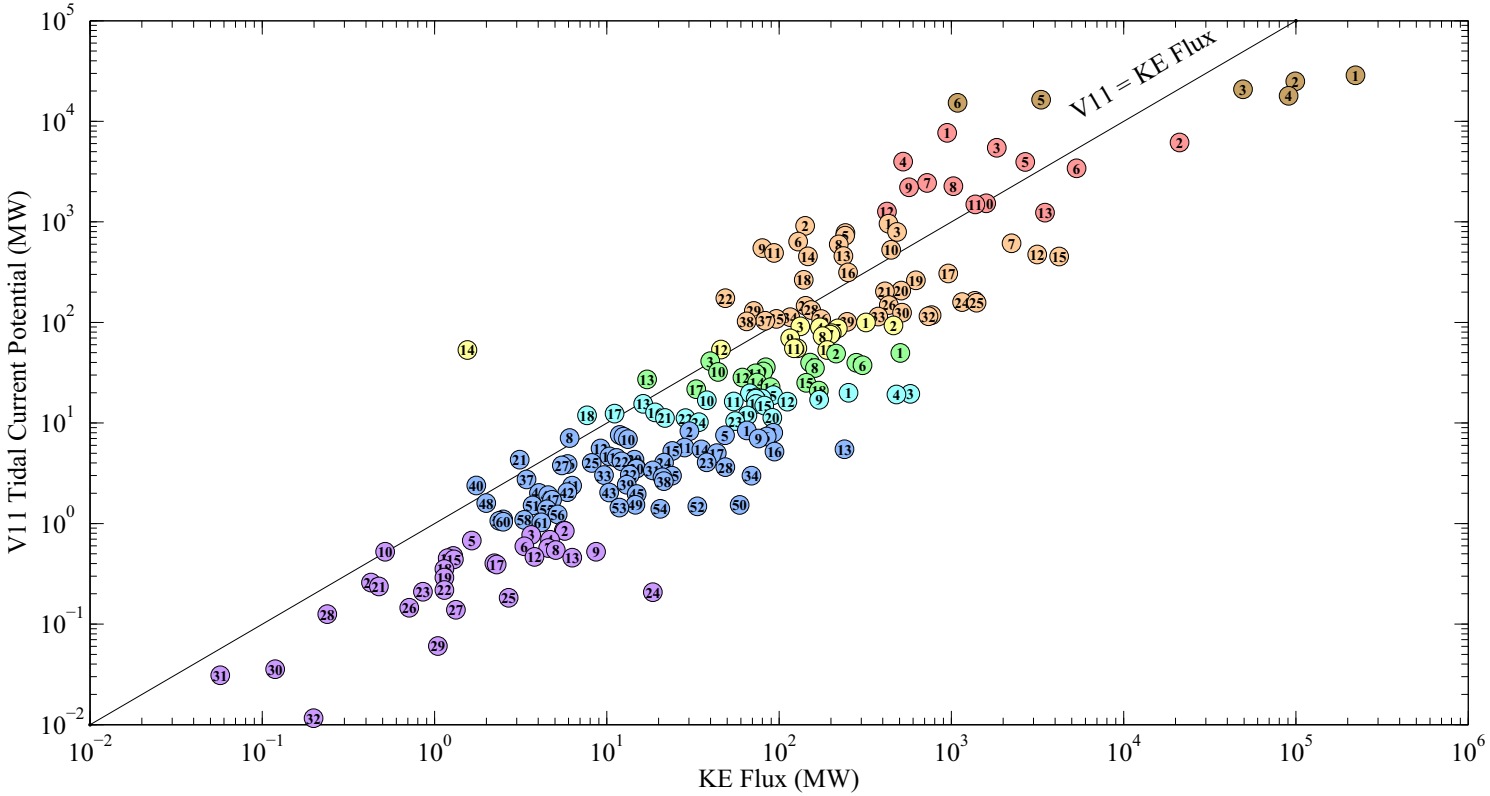


Figure 3.5: Comparison between the upper tidal current potential limits obtained using the V11 and KE Flux models for all the ocean channels in the study. The black line represents the values for which both models give equal potentials. The key for the ocean channel identification can be found in Appendix B.

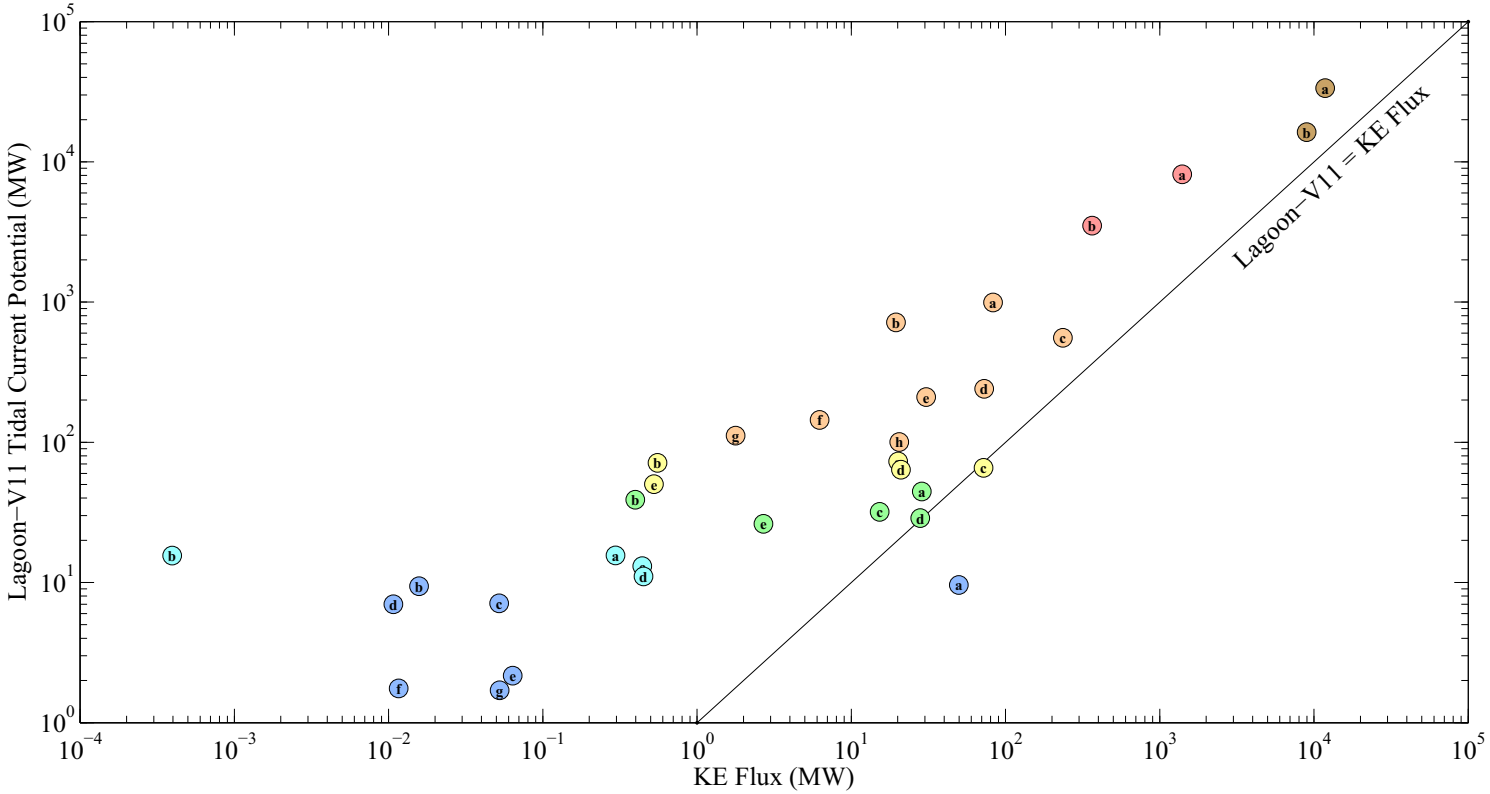


Figure 3.6: Comparison between the upper tidal current potential limits obtained using the Lagoon-V11 and KE Flux models for all the lagoon channels in the study. The black line represents the values for which both models give equal potentials. The key for the lagoon channel identification can be found in Appendix B.

## 3.4 Tidal Current Potential Ranges per Country

The data gathered for the channels included in this study originate from a various range of sources as discussed in Subsection 3.1.1. Although the definitions of the data as collected may vary, consistency exists across the channels belonging to a given country. In this section, the channels are grouped by type and country in order to examine the spread of tidal current potential values produced for each group. The figures enable to highlight any visible effect of the varied sources used on the tidal resource assessment outcomes.

**Ocean Channels** Figure 3.7 shows how the various ranges of potentials obtained using the V11 model compare for each of the countries or group of countries included in this study. According to the definitions of the initial data collected for this research described in Subsection 3.1.2, the average widths and depths as well as the mean peak velocities of the ocean channels display various degrees of variation for a number of countries.

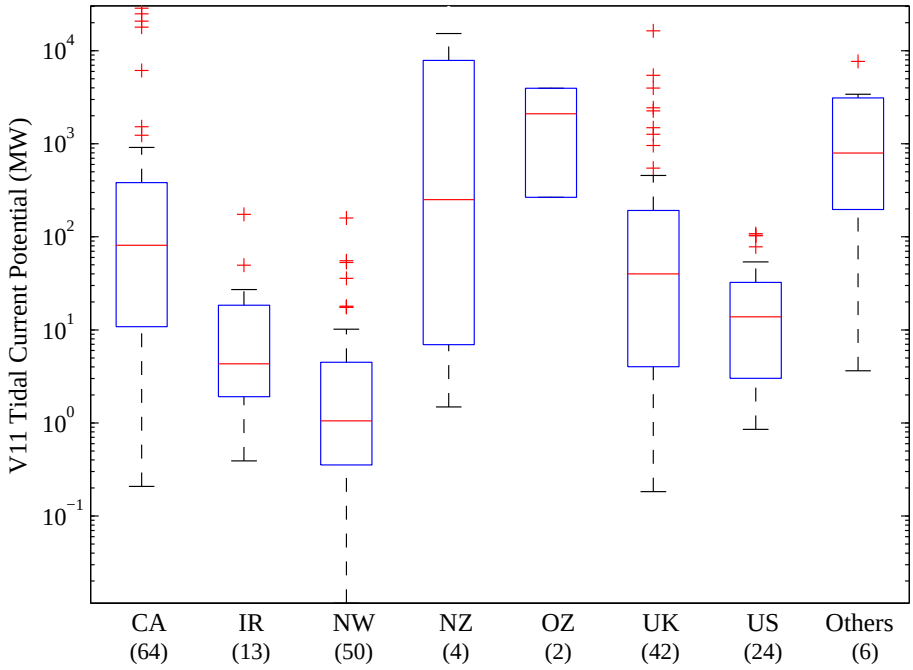


Figure 3.7: Range of potentials of ocean channels calculated via the V11 model for each country or group of countries included in this study. Country codes can be found in the Nomenclature and 'Others' regroup Singapore, Japan, Italy and Chile. The numbers found in the brackets underneath each country code indicate the number of ocean channels included for a given country.

**Canada** The definitions of the width and depth for Canadian sites, which focus on the location of the maximum current, would be expected to produce potentials similar to the ones produced from the general definitions chosen in this study, which correspond to the average width and depth across the area in which the high flow velocity makes for desired exploitation. Since both definitions intend for values of width and depth to be representative of the high speed section of the flow, one can expect them to be very close to one another. The velocity values would be expected to be higher than the ones collected from the general mean peak velocity definition, because their description in the source report only takes into account the spring component of the tidal cycle, albeit considering both the ebb and flood tides. Higher velocities would in return translate into higher potentials. The Canadian sites do comprise the 4 highest ocean channels' potentials in the study. However, these sites are located in the same flow area of the Hudson Strait and tidal power extraction at one of the sites would likely affect the yields of the others, something which has been ignored here. The presence of the top site in this Canadian region highlights the existence of a localised strong potential, which is confirmed by the 3 other nearby sites. The true potentials for the Canadian sites may well be lower than the ones presented here, but the overall span of potentials is not particularly inconsistent with the rest of the data. Moreover, the Canadian sites with the lower potentials have values lower than those of the lowest-potential sites from Ireland, New Zealand, Australia or the USA amongst others as can be seen on Figure 3.7.

**Norway** The definitions of the width and depth for Norwegian sites are not descriptive enough to determine the effects they might have on the potentials as calculated here. The velocity values only take into account the spring component of the tidal cycle and would therefore be expected to be on the upper end of the velocity data collected using the general definition. The anticipated outcome would be higher than true potential values for the Norwegian sites, but they span across from low to lowest potentials compared to the other countries as shown on Figure 3.7. Indeed, only ocean channels from Norway include potential results lower than $100\,kW$ or in the order of $10\,kW$. The low end of the Norwegian sites can be explained by the fact that the source of the data [30] was more inclusive than most of the other reports or papers in terms of minimum flow velocities, as low as $1.03\,ms^{-1}$. The low trend of the overall potentials in comparison with the other countries might be explained by the interpretation made of the velocity data, originally from Norwegian navigational charts (DNL[5]), as representing mean maximum spring speeds, although as explained in [30] some

[5]Den Norske Los: Books made of 8 volumes used for navigation in Norwegian waters and published by the Norwegian Mapping and Cadastre Authority.

could just be mean values.

**USA** The velocity values taken into account for the American sites are described as mean current speeds [28]. These are therefore expected to represent underestimations of the mean peak velocities at the site locations. Consequently, the estimates of the potentials for the American sites would be expected to be lower on average than the ones produced for the other countries present in this study. Figure 3.7 presents results in agreement with the anticipated outcome. Indeed, all of the American ocean channels display potentials in the mid-to-low range in comparison with the ocean channels of the other countries represented here.

**Chile & Italy** The information provided in the sources with regards to the velocity values at the Chilean and Italian sites are not descriptive enough to determine whether they should incur a deviation in potentials from the results obtained for the other countries in the study. Both definitions could imply mean peak velocity values, which would correspond to the general definition chosen in this study. The Chilean and Italian sites belong to the box labelled 'Others' on Figure 3.7 and its overall span is not particularly inconsistent with the rest of the data.

**Lagoon Channels** There were no country-specific differences in the collections of length, lagoon surface area and tidal elevation data, therefore inconsistencies in potentials between countries would have to have arisen from depth or width data. Variations for width and depth data only concerned Canada and Norway. There is no lagoon channel from Norway and only one from Canada, which makes it impossible to discuss patterns of inconsistencies that could have originated from width and/or depth data.

Although it cannot be asserted that no data issue exists for either ocean or lagoon channels, no unreasonable inconsistencies are present in the dataset used in this study. These data are now used to establish the upper limits of the tidal current potential resources of the 11 countries included here.

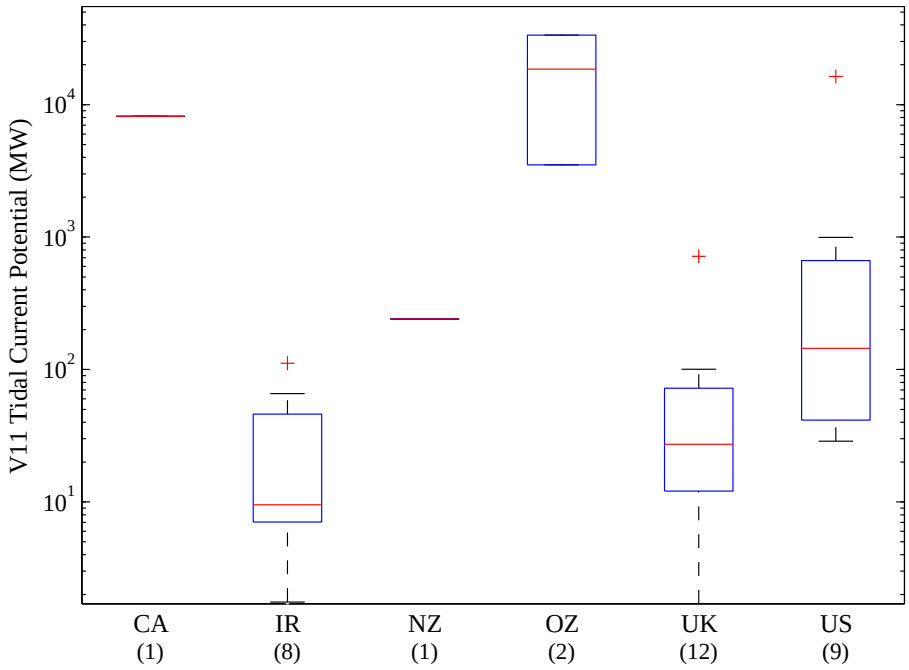


Figure 3.8: Range of potentials of lagoon channels calculated via the Lagoon-V11 model for each country included in this study comprising lagoon-type channels. Country codes can be found in the Nomenclature. The numbers found in the brackets underneath each country code indicate the number of lagoon channels included for a given country.

## 3.5 Tidal Current Potential Estimations

The V11 and Lagoon-V11 models for calculating channels' potentials are approximate versions of the GC05 and Lagoon-GC05 models [57]. However, they provide adequate levels of accuracy for the purpose of completing preliminary potential resource assessments considering the existing uncertainties on the collected data. The substantial cost of gathering data to produce GC05 upper tidal current potential limits has proven to be a barrier to its widespread use in preliminary-type assessments of tidal resources, despite evidence in the lack of validity of the KE Flux model [54, 30]. The V11 and Lagoon-V11 models are being used throughout this study because of the accessibility of their required input data and because of the possibility offered by the more advanced V10 model to produce realisable power estimates as discussed in Chapter 5.

The preliminary tidal resource estimations proposed below present the potentials from both ocean and lagoon channels for each country or group of countries included in this thesis. It is assumed the turbines occupy the entire cross-sections of the channels. Hydrodynamic interactions between turbines, i.e. mixing losses, and electro-mechanical losses of energy have not been taken into account. No consideration was made for restrictions due to the environmental impact of extracting the resource, or specific local constraints such as requirements for navigation, existing structures, fisheries... The results for all the countries and individual sites are presented in Table C.1 on page 143 and Table C.2 on page 155 for ocean and lagoon channels respectively.

The lists of sites for each country are not exhaustive and although one may find country-wide resource assessment results useful, the figures produced here should be considered with prudence for three reasons. Firstly, potential interferences between sites have been largely ignored, although these might have a significant impact on a given site's potential. Additionally, the estimations of the errors on the potentials correspond only to the possible deviation of the V11 model from the true potential as calculated using the GC05 model. They do not take into account the propagation of errors from the uncertainties on the collected data. These uncertainties have been ignored in this section because they would be very difficult to gauge meaningfully considering the data originate from third party sources in which no error estimation exists. A better-adapted sensitivity study relative to the input variables and parameter will be conducted in Section 4.3. Finally, estimations made at substantially wide sites must be considered with more caution, because of the assumptions of a one-dimensional uniform flow velocity across the channels made in the GC05 and V11 models. The resulting effect on the accuracy of channels' potential estimates is unknown.

Comparisons between the results obtained here and existing studies or reports are done for each country whenever appropriate. The UK and Ireland are treated separately from the rest of the countries because their respective databases of channels are believed to be exhaustive, while the ones relating to the other countries are known to be incomplete. Table 3.2 presents a summary of the potentials for each of the 11 countries included as well as the portions of the contributions originating from ocean and lagoon channels. When appropriate, results produced from previous studies are also included in this table.

### 3.5.1 The UK

Tables C.1 and C.2 include the potentials for the ocean and lagoon channels of the UK respectively. The tidal current potential resource from both types of channels across the UK adds up to approximately $37\,GW \pm 6\,GW$.

#### Comparison with Black & Veatch Reports

**Method and Data** Three reports regarding the UK's tidal energy resource have been produced by Black & Veatch for the Carbon Trust in 2004, 2005 and 2011 [4, 5, 3]. The data sources used for these reports include navigational charts, tide tables and the 2008 version of the Marine Energy Atlas (MEA) for the latest one. The sources and thus the quality of the data used in these reports correspond closely to what was utilised here, therefore the errors carried by the collected data in both assessment works should be comparable. The first two reports produced estimates based on the KE Flux model and corrected via a 'Significant Impact Factor' (SIF) meant to take into account the various restrictions to power extraction as aforementioned. Modifications to the number of included sites, their properties and SIFs were made from the 2004 report for the 2005 update. The 2011 report was based on three numerical models closely related to the GC05 model and the results yielded from it when restrictions in the form of maximum acceptable flow reductions are applied as discussed in [27]. Arguments can be raised against the applicability of the GC05 model to specific areas within flow restrictions or around headlands as it is done for nearly all the sites in the 2011 report. The existence of alternative flow pathways is underlined in the report as a potential caveat to the methodology used. However, the conclusion made is that in the presence of alternative flow pathways the potentials obtained would simply give an upper bound of the existing tidal current potential for a given channel. The GC05 and GC07 models are intended to be used in the context of channel-type waterways with the assumption of a one-dimensional flow independent from the across-channel position [25, 26].

Applying the GC07 model to only the small fraction of a channel in which the velocity is high enough to warrant an interest for tidal energy extraction purposes implies that a partial fence of corresponding size is placed in a channel in which the velocity reaches the desired rating all across. The assumption of a flow velocity independent from the across-channel position makes the GC05, GC07 and V11 models not well suited for large channels or any channel with a substantial velocity difference across it. The same issue is being faced in this study. No better two-dimensional assessment method has been developed at this date, therefore it was decided that the channels would be regarded in their entirety with velocity data taken as the averages of the flow information presented on the navigational charts or other relevant sources across the channel areas. One could only speculate on the consequences on the accuracy of the results presented here of the choice of methodology made. However, we should expect that the more varied the across-channel flow velocity is, which generally means the wider the channel is, the less likely the potential calculations are to be good representations of the local tidal resources.

**Results** The potential of the UK was estimated to be around $12.5\,GW$ in both the 2004 and 2005 Black & Veatch reports. The 2005 report introduced a more stringent SIF, which caused the extractable resource estimation, i.e. the proportion of the potential that could in fact be extracted, to drop slightly [4, 5]. The 2011 Black & Veatch report presents an estimate of about $39\,GW$ for the UK's potential [3]. A very close estimation of the UK's potential of $37\,GW$ was produced in this study. 30 sites were selected for the latest Black & Veatch report after applying the following two criteria meant to ensure reasonable project economics: mean annualised power density over $1.5\,kW\,m^{-2}$ and minimum depth of $15\,m$. Power density is used as a proxy for current velocity as it is directly proportional to the cube of the velocity. However, neither the power density nor the current velocity are enough to determine the potential of a given site, because other significant factors, such as the back effect on the flow of the deployment of turbines must also be taken into account. This study, in which the only limit introduced was of a minimum mean peak velocity of $1\,m\,s^{-1}$, comprises, for the UK, 42 ocean channels and 12 lagoon channels. However, the lagoon channels only account for less than 3% of the country's overall tidal resource as calculated here. Amongst the ocean channels, 8 of them account for 94% of the ocean-channel derived resource and 17 for 99% of it. Similarly 5 of the 12 lagoon channels account for 91% of the lagoon-channel derived resource. Following a similar pattern, 10 of the Black & Veatch 2011 sites account for 80% of the calculated tidal current potential resource. Direct comparisons undergone site by site between the current study and the 2011 Black & Veatch report cannot be realised,

because, although some of the sites share a common name and general geographical location, the outlines of the channel areas by and large do not correspond to one another. However, comments can be made with regards to the sites which were included in one of the study and neglected in the other. The areas corresponding to the sites named *South Jersey* and *East Casquets* rated fourth and fifth in the 2011 Black & Veatch report and were not included in this study because of the lack of an enclosed space to use as a channel and missing velocity data respectively. No sites were included in the 2011 Black & Veatch report at the locations of this study's *English Channel*, *North Channel - The Rhins*, *North Isle of Man*, and *Dover Strait,* respectively rated here at first, third, seventh and tenth in terms of their potential for the UK.

### 3.5.2 Ireland

Tables C.1 and C.2 include the potentials for the ocean and lagoon channels of Ireland respectively. Four sites located or in connection with Northern Ireland, *North Channel - The Rhins*, *West Islay*, *North Channel - Kintyre Peninsula* and *Strangford Lough*, have been included in the resource estimation for the UK and excluded from this section. One site located in a disputed area, *Lough Foyle*, was included in this section and excluded from the estimation for the UK. The Irish resource assessment includes 13 ocean channels and 8 lagoon channels. The total tidal current potential resource is estimated to amount $530\,MW$ $\pm 80\,MW$, with $290\,MW$ $\pm 40\,MW$ and $240\,MW$ $\pm 40\,MW$ originating from ocean and lagoon channels respectively. Similarly to the UK, most the resource for both ocean and lagoon channels comes from a small number of sites: 4 of the 13 ocean channels account for 91% of the ocean-derived resource while 4 of the 8 lagoon channels account for 89% of the lagoon-derived resource. Contrary to the UK, the lagoon channels' contribution to the overall resource, at 45%, is non-negligible. A comparison between the results obtained here and the ones presented in a 2004 report published by Sustainable Energy Ireland (SEI) is difficult as the methodologies differ greatly [52]. SEI produced an estimate of $26\,GW$ for the theoretical resource over an area including the Republic of Ireland and Northern Ireland. Part of the collected data came from Admiralty charts and tidal stream atlases which is similar to the data sources used here. However, the KE Flux model was employed over large stretches of water from the 10m depth contour line to the $12\,NMi$ territorial limit in all locations where the peak tidal velocity reached a minimum of $1.5\,ms^{-1}$. An evaluation of the Irish tidal current potential resource done over both the Republic of Ireland and Northern Ireland for this study produces a value of $8.5\,GW$ $\pm 1.3\,GW$, still well under the SEI estimate. No site by site comparison can be made as no details were given pertaining to the production of the $26\,GW$

value on a site by site basis.

### 3.5.3 Other Countries

A phenomenon of concentration of the resource within a small cluster of sites is observed throughout the various countries represented above and below. Such a phenomenon is an interesting occurrence as it confirms the suitability of specific sites regardless of their true potential value. This should, in turn, encourage further investments in order to determine accurately the physical characteristics of these particular channels, as it is required for good quality assessments of the available tidal resources.

**Canada** This study comprises 65 of the 191 sites from the original report [54], 64 ocean channels as shown in Table C.1 and 1 lagoon channel as presented in Table C.2. The largest and most prominent sites are included here as they were treated in details in the original report, providing thus the necessary data. An estimate of $110\,GW \pm 17\,GW$ for the potential of Canada based on a deficient but relevant sample of the possible sites was produced here. This is by far the largest potential of all the countries represented in this study with nearly three times the potential of the second country, the UK (although one should be mindful that most countries have non-exhaustive lists of channels included). As observed previously for the UK and Ireland, a few sites concentrate most of the resource with 5 sites accounting for 90% of the ocean-derived contribution. The input from the only lagoon channel included is substantial at about 8% of the total resource for the country. In comparison, the potential for the country determined in the original 2006 report from the Canadian Hydraulics Centre using the KE Flux model totalled approximately $42\,GW$ . This value corresponds to about 38% of the tidal current potential resource estimation produced here [54]. Both studies are in agreement with the location of the most promising sites within the Hudson Strait, although the specific potentials diverge greatly. It is interesting to notice that the top four Canadian sites are not only at the top of the Canadian table, they also represent the highest potentials of any sites located in any of the countries included in this study. However, these Hudson Strait channels could not possibly all function at the potentials presented here, because of the interactions bound to exist between nearby sites.

**Norway** This study comprises 50 of the 104 sites from the original paper [30], all of them ocean channels as seen in Table C.1. An estimate of $440\,MW \pm 66\,MW$ for the potential of Norway based on a deficient sample of the possible sites was produced here. The overall figure for the potential of the country is comparable to that of Ireland. Although such a value

is reached with more than double the number of sites as Ireland, 97% of the resource is attained within the same number of sites. As discussed previously for other countries, a small number of sites, here 12 sites, shares 90% of the overall resource. The original paper produced a noticeably larger value for the country's potential of $4.7\,GW$ via the KE Flux model. It represents approximately ten times the amount estimated in this study. Although some of the mid-range rating sites in the original paper are missing here, it is not enough to account for the large difference in the assessment estimates produced. Nevertheless, both studies are in agreement regarding the significance of the contribution from the *Moskenstraumen* site to the overall resource. It is found to contribute to almost one third, 27%, of the country's overall resource in the original paper, as 1 of 104 sites, against just over one third, 36%, of it in this study, as 1 of 50 sites.

**New Zealand** The assessment for New Zealand only comprises 5 sites, 4 ocean channels and 1 lagoon channel as shown in Tables C.1 and C.2. It is likely that other sites could contribute to the overall tidal potential resource of the country. However, it is doubtful that any other input would reach values larger than that of the *Foveaux Strait* for an ocean channel or *Kaipara Harbour* for a lagoon channel. With *Cook Strait*'s potential two orders of magnitude higher than that of any of these 2 channels, it is reasonable to expect the potential for the whole country to be around $16\,GW \pm 2.4\,GW$. Once more, the vast majority of the country's potential is concentrated in a few channels; here, we have one channel contributing to 95% of the overall resource.

**Australia** The assessment for Australia only comprises 4 sites, 2 ocean channels and 2 lagoon channels as shown in Tables C.1 and C.2. The overall tidal current potential resource estimation comes to $42\,GW \pm 6.3\,GW$. A thorough investigation of its coastline would be necessary to determine the true potential of the country. *King Sound*, on its own, is a site showing a significant potential, the highest of all the lagoon channels present in this study. The value of $34\,GW \pm 5.1\,GW$ is very close to the potential calculated for the entire UK. If its remote location on the North Western Australian coastline does not prove to be a large obstacle to the redistribution of the power gathered, such a site could be extremely valuable for the country's tidal power production. The potentials of 2 other sites included here, *Banks Strait* and *Broad Sound* could also constitute non-negligible contributions to the country's tidal power production.

**The USA** The assessment for the USA comprises 33 of the 206 sites in the original study [28], 24 ocean channels and 9 lagoon channels as shown in Tables C.1 and C.2. Only 4 of the ocean channels are situated outside the state of Alaska. In this study, the overall potential for the USA amounts to about $19\,GW \pm 3\,GW$, including about $600\,MW \pm 90\,MW$ from ocean channels and $16\,GW \pm 2\,GW$ from lagoon channels, largely dominated by the input from *Cook Inlet*. Most of the resource is once again concentrated in a small number of channels with 12 of the ocean ones adding up to 92% and 1 lagoon channel, *Cook Inlet,* to 89% of their respective contribution to the overall resource. Width and Depth data as presented in the original study were not used for the purpose of potential calculations because of the existing significant divergence between these and the data represented on nautical charts over the areas displaying the maximum flow rates on the Georgia Tech national database.[6] The potentials in the original study were calculated using the GC05 model, but as aforementioned using different data from the ones used here. It is therefore not surprising that the potentials produced for the ocean channels can show variations exceeding 15% between the two assessment works. Calculations in this study have generally led to lesser potentials for ocean channels than the ones produced in the original study. Comparable results were obtained for the lagoon channels including the one with the highest potential, *Cook Inlet,* for which the difference in potential is about 12% between the two studies.

**Singapore, Chile, Japan and Italy** This section regroups ocean channels mentioned in various studies [4, 20, 18] and from various parts of the world without meaningful connections apart from the limited number of them in each given country. Their tidal current resources are presented in Table C.1. Despite the sparseness of the channels taken into account in this study, the tidal current potential resources for Singapore, Chile or Japan as calculated here are noteworthy with $7.7\,GW \pm 1.2\,GW$, $4.9\,GW \pm 0.7\,GW$ and $2.2\,GW \pm 0.3\,GW$ respectively. The resource from the *Strait of Messina*, the only Italian channel included, is low in comparison with $20\,MW \pm 3\,MW$.

[6] The database has been made available at the following url http://www.tidalstreampower.gatech.edu/

Table 3.2: Upper limit of the tidal current potential resource for the 11 countries included in this study and percentages of the contribution that can be attributed to ocean and lagoon channels. Country codes can be found in the Nomenclature. When applicable, results produced in previous studies are also included.

| **Country Code** | **Upper Limit of Potential** | **Ocean Channels' Contribution** | **Lagoon Channels' Contribution** | **From Previous Studies** |
|---|---|---|---|---|
| UK | $37\,GW \pm 6\,GW$ | 97% | 3% | $39\,GW$ [3] |
| IR | $530\,MW \pm 80\,MW$ | 55% | 45% | $26\,GW$ [52] |
| CA | $110\,GW \pm 17\,GW$ | 93% | 7% | $42\,GW$ [54] |
| NW | $440\,MW \pm 66\,MW$ | 100% | 0% | $4.7\,GW$ [30] |
| NZ | $16\,GW \pm 2.4\,GW$ | 98% | 2% | |
| OZ | $42\,GW \pm 6.3\,GW$ | 10% | 90% | |
| US | $19\,GW \pm 3\,GW$ | 16% | 84% | $51\,GW$ [28] |
| SG | $7.7\,GW \pm 1.2\,GW$, | 100% | 0% | |
| CH | $4.9\,GW \pm 0.7\,GW$ | 100% | 0% | |
| JP | $2.2\,GW \pm 0.3\,GW$ | 100% | 0% | |
| IT | $20\,MW \pm 3\,MW$ | 100% | 0% | |

## 3.6 Conclusion

In order to complete the work required for this thesis, a large database of ocean and lagoon channels had to be built. Required data were gathered for 206 ocean and 33 lagoon channels originating from 11 and 6 different countries respectively. Both the ocean and lagoon channels showed significant range diversities with regards to their respective input variables. The V11 and Lagoon-V11 models were confirmed to be suitable and most appropriate for such a large scale assessment project. Contrastedly, the KE Flux model was shown to be unreliable for the purpose of producing tidal potential site assessments.

Despite making use of a wide range of sources to collect the required physical characteristics of the channels, no significant inconsistencies were identified across the countries' ranges of potential results, neither for ocean, nor for lagoon channels. Tidal current potential resource assessments were produced for the 11 countries included in the study and a summary of these results can be found in Table 3.2. Significantly high tidal resource estimates were produced for a number of countries. The assessments for the UK and Ireland were based on complete databases of channels and gave estimates of $37\,GW \pm 6\,GW$ and $530\,MW \pm 80\,MW$ respectively. These results are closed to values found in other studies for the UK, but well below previous estimates for Ireland.

The tidal current potential resource assessments for the other countries were based on partial databases of channels. Canada, with tidal current potential resource estimates of $110\,GW \pm 17\,GW$, was found to comprise a substantial number of the most promising sites, particularly in the Hudson Strait area. A previous country-wide resource estimation came up to less than half this figure. The assessment for Norway gave a low result of $440\,MW \pm 66\,MW$, approximately 10% of previously produced values for the country. Very few sites were included for New Zealand and Australia, yet the tidal current potential resource estimates for these countries of $16\,GW \pm 2.4\,GW$ and $42\,GW \pm 6.3\,GW$ respectively were substantially high. Australia includes the most promising lagoon site, *King Sound*. The USA's tidal current potential resource assessment produced figures of $19\,GW \pm 3\,GW$ with sites mainly located in Alaska. The remaining 4 countries, Singapore, Chile, Japan and Italy, included very few sites and their tidal current potential resources amounted to $7.7\,GW \pm 1.2\,GW$, $4.9\,GW \pm 0.7\,GW$ , $2.2\,GW \pm 0.3\,GW$ and $20\,MW \pm 3\,MW$ respectively.

# Chapter 4

# Pattern Investigations, Flow Reduction & Sensitivity Study

Having a large database of ocean and lagoon channels makes it possible to investigate the existence of potential patterns. Questions will be tested against potentially relevant parameters to determine whether trends exist. Acceptable flow reduction is a constraint which has been previously discussed [5, 10, 27], as the implantation of in-stream turbines in a channel alters the flow within. The range of flow reductions reached at peak power potentials, as well as the ranges of potential values that can be attained at given flow reductions will be examined. Comparisons between various flow reductions may help determine what could be acceptable from both productivity and environmental perspectives at a given site. The last section of this chapter will be focused on determining the key elements responsible for the accuracy of tidal current potential assessments. Knowing the variables which can most affect the potential values may help focus more of the resources used during the data gathering process specifically on the essential ones.

## 4.1 Discriminatory Parameters

In this section, potentially interesting non-dimensional quantities, pertaining to the channels included here and taken directly from the V11 equations or derived from their non-dimensionalisations, are tested against some of the results produced in this study to investigate and eventually expose existing patterns amongst both ocean and lagoon channels. Exploring patterns from the perspective of properties or characteristics of authentic channels as opposed to mathematical equations applicable to virtually any channel's attributes may undercover specific groupings or relationships rising from the factually limited range of chan-

nels found in nature. The non-dimensional parameters are tested against the V11 potentials of the channels in order to establish whether specific parameter values can help determine what might constitute a 'good' channel for the purpose of tidal power extraction. They are also tested against the distance between potentials calculated via the KE Flux model and the V11 model in order to expose the parameter values which may affect the quality of the KE Flux estimations. Non-dimensional quantities, which may act as discriminatory parameters, are now extracted directly from the V11 and Lagoon-V11 equations for future trend tests.

### 4.1.1 Non-Dimensional Quantities from Equations

A set of potentially interesting non-dimensional quantities can be directly extracted from the equations used in V11 potential calculations. These parameters include for ocean channels: a quantity representative of the resistance to the flow in the undisturbed channel, $\lambda_0$[1], a quantity indicative of the flow dynamics, $\alpha$, and a quantity representative of the resistance to the flow of water due to the natural conditions and the farm implantation, $\lambda_{peak}$. The lagoon channels' parameters comprise: a lagoon parameter, $\beta_L$, and variations of the three parameters mentioned above, $\lambda_0$[2], $\alpha^*$, and $\lambda_{peak}$. In the ensuing two subsections, their distributions across the ranges of channels will be examined and the existence of potential patterns will be explored.

#### Distribution of Channels

**Ocean Channels** Figure 4.1a presents the distribution of ocean channels according to their $\alpha$-values. It shows a large range of values spread over more than three orders of magnitude. The flow dynamics is affected by the geometry of the channel, its width, depth and length, as well as the tidal frequency and transport scale. The tidal frequency is being kept constant for all channels with an assumed semi-diurnal tide domination. A high transport-scale value and low width, depth and length values for a given channel indicate it is dominated by bottom friction through a large $\alpha$-value, whereas the opposite ranges signify a channel in which inertia controls the flow dynamics. Because the channels represent a sample of what can be found in nature, a spread close to a normal distribution is to be expected. One would anticipate a concentration of channels around mid-range $\alpha$-values and less channels around more extreme $\alpha$-values. This can be seen on Figure 4.1a, where 70%

[1] $\lambda_0$ is defined by the following equation for ocean channels: $\lambda_0 = \frac{8}{3\pi}\frac{\alpha}{}\frac{L}{h}C_D$.

[2] $\lambda_0$ is defined by the following equation for lagoon channels: $\lambda_0 = \frac{8\alpha^*}{3\pi}\frac{L}{h}C_D$.

of the channels have mid-range $\alpha$-values between 1 and 100. Despite lower percentages of 10% and 19%, channels from the margins have non-negligible representations. Indeed, 21 channels have $\alpha$-values below 1, including one with an $\alpha$-value lower than 0.1, and 40 have $\alpha$-values above 100, including two with $\alpha$-values higher than 1,000. We can conclude from the distribution of $\alpha$-values across the channels that a significant range of various channels' flow dynamics is well represented here and could thus be used to explore related underlying patterns.

Figure 4.1b and Figure 4.1c present the distributions of ocean channels according to their $\lambda_0$-values and $\lambda_{peak}$-values respectively. For ocean channels, $\lambda_{peak}$ is a linear expression derived from $\lambda_0$. Both figures show a large spread of values over more than three orders of magnitudes. The resistance to the flow of water is dependent on the bottom friction, the flow dynamics, as well as the length and the depth of a given channel. The bottom friction, represented here by the drag coefficient for background bottom friction based on the channel's horizontal area, $C_D$, is being kept constant for all channels in the absence of better information. Therefore, the only three variables which affect a channel's $\lambda$-values are its flow dynamics $\alpha$, its length $L$, and its depth $h$. The influence of the flow dynamics means that high $\lambda$-values would tend to represent shallow and narrow sites, whereas low $\lambda$-values would suggest deeper and wider sites. As per the $\alpha$-values aforementioned, mid-range $\lambda$-values are well represented on Figure 4.1b, with 39% of them in the 1 to 10 range and 23% in the 10 to 100 range. More extreme $\lambda$-values, over 100, although less represented, still account for a non-negligible number of 16 sites. The relatively strong representation of channels with $\lambda$-values below 1 suggests a good number of rather deep and wide sites, of comparatively short lengths, which could explain the somewhat lower percentage of very low $\alpha$-values found on Figure 4.1a. Taking into consideration the criterion of substantially fast-flowing water, it is interesting to note this relatively high number of deeper and wider sites. Indeed, one could have expected that achieving minimum flow velocity requirements would have induced more of a shortage of such candidates. However, what is observed here is more of a deficiency in narrower and shallower channels with higher $\lambda$-values. Such a result could be explained by the fact that most studies used as sources of channel inputs included minimum depth requirements, thus eliminating these deemed too-shallow and possibly narrow sites.

**Lagoon Channels** Although the definitions of the non-dimensional quantities extracted from the V11 equations for lagoon channels vary from the ones for ocean channels, the same ranges of values have been chosen for the bar graphs on Figure 4.2 to potentially enable some comparison. The first quantity, $\alpha^*$, like $\alpha$ aforementioned, gives some indication of

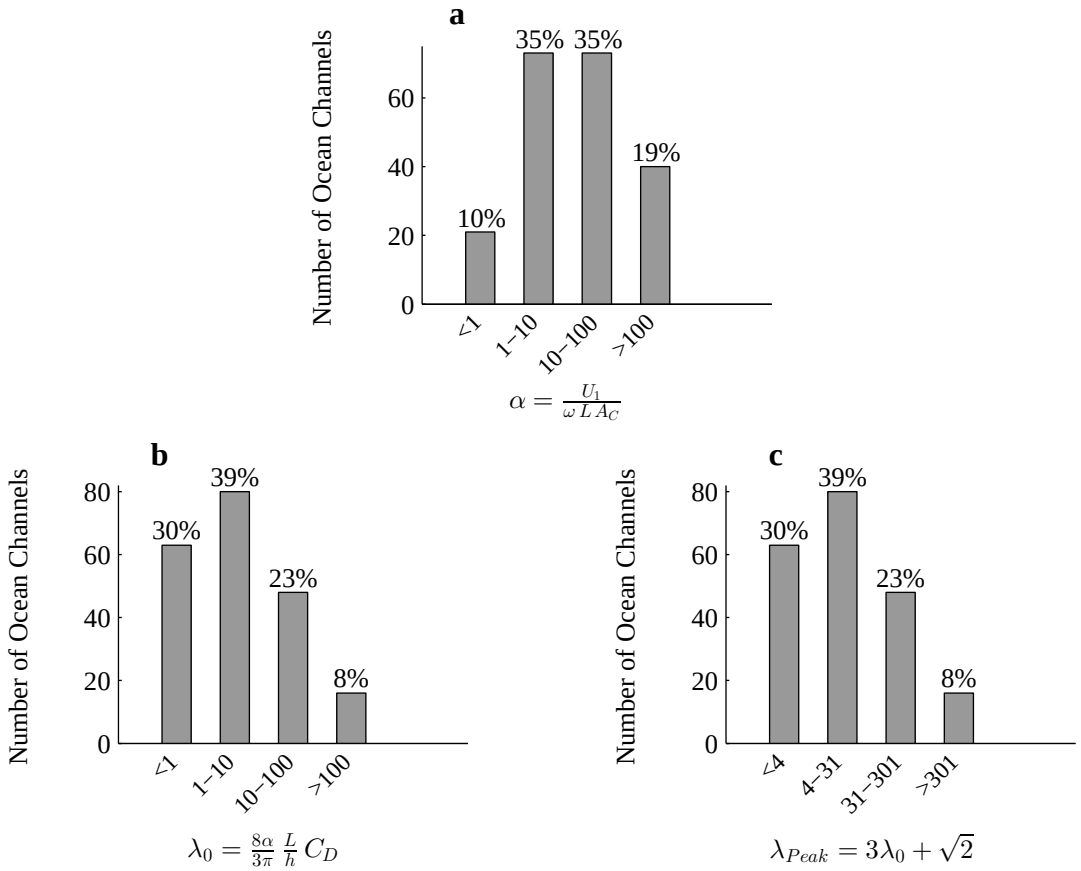


Figure 4.1: Distribution of ocean channels according to dimensionless quantities extracted from the V11 equations, comprised of $\alpha$, $\lambda_0$ and $\lambda_{peak}$ .

a channel's flow dynamics. Its distribution across the lagoon channels is shown on Figure 4.2a. It spreads over more than three orders of magnitude and 6 channels have an $\alpha^*$-value of more than 1,000, including 2 above 10,000. Although most of the channels, 48%, can be found in a mid-range bracket of $\alpha^*$-values, between 10 and 100, the channel distribution leans towards higher $\alpha^*$-values. No channel is found with $\alpha^*$-values below 1 and only 12% of the channels have $\alpha^*$-values in the 1 to 10 bracket. On the other hand, the interval grouping all the channels with $\alpha^*$-values above 100 comprises 39% of the lagoon channels. With the acceleration due to gravity, $g$, and the tidal frequency, $\omega$, fixed for all channels, the only two variables which have an influence on $\alpha^*$ are the length of the channel, $L$, and the tidal elevation in the ocean, $\eta_{01}$. Owing to the tidal elevation in the ocean being invariably negligible in comparison to the length of a channel and the extra weight carried by the length in Equation 2.14 from its exponent, it arises that the distribution of the channels on Figure 4.2a indicates that lagoon channels with shorter lengths are more represented than longer

ones.

Figure 4.2b presents the distribution of lagoon channels according to their $\beta_L$-values. It shows lagoon channels spread over four orders of magnitude with regards to $\beta_L$-values. The intervals representing $\beta_L$-values below 10, spanning between 10 and 100 and between 100 and 1,000 are very closely distributed and comprise 36%, 27% and 33% of the channels respectively. Only a single channel displays a $\beta_L$-value over 1,000. In accordance with Equation 2.15, the $\beta_L$ quantity tends to represent wide, deep and short channels ending in small lagoons through higher values and narrow, shallow and long channels ending in large lagoons through lower values. The good representation of channels with low $\beta_L$-values can be explained by the corresponding physical attributes aforementioned. These characteristics fit what could constitute strong candidates for high flow velocities, through substantial restrictions stemming from their narrowness and shallowness as well as by virtue of potentially large tidal prisms brought about by large lagoon surface areas.

Figure 4.2c presents the distribution of lagoon channels according to their $\lambda_0$-values. It shows lagoon channels distributed according to $\lambda_0$-values spanning over three order of magnitudes. The range of $\lambda_0$ -values between 10 and 100 comprises the majority of the channel, with 67%. The rest of them are divided either side with 12% in the 1 to 10 interval and 21% in the 100 or more bracket. The drag coefficient for background bottom friction based on the channel's horizontal area, $C_D$, as well as the acceleration due to gravity, $g$, and the tidal frequency, $\omega$, emanating from the $\alpha^*$ found in the equation characterising $\lambda_0$, are being kept constant for all channels. Therefore, the three variables influencing $\lambda_0$-values are the tidal elevation in the ocean, $\eta_{01}$, the length $L$, and the depth $h$, of the channels. High $\lambda_0$-values would tend to represent short and shallow channels with high tidal ranges, whereas low $\lambda_0$-equivalents would tend to indicate long and deep channels with lower tidal ranges. Figure 4.2c shows a stronger representation of the mid-range channels. Shorter and shallower channels are more likely to display the high flow velocities we are seeking here. However, these 'too-shallow' channels would not meet the minimum depth requirements introduced in many of the original reports and therefore have already been discarded. This depth argument might explain the poorer representation of sites with $\lambda_0$-values under 10.

Figure 4.2d presents the distribution of lagoon channels according to their $\lambda_{peak}$-values. It is strongly influenced by the contribution from $\beta_L$ in Equation 2.13. The $\lambda_{peak}$-values are spread over three orders of magnitude leaning towards the higher ones, with 52% of the channels in the over 1,000 interval. The mid-range bracket of 100 to 1,000 comprises 30% of the channels, while only 18% of the channels are found in the 10 to 100 interval, the lowest interval with at least one channel within. Patterns with regards to the V11 and Lagoon-V11

potentials reached and the quality of the KE Flux estimations are now examined.

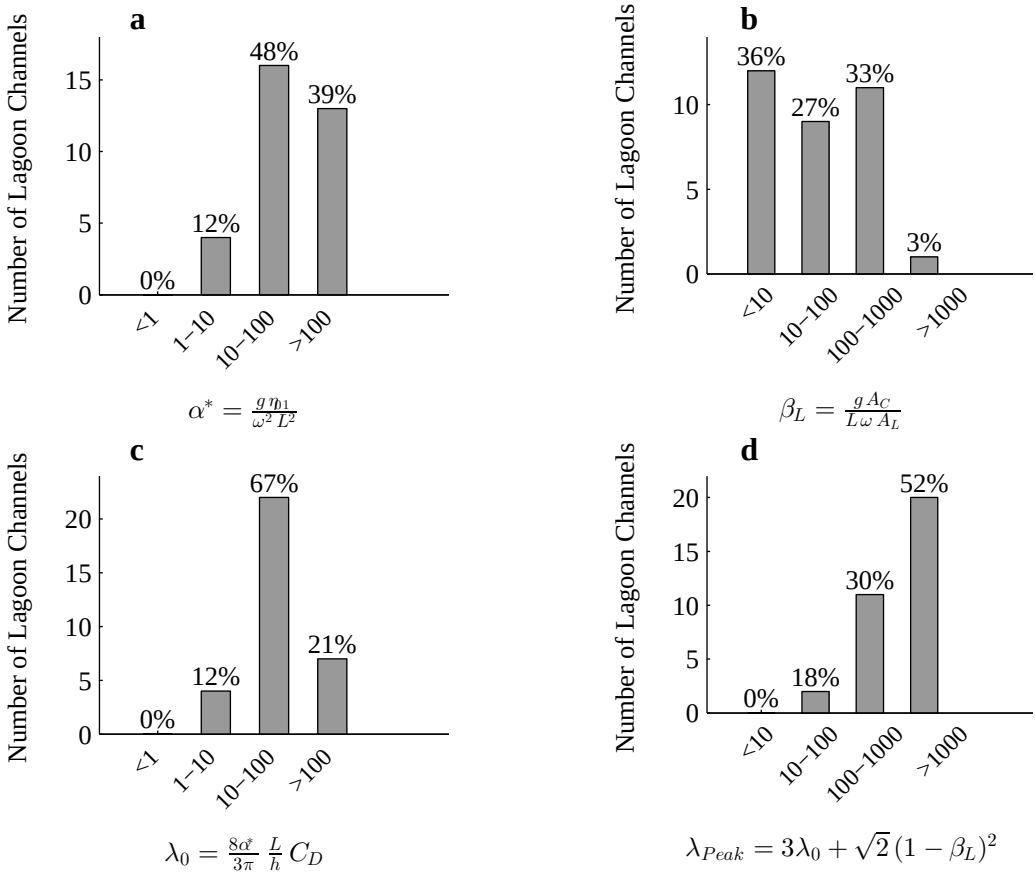


Figure 4.2: Distribution of lagoon channels according to dimensionless quantities extracted from the V11 equations, comprised of $\alpha^*$, $\beta_L$, $\lambda_0$ and $\lambda_{peak}$ .

**Investigation of Possible Patterns** The tests conducted between the non-dimensional quantities and the V11 or Lagoon-V11 potentials did not uncover any latent relationship, neither for the ocean nor for the lagoon channels. Similarly, the tests undertaken between the non-dimensional quantities and the quality of the KE Flux estimations[3] did not highlight an existing trend between any of them for ocean channels. On the other hand, the same tests conducted for lagoon channels did expose an existing trend in relation to the lagoon parameter $\beta_L$. This relationship is presented on Figure 4.3 and offers the results discussed thereafter. These results may only be valid if the definitions of the variables required to calculate the potentials are kept the same as the ones used in this study.

[3]The quality of the KE Flux estimations is determined through the relative error between the KE Flux and the V11 or Lagoon-V11 upper tidal current potential limit estimates for ocean and lagoon channels respectively.

- For $\beta_L < 2.5$:

  The KE Flux produces estimates of the potentials higher than the ones generated by the Lagoon-V11 model. The lower the value of $\beta_L$, the larger the relative error between the KE Flux and the Lagoon-V11 potential estimations.

- For $2.5 < \beta_L < 30$:

  The KE Flux produces estimates of the potentials lower than the ones generated by the Lagoon-V11 model. The relative error between the KE Flux and the Lagoon-V11 potential estimations is less than 100%.

- For $\beta_L > 30$:

  The KE Flux produces estimates of the potentials lower than the ones generated by the Lagoon-V11 model. The relative error between the KE Flux and the Lagoon-V11 potential estimations is more than 90%.

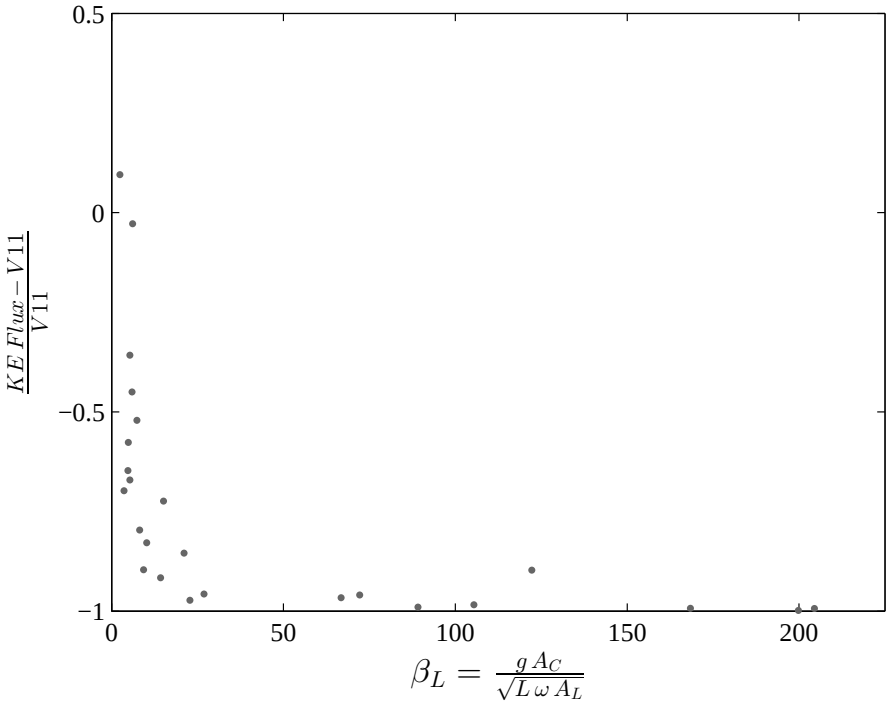


Figure 4.3: Variation in the quality of the KE Flux estimates with regards to the lagoon parameter $\beta_L$ for lagoon channels.

The non-dimensional quantities used here as potential discriminatory parameters were directly extracted from the V11 and Lagoon-V11 equations. New dimensionless parameters can be derived from the non-dimensionalisations of the V11 and Lagoon-V11 equations.

This process is followed next and further possible latent relationships are then researched in relation to these new parameters.

### 4.1.2 Non-Dimensional Parameters from Equations

The dimensionless quantities used in the previous section appear in their exact same form in the V11 and Lagoon-V11 equations. A new set of non-dimensional parameters can be derived from the non-dimensionaliations of the V11 and Lagoon-V11 equations. The same process can then be followed to investigate whether trends exist between these parameters and the potentials reached or the quality of the KE Flux estimations. The non-dimensionalisation processes for the V11 and Lagoon-V11 equations are now developed.

**Non-Dimensionalisation of Equations** In this section, dimensional analysis is conducted in order to determine a list of relevant dimensionless parameters and investigate the existence of patterns between the values associated with these parameters and a range of questions related to the results previously obtained.

The variables used to determined the potentials of ocean and lagoon channels are different, therefore two separate non-dimensionalisations will be developed below: one for ocean channels and one for lagoon channels. Buckingham theorem is used to work out the number of dimensionless parameters needed to, in concert, fully represent each system and to construct them.

**Ocean Channels** The variables number four and are: the average depth of the channel, $h$, its average width, $w$, its length, $L$, and the mean peak velocity of its along-channel flow, $v$. The parameters number four and are: the acceleration due to gravity, $g$, the volumetric mass density, $\rho$, the tidal frequency, $\omega$, and the drag coefficient for background bottom friction based on the channel's horizontal area, $C_D$. The relevant physical dimensions are mass $M$, length $L$ and time $T$. Therefore, according to the theorem of Buckingham the system has five dimensionless quantities, which, in concert, describe it in its entirety.

We form the product:

$$v^{\alpha} L^{\beta} h^{\gamma} w^{\delta} C_D^{\varepsilon} g^{\zeta} \omega^{\eta} \rho^{\theta}$$

using the variables and parameters aforementioned and substitute the dimensions to generate

the following product:

$$\left(\frac{L}{T}\right)^{\alpha} L^{\beta} L^{\gamma} L^{\delta} 1^{\varepsilon} \left(\frac{L}{T^2}\right)^{\zeta} \left(\frac{1}{T}\right)^{\eta} \left(\frac{M}{L^3}\right)^{\theta}$$

Following the condition of non-dimensionalisation, we obtain the following system of linear equations for the exponents:

$$\begin{cases} \alpha+\beta+\gamma+\delta+\zeta-3\theta=0 \\ -\alpha-2\zeta-\eta=0 \\ \theta=0 \\ \varepsilon = free\ parameter \end{cases}$$

which can be simplified to:

$$\begin{cases} \alpha+\beta+\gamma+\delta+\zeta=0 \\ \alpha+2\zeta+\eta=0 \\ \varepsilon=1 \end{cases}$$

We have a system of 2 linear equations with 6 unknowns. Thus, 4 unknowns can be treated as free parameters.
Let us choose:

$$\begin{array}{llll} (\alpha,\eta,\beta,\delta)= & (1,0,0,0)\rightarrow & \zeta=-\frac{1}{2}, & \gamma=-\frac{1}{2} \\ & (0,1,0,0)\rightarrow & \zeta=-\frac{1}{2}, & \gamma=\frac{1}{2} \\ & (0,0,1,0)\rightarrow & \zeta=0, & \gamma=-1 \\ & (0,0,0,1)\rightarrow & \zeta=0, & \gamma=-1 \end{array}$$

respectively giving rise to the five dimensionless quantities:

$$\frac{v}{\sqrt{gh}}, \omega\sqrt{\frac{h}{g}}, \frac{L}{h}, \frac{w}{h}, C_D$$

**Lagoon Channels** The variables number five and are: the average depth of the channel $h$, its average width $w$, its length $L$, the average surface area of the lagoon, $A_L$, and the amplitude of the tidal elevation in the ocean, $\eta_{01}$. The parameters number four and are: the acceleration due to gravity, $g$, the volumetric mass density, $\rho$, the tidal frequency, $\omega$, and the drag coefficient for background bottom friction based on the channel's horizontal area, $C_D$. The relevant physical dimensions are mass $M$, length $L$ and time $T$. Therefore, according to the theorem of Buckingham the system has six dimensionless quantities, which, in concert, describe it in its entirety.

We form the product:

$$L^{\alpha}\, h^{\beta}\, w^{\gamma}\, \eta_{01}^{\delta}\, A_L^{\varepsilon} C_D^{\zeta}\, g^{\eta}\, \omega^{\theta}\, \rho^{\iota}$$

using the variables and parameters aforementioned and substitute the dimensions to generate the following product:

$$L^{\alpha} L^{\beta} L^{\gamma} L^{\delta} \left(L^2\right)^{\varepsilon} 1^{\zeta} \left(\frac{L}{T^2}\right)^{\eta} \left(\frac{1}{T}\right)^{\theta} \left(\frac{M}{L^3}\right)^{\iota}$$

Following the condition of non-dimensionalisation, we obtain the following system of linear equations for the exponents:

$$\begin{cases} \alpha+\beta+\gamma+\delta+2\varepsilon+\eta-3\iota=0 \\ 2\eta+\theta=0 \\ \iota=0 \\ \zeta=free\ parameter \end{cases}$$

which can be simplified to:

$$\begin{cases} \alpha+\beta+\gamma+\delta+2\varepsilon+\eta=0 \\ 2\eta+\theta=0 \\ \zeta=1 \end{cases}$$

We have a system of 2 linear equations with 7 unknowns. Thus, 5 unknowns can be treated as free parameters.

Let us choose:

$$
\begin{aligned}
(\alpha,\beta,\gamma,\delta,\eta) = \quad & (0,-\frac{3}{2},-1,1,-\frac{1}{2}) \rightarrow \quad \varepsilon = 1, \quad \theta = 1 \\
& (0,\frac{1}{2},0,0,-\frac{1}{2}) \rightarrow \quad \varepsilon = 0, \quad \theta = 1 \\
& (1,-1,0,0,0) \rightarrow \quad \varepsilon = 0, \quad \theta = 0 \\
& (0,-1,1,0,0) \rightarrow \quad \varepsilon = 0, \quad \theta = 0 \\
& (1,0,0,1,0) \rightarrow \quad \varepsilon = 0, \quad \theta = 0
\end{aligned}
$$

respectively giving rise to the six dimensionless quantities:

$$
\frac{\eta_{01} A_L \omega}{w h^{3/2} \sqrt{g}}, \omega\sqrt{\frac{h}{g}}, \frac{L}{h}, \frac{w}{h}, \frac{\eta_{01}}{h}, C_D
$$

The first of the dimensionless quantities can be simplified using the definitions of a few physical characteristics of the system. The simplification is done below.
The tidal prism, $\Omega$, can be expressed as follows:

$$
\Omega = 2\,\eta_{01} A_L
$$

The volume transport, $U$, can in turn be expressed using the tidal prism expression as:

$$
U = \frac{\Omega}{T/2} = \frac{2\,\Omega}{T} = \frac{4\,\eta_{01} A_L}{T}
$$

The volume transport can also be expressed as a function of the along-flow velocity, $v$, and the cross-sectional area of the channel, $A_C$:

$$
U = v A_C = v w h
$$

Combining the two previous expressions for the volume transport gives a new expression for the along-flow velocity:

$$
v w h = \frac{4\,\eta_{01} A_L}{T} \Longrightarrow v = \frac{4\,\eta_{01} A_L}{T\,w h}
$$

From $\omega = \dfrac{2\pi}{T}$, the first dimensionless quantity can be rewritten as:

$$
\frac{\eta_{01} A_L \omega}{w h^{3/2} \sqrt{g}} = \frac{2\pi\,\eta_{01} A_L}{T\,w h \sqrt{g\,h}}
$$

Substituting the new expression for the along-flow velocity in the first dimensionless quantity's expression gives:

$$\frac{\eta_{01} A_L \omega}{w h^{3/2} \sqrt{g}} = \frac{2\pi \eta_{01} A_L}{T w h \sqrt{g h}} = \frac{\pi}{2} \frac{v}{\sqrt{gh}}$$

We end up with a scaled expression of the Froude number. The scaling coefficient of $\frac{\pi}{2}$ matters little here and the six relevant dimensionless quantities for lagoon channels can be rewritten as the five previously found for the ocean channels $\frac{v}{\sqrt{gh}}, \omega\sqrt{\frac{h}{g}}, \frac{L}{h}, \frac{w}{h}, C_D$ with the addition of $\frac{\eta_{01}}{h}$.

**Distribution of Channels**

**Ocean Channels** Figure 4.4 presents the distribution of the ocean channels according to the parameters determined through the dimensional analysis of the V11 equations pertinent to ocean channels, with the exception of $C_D$. The drag coefficient for background bottom friction based on the channel's horizontal area is excluded from this section because, in the absence of better information, it was fixed for all channels to 0.0025. Its distribution across all channels is therefore of no interest.

The Froude number encompasses information relative to the flow velocity and the depth of the channels. High Froude numbers are indicative of fast-flowing shallow sites, whereas low Froude numbers suggest slow-flowing deeper sites. The ocean channels included in this study have been chosen for the relatively high velocities of the flows within, which would be expected to ensue relatively high Froude numbers. However, the results presented on Figure 4.4a show a large majority of channels with low Froude numbers. Indeed, more than 95% of the ocean channels have Froude numbers below 0.6. These low Froude number values could indicate a trend of relatively deep depths for the given flow velocities for most of the ocean channels included in the study.

The non-dimensional parameter $\omega\sqrt{\frac{h}{g}}$ is representative of the existing depth range across the sites, because depth is the only varying quantity within its definition. Indeed, both the acceleration due to gravity, $g$, and the tidal frequency, $\omega$, have fixed values for all the channels. This parameter carries no other particular meaning on its own and the existence of any trend in relation to it should be discussed in terms of a depth relationship (see Figure 4.4b).

The $\frac{L}{h}$ parameter is partly indicative of the geometrical characteristics of the channels. The higher its value, the longer a channel is relative to its depth and vice versa. It is distributed, as shown on Figure 4.4c, across five orders of magnitude with values spreading from approximately 5.6 to 18,000. However, close to 94% of the channels belong to the $10^1$ or $10^2$

orders of magnitude. The inherent quality of such a parameter is the fact that it represents real channels' geometries. A concentration of channels around centre values is therefore not surprising as it reflects what is expected to be found in nature. It shows that ocean channels tend to be one hundred to several thousands times longer than they are deep.

Similarly to the previous parameter, $\frac{w}{h}$ is also partly indicative of the geometrical characteristics of the channels. The higher its value, the wider a channel is relative to its depth and vice versa. It is distributed, as presented on Figure 4.4d, across four orders of magnitude with values spreading from approximately 2.3 to 1,800. However, close to 91% of the channels belong to the $10^1$ or $10^2$ orders of magnitude including about 64% within the $10^1$ order of magnitude. Thus, ocean channels tend to be several tens of times wider than they are deep.

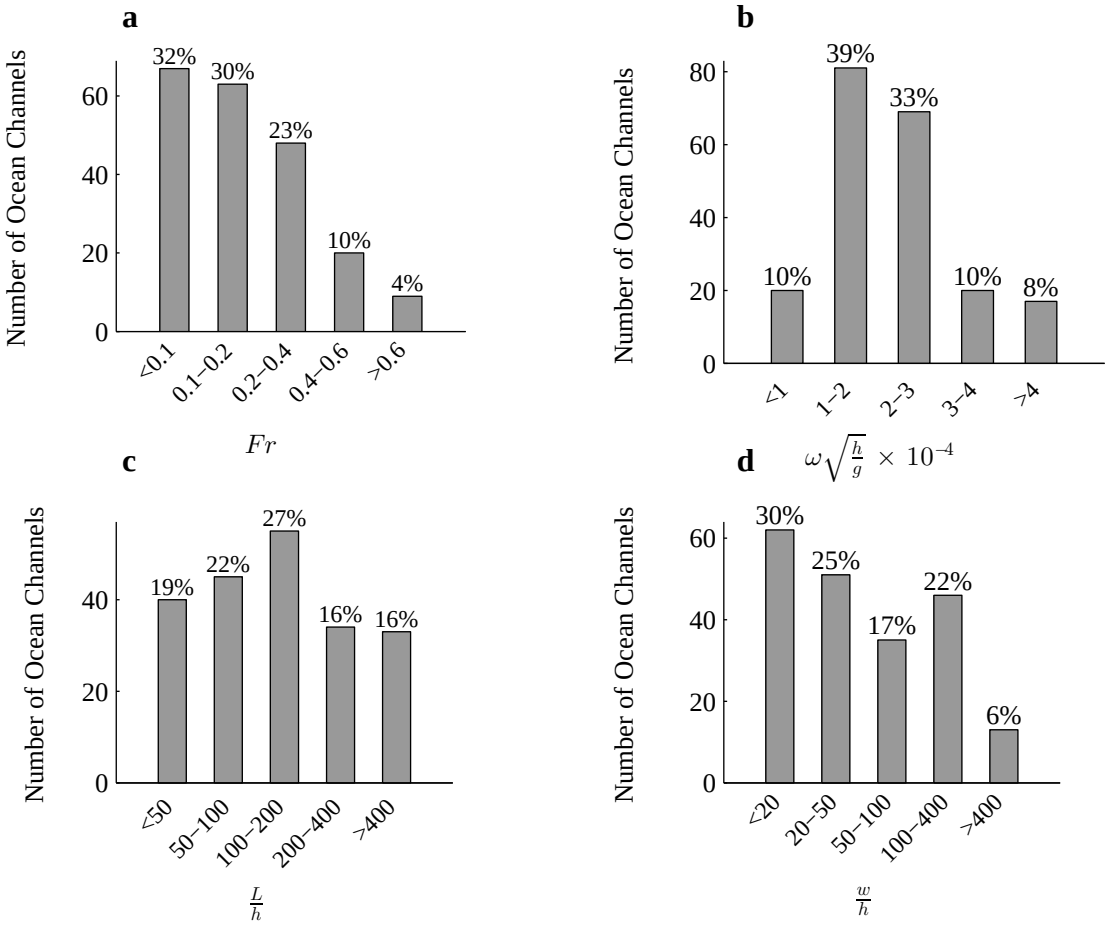


Figure 4.4: Distribution of ocean channels according to four of the non-dimensional parameters generated from the non-dimensionalisation of the V11 equations consisting of $Fr$, $\omega\sqrt{\frac{h}{g}}$, $\frac{L}{h}$ and $\frac{w}{h}$.

**Lagoon Channels** Figure 4.5 presents the distribution of the lagoon channels according to the parameters determined through the dimensional analysis of the V11 equations pertinent to lagoon channels. Four of those five parameters correspond to the ocean parameters, whose distribution across ocean channels was discussed in the previous section. $C_D$ is not included here as was explained earlier in this section.

Similarly to ocean channels, the Froude number values for the lagoon channels are in majority very low with about 88% of them under 0.2, as can be seen on Figure 4.5a. This result could indicate, in much the same way as the ocean channels, a trend of relatively deep depths for the flow velocities of most of the lagoon channels taken into account in this study.

The non-dimensional parameter $\omega\sqrt{\frac{h}{g}}$ is the same as the one found for the ocean channels and similarly only varies with the depths of the channels considered. Any pattern uncovered involving this parameter would echo a latent trend relative to the depths of the channels (see Figure 4.5b).

The $\frac{L}{h}$ parameter values span over three orders of magnitude from approximately 11 to 1,200 as shown on Figure 4.5c. Two thirds of the channels have $\frac{L}{h}$-values within the $10^2$ order of magnitude. Thus, lagoon channels tend to be several hundreds times longer than they are deep. In comparison to ocean channels, lagoon channels tend to be shorter for a given depth.

The $\frac{w}{h}$ parameter values are spread over three orders of magnitude from about 13 to 1,900 as can be seen on Figure 4.5d. More than half of the channels have $\frac{w}{h}$-values within the $10^1$ order of magnitude. Thus, lagoon channels tend to be some ten of times wider than they are deep. This result aligns well with the width to depth comparison undergone through the $\frac{w}{h}$ parameter for ocean channels.

The $\frac{\eta_{01}}{h}$ parameter is specific to lagoon channels. It is equivalent to $\frac{\eta_{01} A_L}{h A_L}$ which represents the fraction of the water volume in the lagoon contributing to half of the flow from the ebb or flood tide. For a tidal elevation in the ocean negligible in comparison to the water depth of the lagoon, it represents the tidal flushing. Figure 4.5e presents the spread of values for this ratio over the lagoon channels. For approximately 42% of the channels, the tidal elevation in the ocean adds up to less than 10% of the average channel depth. Just over one third of the channels have tidal elevations representing 10% to 20% of their average depths. About 21% of the channels have tidal elevations $\eta_{01}$ adding up to more than 20% of the channels' average depths. The proportion of water in the lagoon renewed through each tidal cycle does not necessarily give a good indication of the tidal prism or the velocity of the flow, not without additional information regarding the lagoon surface area and the cross-sectional

area of the channel. Thus, no meaningful conclusion can be drawn from the spread of values discussed above.

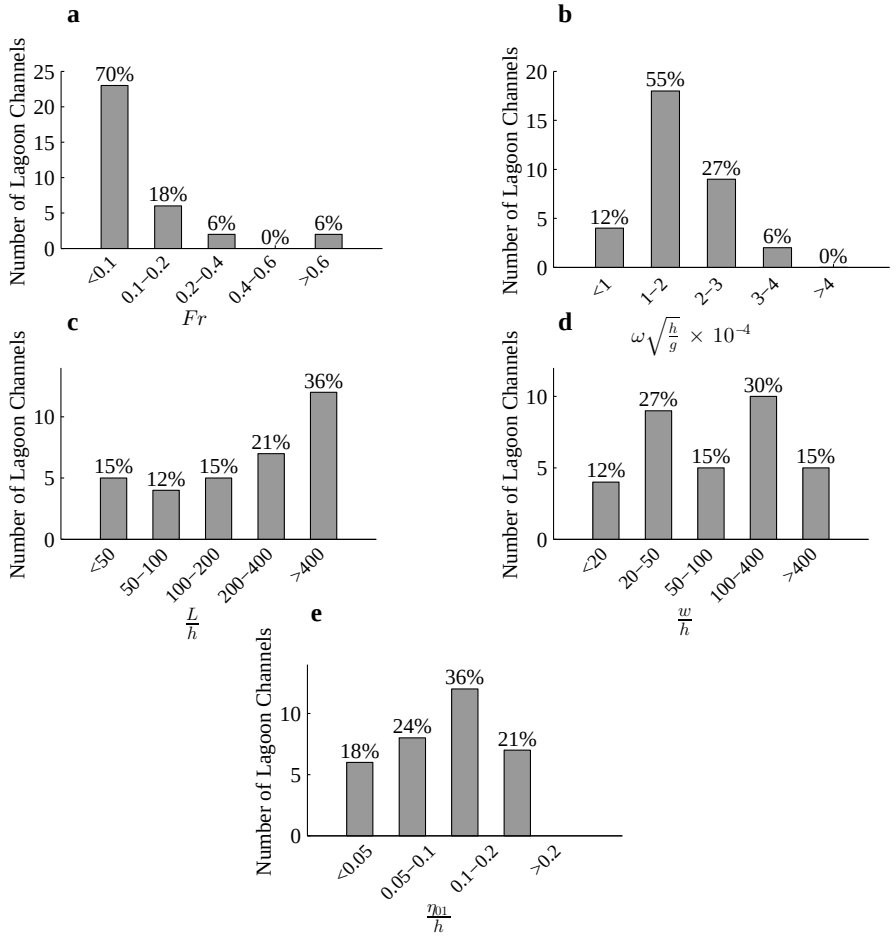


Figure 4.5: Distribution of lagoon channels according to five of the non-dimensional parameters generated from the non-dimensionalisation of the V11 equations consisting of $Fr$, $\omega\sqrt{\frac{h}{g}}$, $\frac{L}{h}$, $\frac{w}{h}$ and $\frac{\eta_{01}}{h}$.

Patterns with regards to the V11 and Lagoon-V11 potentials reached and the quality of the KE Flux estimations are now examined.

**Investigation of Possible Patterns** The tests conducted between the non-dimensional parameters and the V11 and Lagoon-V11 potentials did not uncover any latent relationship, neither for the ocean nor for the lagoon channels. Similarly, the tests undertaken between

the non-dimensional parameters and the quality of the KE Flux estimations[4] did not highlight an existing trend between them for lagoon channels. On the other hand, the same tests conducted for ocean channels did expose an existing trend in relation to the parameter $\frac{L}{h}$. This relationship is presented on Figure 4.6 and offers the results discussed thereafter. These results may only be valid if the definitions of the variables required to calculate the potentials are kept as per the descriptions made in this study.

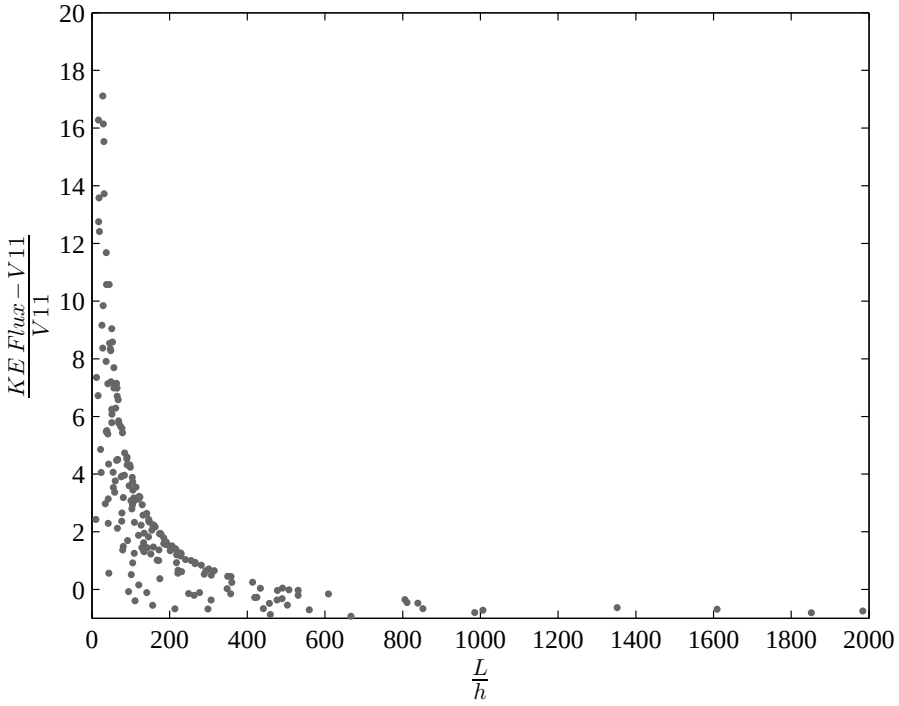


Figure 4.6: Variation in the quality of the KE Flux estimates with regards to the discriminatory parameter $\frac{L}{h}$ for ocean channels.

- For $\frac{L}{h} > 500$:

  The KE Flux produces estimates of the potentials lower than the ones generated by the V11 model. The relative error between the KE Flux and the V11 potential estimations is likely to increase with increasing values of $\frac{L}{h}$.

- For $400 < \frac{L}{h} < 500$:

  The KE Flux produces estimates of the potentials likely to be lower than the ones generated by the V11 model. The relative error between the KE Flux and the V11 potential estimations is less than 100%.

[4]The quality of the KE Flux estimations is determined through the relative error between the KE Flux and the V11 or Lagoon-V11 upper tidal current potential limit estimates for ocean and lagoon channels respectively.

- For $200 < \frac{L}{h} < 400$:

  The KE Flux produces estimates of the potentials likely to be higher than the ones generated by the V11 model. The relative error between the KE Flux and the V11 potential estimations can be over 100%.

- For $50 < \frac{L}{h} < 200$:

  The KE Flux produces estimates of the potentials very likely to be higher than the ones generated by the V11 model. The relative error between the KE Flux and the V11 potential estimations is very likely to be more than 100%.

- For $\frac{L}{h} < 50$:

  The KE Flux produces estimates of the potentials higher than the ones generated by the V11 model. The relative error between the KE Flux and the V11 potential estimations is likely to increase with decreasing values of $\frac{L}{h}$.

The next section looks into links between flow reduction values and the power potentials that can be achieved.

## 4.2 Flow Reduction

The implantation of a tidal farm at a given site has the potential to significantly alter its natural state through power extraction, therefore limitations specifically relating to the reduction in the flow velocity are expected to be put in place for most channels. The notion of acceptable flow reduction was introduced in previous resource assessments or models [5, 10, 27]. This section discusses the flow reductions reached at peak power potentials, as well as the effect on the potentials of restricting the allowed reduction in the flow velocities to 5% to 40% of the natural flow speeds in 5% increments.

For better clarity the following convention has been adopted when discussing flow reductions. The flow reduction, which corresponds to the ratio of the volume transport at a given power potential over the volume transport in the undisturbed channel, $\frac{U_0}{U_{0UD}}$, will always be given as a fraction of 1, whereas the equivalent reductions in the flow velocity will always be given as a percentage. For example, a flow reduction of 0.95 corresponds to a 5% reduction in the flow velocity.

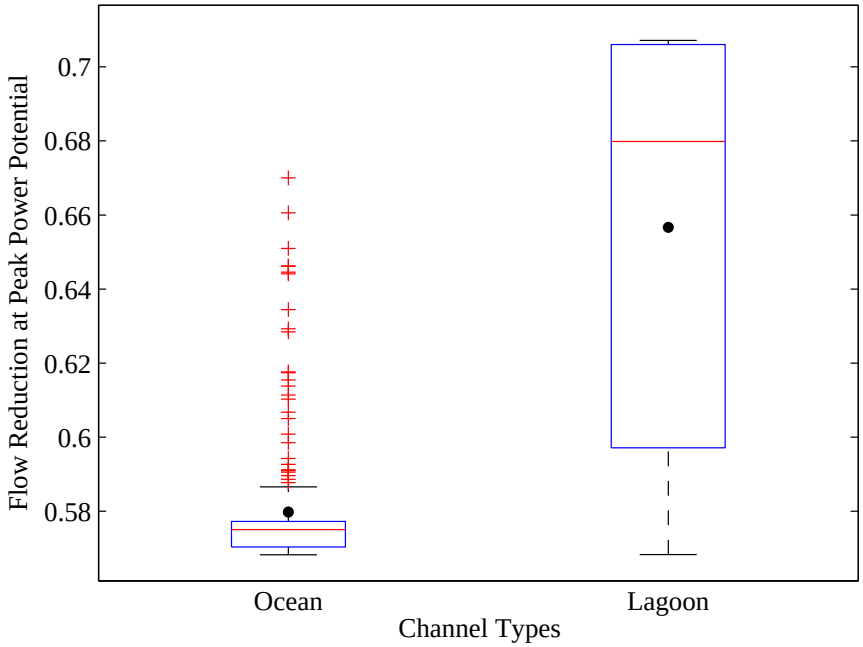


Figure 4.7: Distribution of flow reductions at peak power potentials for both ocean and lagoon channels.

### 4.2.1 Flow Reduction at Peak Power Potential

The range of flow reductions at peak power potentials for both the ocean and lagoon channels included in this study is presented on Figure 4.7. Ignoring the outliers, the spread of flow reductions is substantially more restricted for ocean channels than it is for lagoon ones, with ranges of 0.56 to 0.59 and 0.56 to 0.71 respectively, and this, despite ocean channels having more than 6 times the amount of sites. The outliers bring the maximum flow velocities attained at peak power potential for the ocean channels to 0.67 of the natural flow speeds, which is very close to the lagoon channels' mean value of 0.66. The mean value for the flow reduction of ocean channels, 0.58, indicates that on average the current velocity is reduced by 42%, which corresponds to previously reported values [27]. Lagoon channels tend to have lesser reductions in flow velocities at peak power potentials than ocean channels.

Tests were conducted between the non-dimensional quantities and parameters and the flow reductions at peak power potentials. These did not uncover any latent relationship for lagoon channels. On the other hand, they did expose an existing trend for ocean channels in relation to the Froude number, $Fr$. This relationship is presented on Figure 4.8 and offers the results discussed thereafter. These results may only be valid if the definitions of the variables

required to calculate the power potentials are kept as per the descriptions made in this study.

- For $Fr > 0.2$:

  The reduction in the flow velocity at peak power potential is between 42% and 44%.

- For $0.1 < Fr < 0.2$:

  The reduction in the flow velocity at peak power potential is very likely to be between 42% and 44%.

- For $0.075 < Fr < 0.1$:

  The reduction in the flow velocity at peak power potential is likely to be between 42% and 44%.

- For $0.05 < Fr < 0.075$:

  The reduction in the flow velocity at peak power potential is likely to be less than 42%.

- For $Fr < 0.05$:

  The reduction in the flow velocity at peak power potential is less than 42%.

The power efficiencies that can be achieved at given flow reductions are now investigated.

### 4.2.2 Power Efficiencies at given Flow Reductions

The ranges of power efficiencies, here the ratios of achieved power potentials, for ocean channels at flow reductions, $\frac{U_0}{U_{0UD}}$, varying from 0.95 to 0.6 over the peak power potentials are presented on Figure 4.9. The larger increases in power efficiencies over the 5% diminution increments in the current speeds are realised for the highest flow reductions, i.e. lowest reductions in flow velocities in comparison to the natural regime. The power efficiency for a reduction of 5% in the flow velocity averages at 26% and increases by 21 points to 47% with the flow speed reduced by 10%, then by 17 points to 64% with the flow speed reduced by 15%. The subsequent increases in power efficiency are further and further diminished producing mean values of 77%, 87%, 94%, 98% and just under 100% for 20%, 25%, 30%, 35% and 40% reductions in flow velocities respectively. The spread of the power efficiencies for a given flow reduction including the outliers decreases with larger reductions in the flow speeds.

The ranges of power efficiencies for lagoon channels at flow reductions varying from 0.95 to 0.6 are presented on Figure 4.10. The larger increases in power efficiencies over the

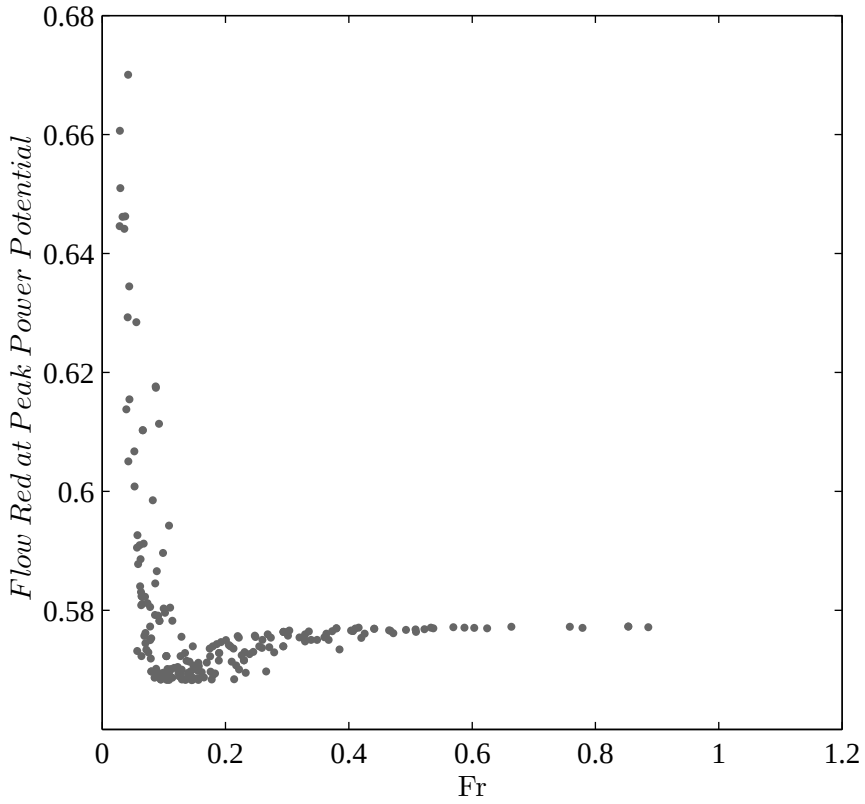


Figure 4.8: Variation in the flow reduction at peak power potential with regards to the Froude number for ocean channels.

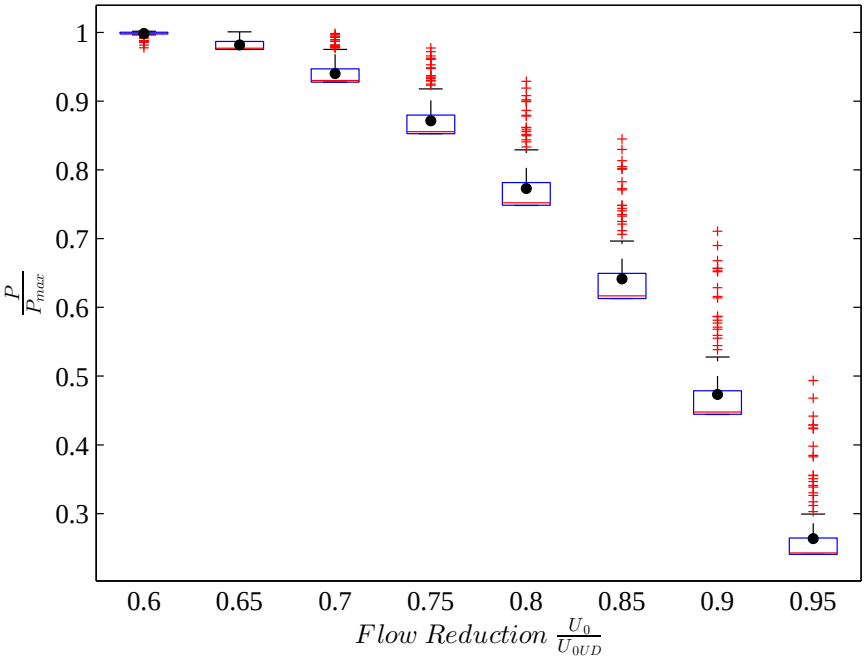


Figure 4.9: Distributions of power efficiencies at given flow reductions of 0.95 to 0.6 in 0.05 increments for ocean channels.

5% diminution increments in the current speeds are realised for the highest flow reductions, i.e. lowest reductions in flow velocities in comparison to the natural regime. The power efficiency for a reduction of 5% in the flow velocity averages at 46% and increases by 21 points to 67% with the flow speed reduced by 10%, then by 13 points to 80% with the flow speed reduced by 15%. The subsequent increases in power efficiencies are further and further diminished producing mean values of 90%, 95%, 98%, 99% and just under 100% for 20%, 25%, 30%, 35% and 40% reductions in flow velocities respectively. The spread of the power efficiencies for a given flow reduction tends to decrease with lower flow reductions until the 35% reduction in flow speeds is attained, from which it proceeds to increase.

Tests were conducted between the non-dimensional quantities and parameters and the power efficiencies at a flow reduction of 0.9. These exposed existing trends for both ocean and lagoon channels in relation to the Froude number, $Fr$. These relationships are presented on Figures 4.11 and 4.12 and offer the results discussed thereafter. These results may only be valid if the definitions of the variables required to calculate the power potentials are kept as per the descriptions made in this study.

The following results correspond to the ocean channels as shown on Figure 4.11.

- For $Fr > 0.22$:

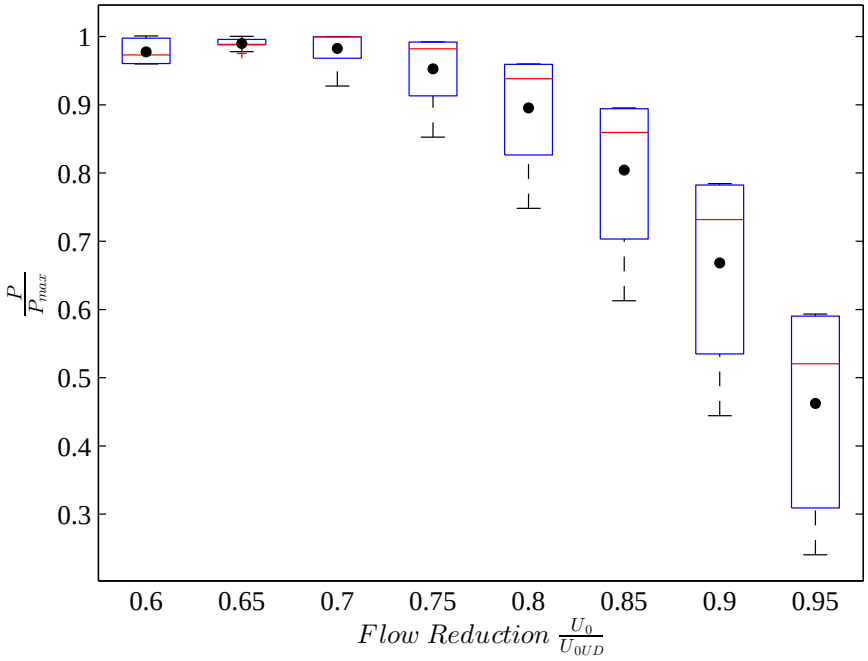


Figure 4.10: Distributions of power efficiencies at given flow reductions of 0.95 to 0.6 in 0.05 increments for lagoon channels.

The potential achieved for a 10% reduction in the flow velocity is less than 45% of the peak power potential. The achieved potentials tend towards an asymptotic value of about 44% of the peak power potential for larger Froude numbers.

- For $0.15 < Fr < 0.22$:

  The potential achieved for a 10% reduction in the flow velocity is likely to be less than 45% of the peak power potential.

- For $0.1 < Fr < 0.15$:

  The potential achieved for a 10% reduction in the flow velocity is likely to be more than 45% of the peak power potential. The achieved potentials tend to be larger for lower Froude numbers.

- For $Fr < 0.1$:

  The potential achieved for a 10% reduction in the flow velocity is more than 45% of the peak power potential.

The following results correspond to the lagoon channels as shown on Figure 4.12.

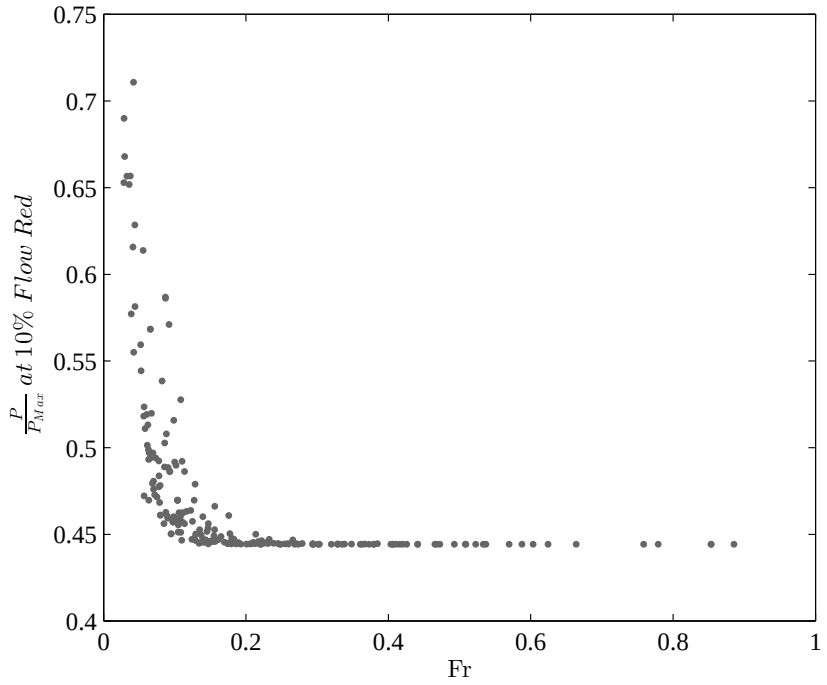


Figure 4.11: Variation in the power efficiency obtained at 10% flow reduction with regards to the Froude number for ocean channels.

- For $Fr > 0.26$:

  The potential achieved for a 10% reduction in the flow velocity is less than 46% of the peak power potential. The achieved potentials tend towards an asymptotic value of about 44% of the peak power potential for larger Froude numbers.

- For $0.08 < Fr < 0.26$:

  The potential achieved for a 10% reduction in the flow velocity is generally between 46% and 67% of the peak power potential. The achieved potentials tend to be larger for lower Froude numbers.

- For $0.027 < Fr < 0.08$:

  The potential achieved for a 10% reduction in the flow velocity is generally between 67% and 78% of the peak power potential. The achieved potentials tend to be larger for lower Froude numbers.

- For $Fr < 0.027$:

  The potential achieved for a 10% reduction in the flow velocity is more than 78% of the peak power potential. The achieved potentials tend to be larger for lower Froude numbers.

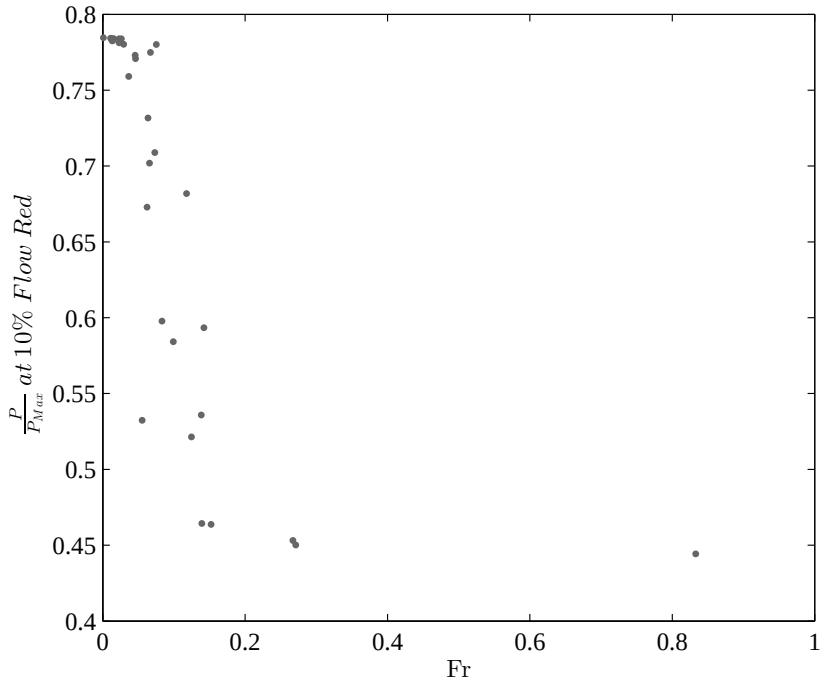


Figure 4.12: Variation in the power efficiency obtained at 10% flow reduction with regards to the Froude number for lagoon channels.

Knowing the variables which can most affect the potential values may help focus more of the resources used during the data gathering process for the purpose of obtaining good quality data, specifically for these essential ones. The next section examines the key data for ocean and lagoon channels through a sensitivity study relative to the input variables.

## 4.3 Sensitivity Study

In this section, a sensitivity study is conducted with regards to the input variables for both ocean and lagoon channels. After the key variables are identified, tests are run in order to determine if variations in the potentials from input variable alterations can be linked to any of the discriminatory parameters previously produced.

### 4.3.1 Sensitivity Study Relative to Input Variables

Because of the limited information regarding the margins of error in the collected data, it is impossible to give a meaningful estimation of the uncertainties on the results presented in this study. However, the impact on the potential of altering each of the input variable or parameter can be studied, allowing to highlight the input data which must be gathered

accurately to ensure good resource estimations can be produced.

**Ocean Channels** The sensitivity of the V11 potentials to each of the input variables as well as the parameter $C_D$ representing background friction is presented on Figure 4.13. Three of the variables, the average width, $w$, the average depth, $h$, and the channel length, $L$, as well as the parameter $C_D$, have a relatively equivalent impact on the potentials calculated using the V11 model. A 10% increase or decrease in the value of any one of them results in an augmentation or diminution in the potential of at most 11% respectively. Similarly, variations of 20% ensue differences of up to 21% in the potentials. The relationships between the potentials and two of these initial variables, the average width, $w$, and the channel length, $L$, and the final product of the series of calculations, the V11 potential, appear to be linear. Indeed, a given relative variation in the width or length results in the very same relative variation in the potential. The relationships between the other two initial variables, the average depth, $h$, and the parameter, $C_D$, seem to be more complex. However, the effect on the potentials from varying any of the two is at worst almost exactly what would be observed had the relationships been linear. The variable which has the largest impact on the V11 potential value for a given ocean channel is the mean peak velocity, $v$. Indeed, an increase of 10% in the mean peak velocities results in augmentations between 20% and 33% for the corresponding potentials, averaging at approximately 28%. An increase of 20% in the mean peak velocity values produces potentials augmented by 42% to 73% with an average of about 61%. The reductions in potentials observed for 10% or 20% decreases in the mean peak velocities are slightly less in comparison with 19% to 28% and 36% to 49%, and averages of 24% and 44% respectively. The impact of the mean peak velocity on the quality of the potentials produced is substantial and accurate site assessments would require improved velocity measurements at least for the key candidates, which represent a large fraction of the available resource.

**Lagoon Channels** Calculations of the potentials of lagoon channels can be affected by the quality of their five initial input variables, the average width, $w$, the average depth, $h$, the length, $L$, the tidal elevation in the ocean, $\eta_{01}$, and the lagoon surface area, $A_L$, as well as the parameter $C_D$ as shown on Figure 4.14. There exists a greater variation in the results obtained for each individual variable or parameter than that observed for ocean channels. Changes in the widths of 10% to 20% result, at worst, in equivalent changes in the potential values, but on average those changes are all less than 5%. Similarly, 10% to 20% alterations in the lagoon surface areas ensue, at worst, equivalent variations in the potential values. However, contrary to the widths, the averages for the lagoon surface areas tend to be just under the 10%

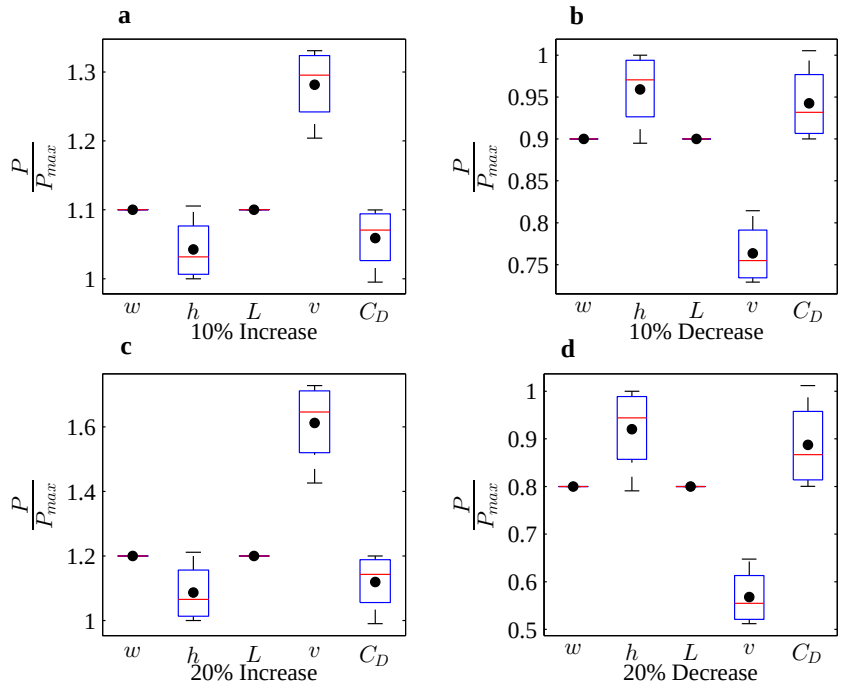


Figure 4.13: Distributions of the power efficiency calculated from altered input variables or parameter for ocean channels. Input variables or parameter are individually increased by 10% (a) and 20% (c) and decreased by 10% (b) and 20% (d).

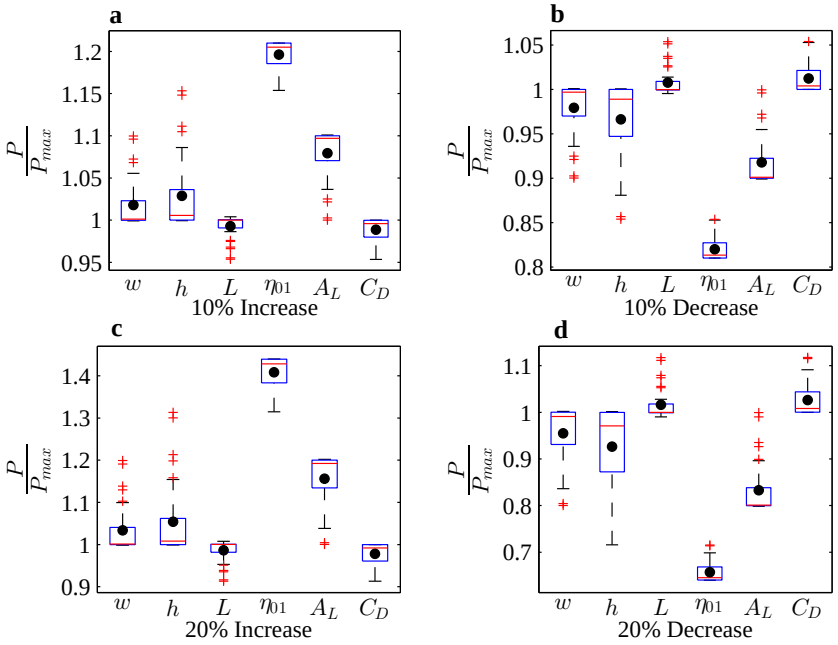


Figure 4.14: Distributions of the power efficiency calculated from altered input variables or parameter for lagoon channels. Input variables or parameter are individually increased by 10% (a) and 20% (c) and decreased by 10% (b) and 20% (d).

or 20% values. Increases and decreases in the length or parameter $C_D$ produce lesser relative diminutions and augmentations of the potentials respectively. Both have mean variations of less than 3% for all cases. The last two variables, the depth $h$ and the tidal elevation $\eta_{01}$ are responsible for the larger differences observed in the potential values. Although alterations in the depth values of 10% or 20% can lead to up to 16% and 32% variations in the potentials respectively, the worst averages are much lower at 4% and 8% respectively. On the other hand, changes in tidal elevations of 10% and 20% can lead to variations in the potentials of up to 21% and 44% and averages as high as 20% and 41% respectively. The tidal elevation in the ocean appears to be the variable with the most influence on the potential calculations for lagoon channels. The effect on the potential of a relatively small variation in the tidal elevation is likely to be substantial. Accurate site assessments would require improvements in its measurement at least at the sites identified as strong candidates for tidal power extraction. The impact of each of the input variables and parameter $C_D$ on the potentials is now tested against the discriminatory parameters previously derived to investigate the possible existence of patterns between them.

### 4.3.2 Sensitivity Study & Discriminatory Parameters

Tests were conducted between the non-dimensional quantities and parameters and the relative change in potentials when a 10% increase in each of the input variables, individually, is applied. These tests exposed existing trends for both ocean and lagoon channels in relation to the Froude number, $Fr$. These relationships are presented on Figures 4.15 and 4.16 and offer the results discussed thereafter. These results may only be valid if the definitions of the variables required to calculate the potentials are kept as per the descriptions made in this study.

**Ocean Channels** The seemingly linear relationships between the potential and the average width, $w$, or the length, $L$, of the ocean channels ensue that no trend was found with regards to either of these two input variables. As shown on Figure 4.15, trends with regards to the other two input variables, the average depth, $h$, and the mean peak velocity, $v$, as well as the background friction parameter $C_D$ were revealed. It appears that the higher the Froude number of a channel, the greater the effect of the variable alteration on the potential when applied to the velocity or $C_D$. On the contrary, greater Froude numbers tend to minimise the effect of depth variation on the potential. All three trends seem to tend towards asymptotes, reached for all of them for a Froude number over approximately 0.4. For the depth graph (Figure 4.15a), the asymptote corresponds to the potential at the initial depth. For the velocity graph (Figure 4.15b), the asymptote corresponds to a potential augmented by 33% from its original value. For the background friction parameter graph (Figure 4.15c), the asymptote corresponds to a potential augmented by 10% from its starting value.

**Lagoon Channels** As shown on Figure 4.16, trends with regards to the five input variables and the background friction parameter $C_D$ were revealed. It appears that the higher the Froude number of a channel, the greater the effect of the variable alteration on the potential when applied to the width, the depth or the length. On the contrary, greater Froude numbers tend to minimise the effect of the variable alteration on the potential when applied to the lagoon surface area, tidal elevation or background friction parameter. All six trends may tend towards asymptotes, but the relatively small amount of data makes it impossible to assert.

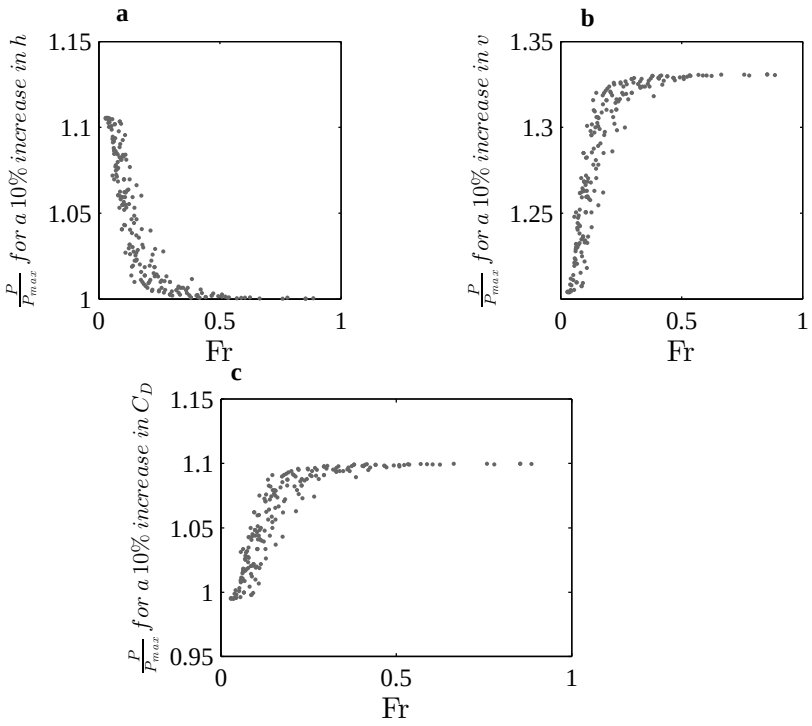


Figure 4.15: Variations in power efficiencies obtained for 10% increases in $h$, $v$ or $C_D$ with regards to the Froude number for ocean channels.

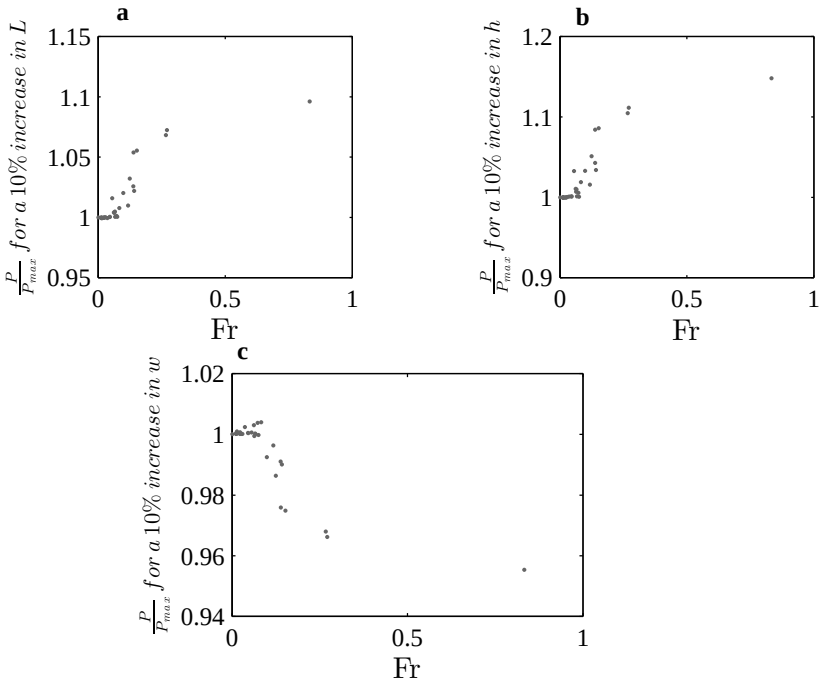


(a) Variations in power efficiencies obtained for 10% increases in $h$, $v$ or $w$ with regards to the Froude number for lagoon channels.

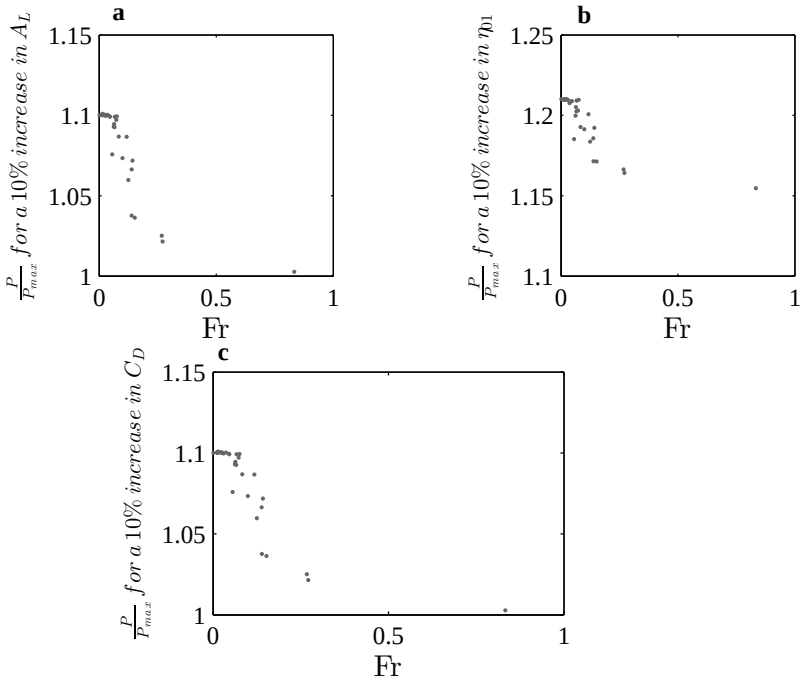


(b) Variations in power efficiencies obtained for 10% increases in $A_L$, $\eta_{01}$ or $C_D$with regards to the Froude number for lagoon channels.

Figure 4.16

## 4.4 Conclusion

Non-dimensional quantities, including $\alpha$, $\lambda_0$ and $\lambda_{peak}$ and $\alpha*$, $\beta_L$, $\lambda_0$ and $\lambda_{peak}$, were extracted directly from the V11 and V11-Lagoon equations respectively to be used as discriminatory parameters. The non-dimensionalisations of the V11 and Lagoon-V11 equations also allowed to derive a series of supplementary discriminatory parameters , comprising $\frac{v}{\sqrt{gh}}$, $\omega\sqrt{\frac{h}{g}}$, $\frac{L}{h}$, $\frac{w}{h}$, $C_D$ for ocean channels and with the addition of $\frac{\eta_{01}}{h}$ for lagoon channels. These discriminatory parameters were tested against the V11 and Lagoon-V11 potentials of the channels, but no pattern was found. Further investigating was done regarding potential relationships between these discriminatory parameters and the quality of the KE Flux estimations. The quality of the KE Flux estimates was determined to be related to the parameter $\frac{L}{h}$ for the ocean channels, while its quality was found to be connected to the discriminatory parameter $\beta_L$ for the lagoon channels.

At peak power potential, the flow reduction values range from 0.56 to 0.59 and 0.56 to 0.71 for ocean and lagoon channels respectively. Tests were conducted between the discriminatory parameters determined from V11 and Lagoon-V11 and the flow reductions at peak power potentials. These tests showed the existence of a pattern with regards to the Froude number for ocean channels and no pattern for lagoon ones. Unsurprisingly, more of a channel's potential can be realised when less restriction pertaining to the flow reduction is put in place. For every increment of 5% in the allowed reduction in the flow velocity until about 40%, the power potential of the channel increases. The biggest increases are found at the highest flow reductions, i.e. when going from 0.95 to 0.9 or 0.9 to 0.85. These increases are generally substantial and can make for significant improvements in the power potentials attained.

The sensitivity study shows that the mean peak velocity, $v$, and the average oceanic tidal elevation, $\eta_{01}$, are the input variables which affect the most the accuracy of the potentials of ocean and lagoon channels respectively. Their influence is quite significant. Accurate measurements for these variables would substantially improve the quality of the resource estimations produced. Tests were conducted between the discriminatory parameters and the power efficiencies attained when each of the input variables and the parameter $C_D$ are altered by 10%, one at a time. These tests showed that trends exist for both ocean and lagoon channels in relation to the Froude number.

# Chapter 5

# Realisable Tidal Current Power Outputs for Ocean Channels

Upper tidal current potential limits represent the available potentials of channels, but for a given channel not all of the available potential can veritably be extracted. Losses are inevitably incurred from mixing in the turbulent wake behind the turbines and between the rotor and grid connection or caused by the drag from supporting structures. Additionally, constraints imposed to preserve the environment or the various usages made of the waterways would be expected to be put in place. These constraints would likely ensue flow reduction or channel blockage restrictions, reducing further the realisable tidal current power at a given site. Determining the realisable output of a given channel gives a more realistic overview of the power that can actually be produced and whether such a figure warrants the deployment of turbines.

In this Chapter, the new method used will firstly be introduced. Realisable powers from two different farm configurations with low blockage ratios will then be calculated for four different flow reductions and the results compared to determine the one with the best yield. The particulars of this 'best' farm configuration will then be analysed. Finally, the realisable outputs for each of the countries included here will be produced. The new method used to produce the ocean channels' realisable powers is now discussed.

## 5.1 Method

The model used in this chapter, the V10 model [56], enables the refinement of the potentials of ocean channels produced in Chapter 3 by taking into account additional parameters. These parameters include mixing and electro-mechanical losses as well as the partial filling of the

channels' cross-sections by means of given blockage ratios for each of the tidal farms' rows. Although the V10 model does allow for the consideration of the drag from support structures, this option has been ignored in this chapter. The required physical characteristics of the channels are the same as the ones needed for the V11 model, thus the data and data sources used here are identical to the ones used in Chapter 3.

Parameters $\rho$, $g$ and $\omega$, as well as $C_D$, which is still treated as a parameter, have been kept unaltered from Chapter 3. The V10 model enables to make allowance for existing constrictions in the channels. However, no information was collected with regards to such geometrical specificities, thus the presence and characteristics of any constriction have been ignored here. The parameter pertaining to the blade area of the turbines has been fixed at $400\,m^2$, which is closely related to the blade area of the largest commercially operating turbine, the Seagen marine current turbine [17].

The pool of channels for this current Chapter was reduced due to the introduction of new requirements. With the blade area of the turbines fixed at $400\,m^2$ and calculations anticipated to apply to tidal farms, i.e. numerous turbines working in concert, a minimum cross-sectional area corresponding to four turbines, $1600\,m^2$, has been introduced. As a results 34 ocean channels were discarded from this part of the study, including 12 from Canada, 21 from Norway and 1 from the UK. In order to make a significant contribution to the tidal power demand, farms need to generate electricity in the order of 100s of $MW$ [61], therefore a minimum depth requirement of $15\,m$ was established. A further 36 ocean channels did not meet this depth threshold and were discarded, including 11 from Canada, 1 from Ireland, 9 from Norway, 7 from the UK, 7 from the USA and 1 from Japan. In order for the across-channel flow to homogenise in between two rows of the tidal farm, a substantial separation between the rows of turbines is required. This minimum separation length was fixed at approximately the length of 10 turbines to $200\,m$. None of the 136 ocean channels left had too-small a length to meet this requirement, therefore no more channel was discarded. Table 5.1 shows the number of ocean channels left as well as the number of ocean channels removed due to the new requirements aforementioned for each of the countries represented in this study and listed in alphabetical order.

The environmental impact of farm implantations continues to be a concern in this Chapter and limits pertaining to the flow reductions will be imposed. The flow alterations, deemed potentially acceptable, and being considered in the subsequent sections include 5%, 10%, 15% and 20% reductions in the flow velocities in comparison to the natural flow speeds.[1] The

[1]For better clarity the same convention introduced in Chapter 4 has been adopted when discussing flow reductions. The flow reduction, which corresponds to the ratio of the volume transport at a given power potential

Table 5.1: Number of ocean channels meeting the cross-sectional area, depth and length requirements for each of the countries included in this study listed in alphabetical order. The number of ocean channels lost to the new requirements is also given. Country codes can be found in the Nomenclature.

| Country Code | Number of Ocean Channels | Number of Lost Ocean Channels |
|---|---|---|
| OZ | 2 | 0 |
| CA | 41 | 23 |
| CH | 3 | 0 |
| IR | 12 | 1 |
| IT | 1 | 0 |
| JP | 1 | 1 |
| NW | 20 | 30 |
| NZ | 4 | 0 |
| SG | 1 | 0 |
| UK | 34 | 8 |
| US | 17 | 7 |
| TOTAL | 136 | 70 |

realisable outputs than can be attained for two different farm configurations with values of less than 20% blockage ratio imposed to all of their rows and at four different flow reductions is discussed next.

## 5.2 Realisable Power Potential Estimations

The potentials for each of the channels included in this study were produced in Chapter 3. The methods used to produce these results ignore unavoidable losses and added constraints. These figures thus represent the upper bounds for the potentials of the channels and the amounts of power than can ultimately be extracted are to be lower. The realisable power of a channel takes into account these added losses and constraints. It therefore better represents the extractable power at a given site. In this section, two different farm configurations, which

over the volume transport in the undisturbed channel, $\frac{U_0}{U_{0UD}}$, will always be given as a fraction of 1, whereas the equivalent reduction in the flow velocity will always be given as a percentage. For example, a flow reduction of 0.95 corresponds to a 5% reduction in the flow velocity.

limit the blockage ratio to a maximum of 20% for each of their rows, are investigated at four different flow reductions to determine the one with the better yield. The particulars of this farm configuration are then examined.

### 5.2.1 At targeted 20% Blockage Ratio

The channels considered for the deployments of tidal farms are, for most of them, waterways in use for commercial or recreational activities. Taking into consideration other users ensue that only a fraction of the channels' cross-sections may be occupied by tidal turbines, leaving the rest free to be made used of for other purposes [60]. In this section, a maximum blockage ratio, $\varepsilon$, of 0.2 is targeted for a maximum of the farm rows. The following process was followed in order to determine the appropriate turbine arrangement for a given farm in a given channel. An initial farm set-up comprised of 1 row and a 0.2 blockage ratio was used and the corresponding flow reduction was calculated. If the flow reduction was beyond the threshold value, the channel was discarded. If not, an additional row with the same 0.2 blockage ratio was added and the flow reduction re-calculated, until the threshold was surpassed. The blockage ratio of the last row was then adjusted, i.e. lowered to meet the given flow reduction requirement. The resulting farms are comprised of series of one or more rows at a blockage ratio of exactly 20% and one last row of a given blockage ratio below or equal to 20%.

Figure 5.1 presents the distribution of the ocean channels considered in this Chapter according to their flow reduction when fitted with one row of turbines filling 20% of their cross-section, which corresponds to the initial farm set-up described above — the simplest one. More than a quarter of the channels, 26%, have flow velocities reduced by more than 20% in this simplest farm configuration. These 35 channels, including 11 from Canada, 3 from Ireland, 1 from Italy, 1 from New Zealand, 8 from Norway, 7 from the UK, 3 from the USA and 1 from Japan, have to be discarded from Section 5.2.1 because the 0.2 blockage ratio target cannot be attained without ignoring the previously set environmental considerations pertaining to acceptable flow reductions. The other 102 channels can be considered for at least the calculations related to the 20% reduction in flow velocities. 23 channels, 17%, have flow velocities reduced by 15% to 20% in the simplest farm configuration. These channels can only be considered for farm configurations resulting in 20% reduction in flow speeds and include 7 channels from Canada, 2 from Ireland, 5 from Norway, 5 from the UK and 4 from the USA. 29 channels, 21%, have flow velocities reduced by 10% to 15% in the basic farm configuration used. These channels can be considered for farm configurations resulting in both 15% and 20% reductions in flow velocities and include 14 channels from Canada, 1

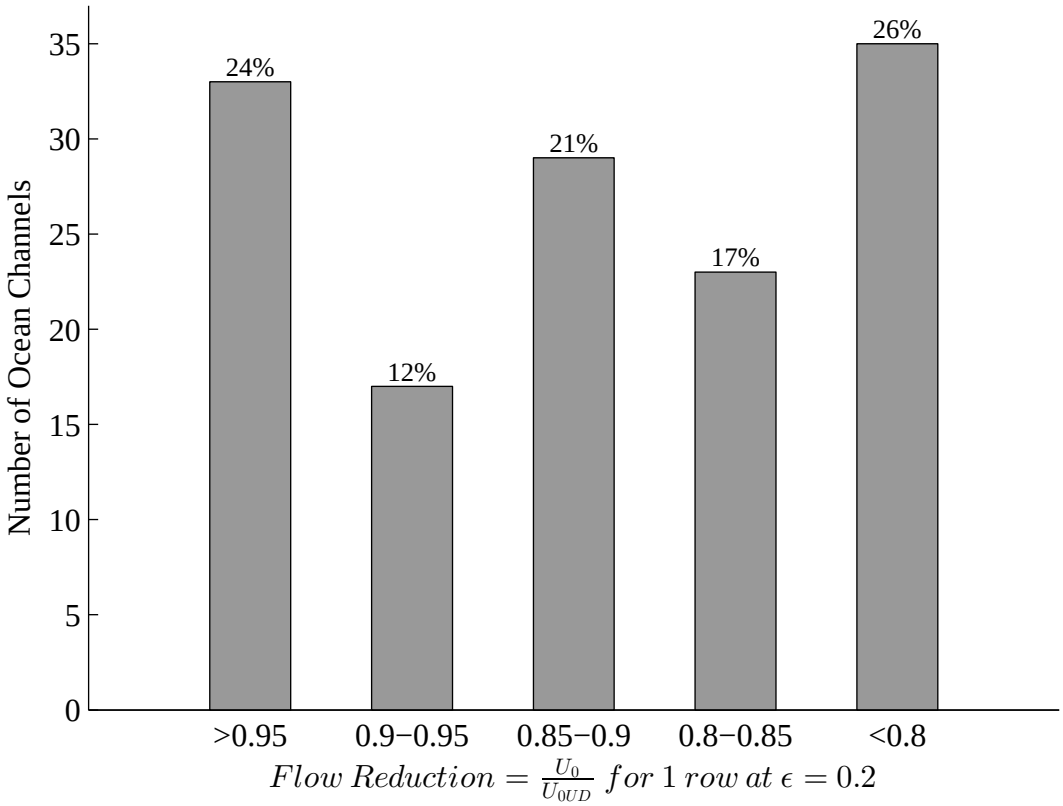


Figure 5.1: Distribution of ocean channels across a series of flow reduction intervals for a farm composed of 1 row of turbines with a blockage ratio, $\varepsilon$, of 0.2.

from Ireland, 4 from Norway, 8 from the UK and 2 from the USA. 17 channels, 12%, have flow velocities reduced by 5% to 10% in the simplest farm configuration. These channels can be considered for farm configurations resulting in 10%, 15% and 20% reductions in flow speeds and include 4 channels from Canada, 1 from Chile, 3 from Ireland, 1 from Norway, 4 from the UK and 4 from the USA. 33 channels, 24%, have flow velocities reduced by less than 5% in the basic farm configuration used. These channels can be considered for farm configurations resulting in all four reductions in flow velocities used (5%, 10%, 15% and 20%) and include 5 channels from Canada, 2 from Chile, 3 from Ireland, 2 from Norway, 2 from Australia, 11 from the UK, 4 from the USA and 1 from Singapore.

Figure 5.2 presents the range of power efficiencies, defined here as the ratios of the realisable powers calculated using V10 with a 0.2 blockage ratio and for flow reductions of 0.95, 0.9, 0.85 and 0.8 over the potentials determined in Chapter 4 for all the ocean channels meeting the cross-sectional area, depth, length and flow reduction requirements. As expected, decreased flow reductions result in overall increased power efficiencies. The mean values for the power efficiencies come to 20%, 35%, 47% and 60% for reductions in flow velocities of 5%, 10%, 15% and 20% respectively. The increases in mean power efficiencies

with each 5% increment in the flow velocity reductions are substantial and average at 13%. It is interesting to note that, on average, a substantial fraction, 60%, of the potential can be achieved by only blocking 20% of the channels' cross-sections and reducing the flow velocities by 20%.

The power efficiencies of the ocean channels included for a given flow reduction are not homogeneous and the spread of values for each flow reduction is substantial enough to create overlaps. At a flow reduction of 0.95, the power efficiencies of the 33 channels used span across 15% to 29%. This upper limit for the power efficiency corresponds to the lower end of the power efficiencies of the 50 channels involved in the 0.9 flow reduction calculations and for which it peaks at 50%. The 79 channels used to produce the 0.85 flow reduction results start at a significantly lower power efficiency of 42% and reach a maximum value of 64%. This is 10 points higher than the minimum power efficiency for the 102 channels involved in the 0.8 flow reduction calculations, spreading from 54% to 77%. Such large spreads in power efficiencies at the various flow reductions indicate that each channel might require a specific approach in order to draw near the wanted power output.

Figure 5.3 presents the range of power efficiencies, defined here as the ratios of the realisable powers calculated using V10 with a 0.2 blockage ratio for all but the last row of turbines and for flow reductions of 0.95, 0.9, 0.85 and 0.8 over the power potentials for flow reductions of 0.95, 0.9, 0.85 and 0.8 determined in Chapter 4 for all the ocean channels meeting the cross-sectional area, depth, length and flow reduction requirements. It appears that more of the power potential at a given flow reduction can be achieved with a 20% blockage ratio for higher reductions in flow velocities, i.e. lower flow reductions. However, the pool of channels between each graph is different and Figure 5.5 for which the pool is constant, and thus more appropriate to produce a comparison, shows this is not true at low reductions in flow velocities. The mean values for the power efficiencies come to 65%, 67%, 71% and 75% for reductions in flow velocities of 5%, 10%, 15% and 20% respectively. The increases in mean power efficiencies with each 5% increment in the flow velocity reductions are relatively low and average at 3%. Excluding the outliers results in limited overlaps between the adjacent flow reductions of no more than 1.5%. The second farm configuration is now introduced.

### 5.2.2 At a Uniform Blockage Ratios Below 20%

If part of a channel's cross-section was to be reserved for navigational purposes, it is conceivable that an obstacle of fixed, regular shape would help simplify its avoidance and help maintain the dimensions of the navigable area, providing the channel's width remains ap-

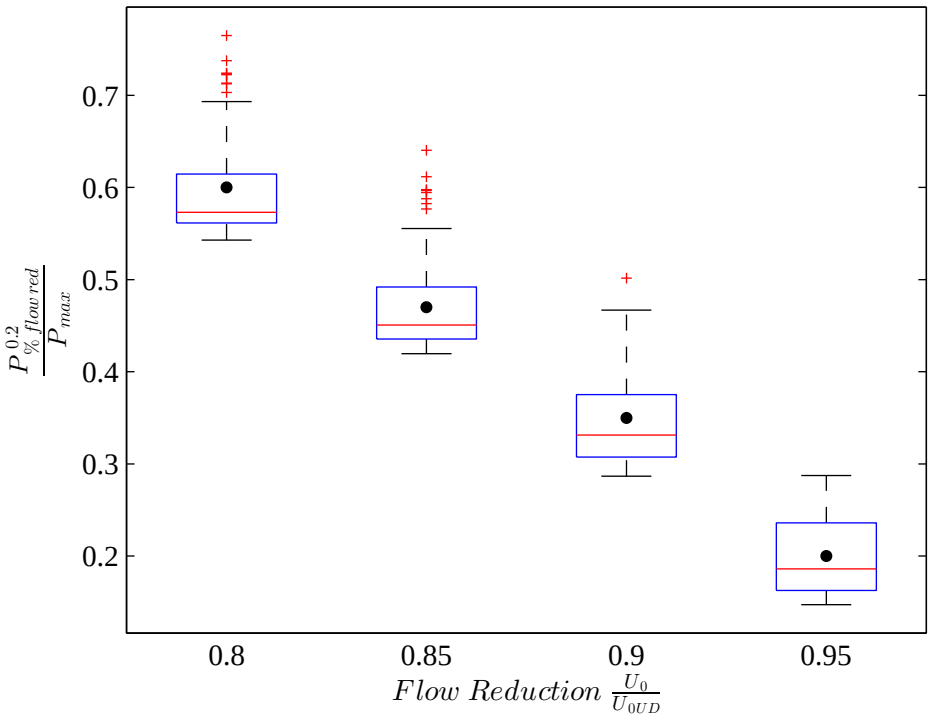


Figure 5.2: Range of power efficiencies from potentials calculated at 5%, 10%, 15% and 20% reductions in flow velocities and a 20% blockage ratio for all but the last row of turbines against the upper tidal current potential limits for all the ocean channels meeting the cross-sectional area, depth, length and flow reduction requirements.

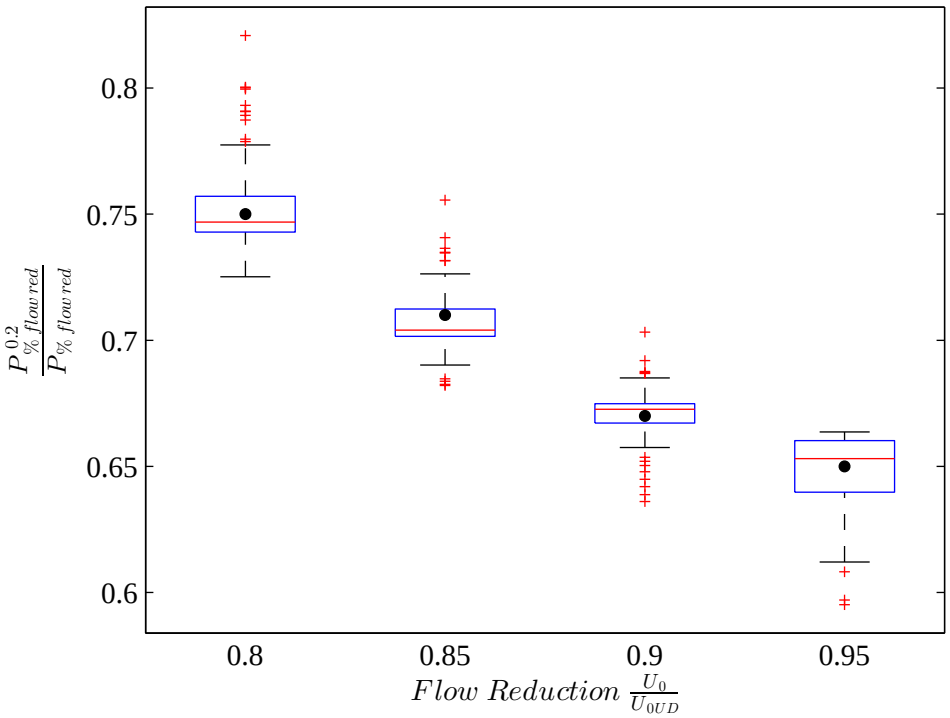


Figure 5.3: Range of power efficiencies from potentials calculated at 5%, 10%, 15% and 20% reductions in flow velocities and a 20% blockage ratio for all but the last row of turbines against the power potentials at the equivalent flow reduction for all the ocean channels meeting the cross-sectional area, depth, length and flow reduction requirements.

proximately stable over the length of the farm. In this section, a fixed blockage ratio, $\varepsilon$, of maximum 0.2 is implemented for the purpose of farm configurations. The following process was followed in order to determine the appropriate turbine arrangement of a given farm in a given channel. An initial farm set-up comprised of 1 row and a 0.2 blockage ratio was used and the corresponding flow reduction was calculated. If the flow reduction was beyond the threshold value, the blockage ratio was decreased until the appropriate flow reduction was attained. If not, an additional row with the same 0.2 blockage ratio was added and the flow reduction re-calculated, until the threshold was surpassed. The number of rows was then kept to this maximum value and the overall blockage ratio adjusted for all the rows until the appropriate flow reduction was obtained. No channel was required to have at least one row at a 20% blockage ratio, therefore all the 136 channels meeting the cross-sectional area, depth and length requirements were utilised in this section.

Figure 5.4 presents the range of power efficiencies, defined here as the ratios of the realisable powers calculated using V10 with a uniform blockage ratio below 0.2 and for flow reductions of 0.95, 0.9, 0.85 and 0.8 over the potentials determined in Chapter 4 for all the ocean channels meeting the cross-sectional area, depth and length requirements. As expected, decreased flow reductions result in overall increased power efficiencies. The mean values for the power efficiencies come to 19%, 34%, 47% and 60% for reductions in flow velocities of 5%, 10%, 15% and 20% respectively. The increases in mean power efficiencies with each 5% increment in the flow velocity reductions are substantial and average at 14%. These results correspond very closely to the ones obtained for a targeted blockage ratio of 0.2 in Section 5.2.1, although with a different pool of channels.. The ranges of power efficiency values for the various flow reductions also match the ones seen on Figure 5.2 very closely. Although the means display almost a linear decrease in power efficiencies with higher flow reductions, the large spreads in power efficiencies at the various flow reductions would encourage a case by case approach in order to draw near the wanted power output.

Figure 5.5 presents the range of power efficiencies, defined here as the ratios of the realisable powers calculated using V10 with a uniform blockage ratio below 0.2 and for flow reductions of 0.95, 0.9, 0.85 and 0.8 over the power potentials for flow reductions of 0.95, 0.9, 0.85 and 0.8 determined in Chapter 4 for the 136 ocean channels meeting the cross-sectional area, depth and length requirements. It shows that between the 0.8, 0.85 and 0.9 flow reductions more of the power potential at a given flow reduction can be achieved with a uniform 20% blockage ratio for higher reductions in flow velocities, i.e. lower flow reductions. The mean values for the power efficiencies come to 69%, 68%, 71% and 75% for reductions in flow velocities of 5%, 10%, 15% and 20% respectively. The mean power

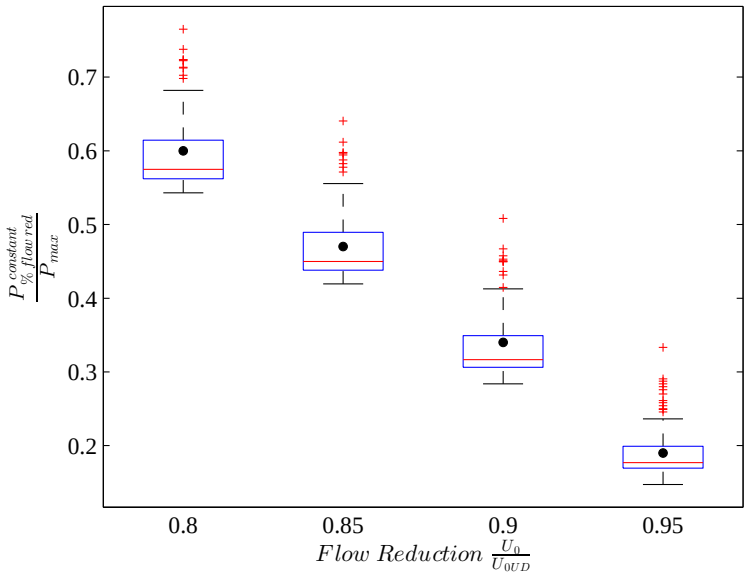


Figure 5.4: Range of power efficiencies from potentials calculated at 5%, 10%, 15% and 20% reductions in flow velocities and a uniform blockage ratio below 0.2 against the upper tidal current potential limits for all the ocean channels meeting the cross-sectional area, depth and length requirements.

efficiency for the 0.95 flow reduction is higher than that of the 0.9 flow reduction by 1%. The spreads of power efficiencies for the 0.8, 0.85 and 0.9 flow reductions are similar to the ones presented on Figure 5.3, with a shift in the outliers likely related to the different pools of data. However, the spread of power efficiencies for the 0.95 flow reduction shows significant variation and is much larger on Figure 5.5. This difference may be imputed to the 35 additional channels, which were discarded from Section 5.2.1.

A farm designed with a uniform blockage ratio of maximum 0.2 appears to offer the same or better yields than that of one designed with a targeted blockage ratio of 0.2 at all the tested flow reductions. The first type of farm configuration also enables the inclusion of all the desired channels, whereas the second causes the pool to be reduced in order to meet the flow reduction requirements. The two phenomena observed might in fact be related, as more channels could ensue better yields. However, the power efficiency of a given channel at a given flow reduction for either type of farm configuration cannot be estimated closely because of the wide ranges of values obtained for the groups of channels used. It appears from the results presented here that only rough estimations of the power efficiencies of ocean channels can be made, within approximately 10% of the true values, using the means of the power efficiencies defined as the ratios of the realisable powers calculated using V10

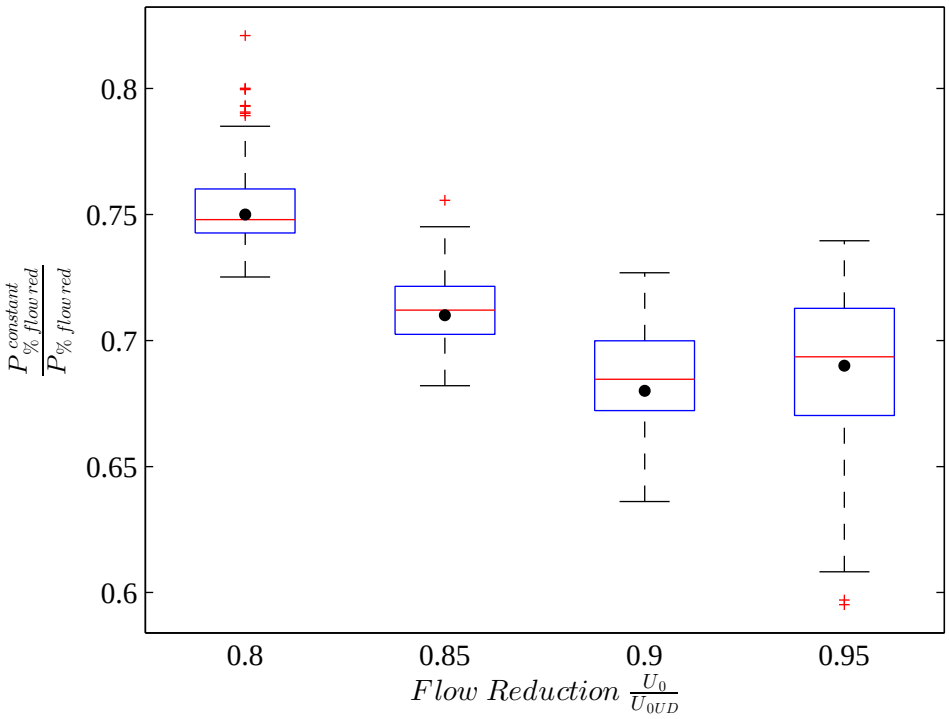


Figure 5.5: Range of power efficiencies from potentials calculated at 5%, 10%, 15% and 20% reductions in flow velocities and a uniform blockage ratio below 0.2 against the potentials at the equivalent flow reduction for all the ocean channels meeting the cross-sectional area, depth and length requirements.

with a uniform blockage ratio below 0.2 and for flow reductions of 0.95, 0.9, 0.85 and 0.8 over the potentials for flow reductions of 0.95, 0.9, 0.85 and 0.8. The particulars of a farm configuration, designed with a uniform blockage ratio of maximum 0.2, are now examined.

### 5.2.3 Particulars of Farm Configuration

This section is based on data collected for the farm configuration with uniform blockage ratio below 20%, because of the better yields and larger channel pool it offers at all flow reductions considered. Figure 5.6 presents the ranges of row numbers for the farm configurations corresponding to the 5%, 10%, 15% and 20% reductions in flow velocities, for turbine blade areas of $400\,m^2$. In order to reduce the flow velocities in the channels by 5%, most farms, 76%, require a single row of turbines, 11% of them need two rows and 13% three or more rows with a maximum of 26 rows for *Cook Strait*, New Zealand. This site also tops the numbers of rows required to reduce the flow velocities by 10%, 15% and 20% with 52, 88 and 149 rows of turbines respectively. A majority of farms, 64%, still only need one row of turbines to achieve a 10% reduction in flow velocities. The quantity of farms requiring two rows remains the same at 11%, but for three rows and more there is a noticeable increase to 25% of them. At 15% reduction in flow velocities, the number of farms needing only a single row of turbines drops to 42%, whereas it increases to 25% and 33% for two rows and three and more rows respectively. At 20% reduction in flow velocities, the majority of farms, 51% requires three or more rows of turbines, while the quantities of farms requiring one or two rows drop to 26% and 23% respectively.

It is interesting to note that even at blockage ratios below 20%, a large portion of the sites require a small number of rows of turbines in order to reach up to 20% reductions in flow velocities. Such channels include high potential ones. Indeed, at 20% reduction in flow velocities, the top four sites, located in Canada, *Nottingham Is - Ungava, Mill - Salisbury Is*, *Salisbury - Notthingham Is*, and *Mill - Baffin Is* only require 2, 3, 4 and 2 rows of turbines respectively. Lower numbers of rows of turbines mean smaller scale farms with therefore a lesser impact on other activities potentially taking place in these waterways.

Figure 5.7 presents the ranges of total numbers of turbines required for the farm configurations corresponding to the 5%, 10%, 15% and 20% reductions in flow velocities, and for turbine blade areas of $400\,m^2$. The number of Seagen-like turbines needed varies greatly with the site and flow reduction chosen. It can be as low as 0.07, 0.15, 0.26 and 0.40 for reductions in flow speeds of 5%, 10%, 15% and 20% respectively, as is found for *Saltstraumen*, Norway. Fractions of a turbine mean that turbines smaller than the Seagen one would need to be deployed to keep the flow velocities high enough. Approximately 15%, 7%, 4%

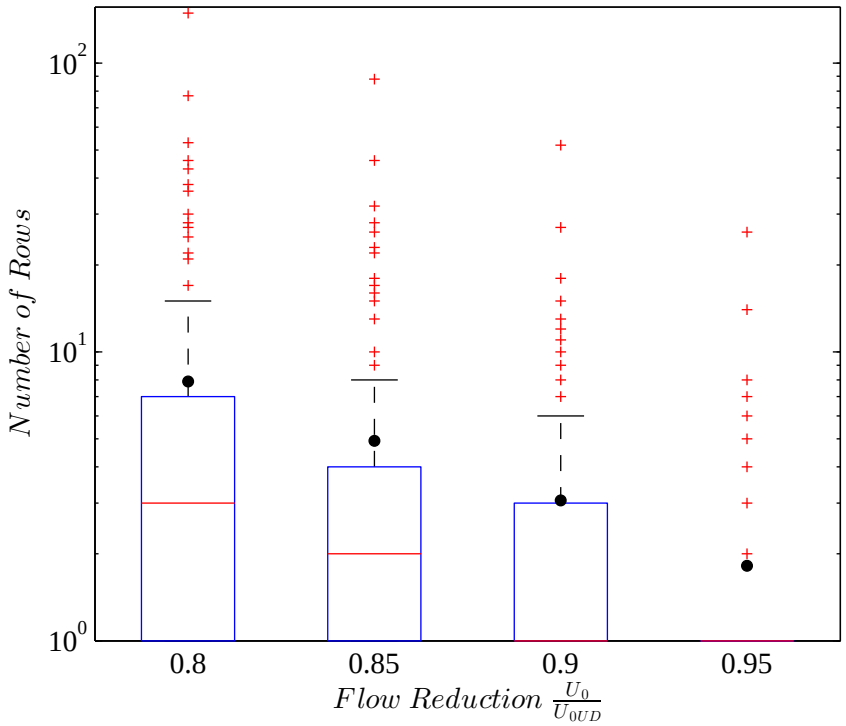


Figure 5.6: Range of row numbers from farm configurations produced for 5%, 10%, 15% and 20% reductions in flow velocities and a uniform blockage ratio below 0.2 for all the ocean channels meeting the cross-sectional area, depth and length requirements and for turbine blade areas of $400\,m^2$.

and 1% of the channels require less than one Seagen turbine to attain 5%, 10%, 15% and 20% reductions in flow velocities respectively. Inversely, the number of Seagen-like turbines needed can reach as high as 4,875, 97,508, 165,010 and 279,400 for reductions in flow speeds of 5%, 10%, 15% and 20% respectively, as is found for *Cook Strait*, New Zealand. These extremely large numbers of turbines indicate that another larger model than the Seagen one might be more appropriate for such sites.

Arrays comprising more than 200 turbines account for about 18%, 21%, 28% and 31% of the 136 sites for reductions in flow speeds of 5%, 10%, 15% and 20% respectively. A large majority of the channels, always at least two thirds, seem to be able to fit turbines of $400\,m^2$ blade area reasonably well at all four flow reductions. However, the most promising sites tend to require several thousands of them with the first of the top ranked channel requiring less than 1,000 turbines for a 5% reduction in flow velocity being *Singapore Strait*, ranked $7^{th}$ in terms of potential and the first requiring less than 200 turbines being *Chacaco Channel*, Chile, ranked $12^{th}$. Of the 50 channels with the highest potentials, 4 do not meet the cross-sectional area or depth requirements. 30% of the 46 channels left require less than 200 turbines and that proportion rises to only 43% for 1,000 turbines or less. Ignoring the other parameters to take into account for turbine implantations such as the depth-range or anchoring mechanism, it appears that the scale of the current Seagen turbine is not large enough for the potentially most prolific sites.

Figure 5.8 presents the ranges of uniform blockage ratios obtained for the farm configurations corresponding to the 5%, 10%, 15% and 20% reductions in flow velocities, and for turbine blade areas of $400\,m^2$. Blockage ratios to achieve 5% reductions in flow velocities vary from approximately 1%, with 2 channels, to 20%, with 19 channels and about half of the 136 channels have blockage ratios of 10% or more. At 10% reductions in flow speeds, 74% of the channels have at least a 10% blockage ratio, including 33 channels, 24%, with a blockage ratio of 20%. The lowest blockage ratio is around 2% for the same 2 channels mentioned at 5% reductions in flow velocities. These 2 channels also have the lowest blockage ratios at 15% and 20% reductions in flow velocities with approximately 3% and 5% respectively. The large majority of the channels, 91% and 96%, have blockage ratios of 10% or more for 15% and 20% reductions in flow speeds respectively, including 38 and 47 channels with a 20% blockage ratio.

Achieving the four flow reductions considered reasonable with a relatively low blockage ratio of at most 20% appears to be unproblematic for any of the channels represented here. The deployment of power-efficient farms within environmental constraints even in highly used waterways seems therefore to be almost a nullified issue pending any site-specific point

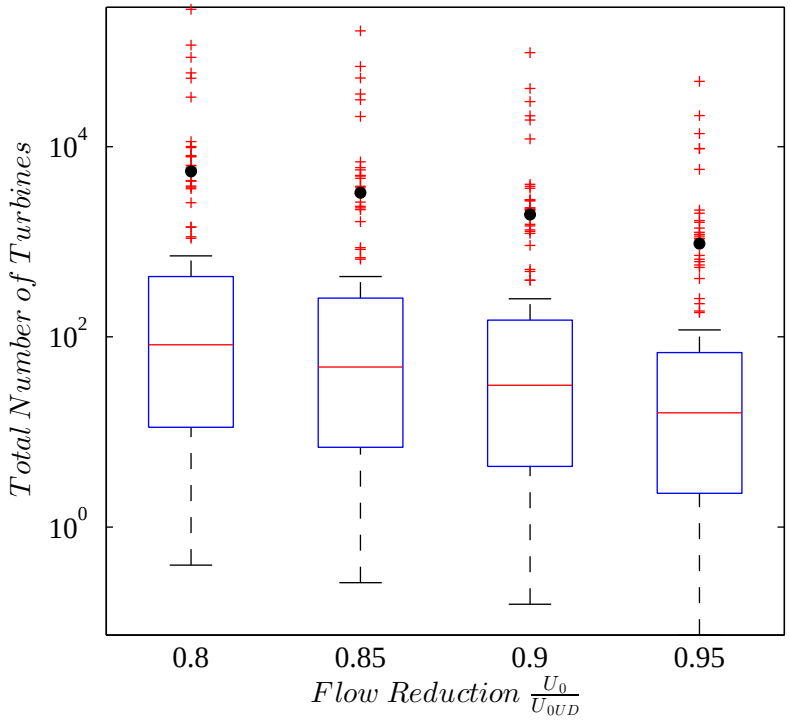


Figure 5.7: Range of total numbers of turbines from farm configurations produced for 5%, 10%, 15% and 20% reductions in flow velocities and a uniform blockage ratio below 0.2 for all the ocean channels meeting the cross-sectional area, depth and length requirements and for turbine blade areas of $400\,m^2$.

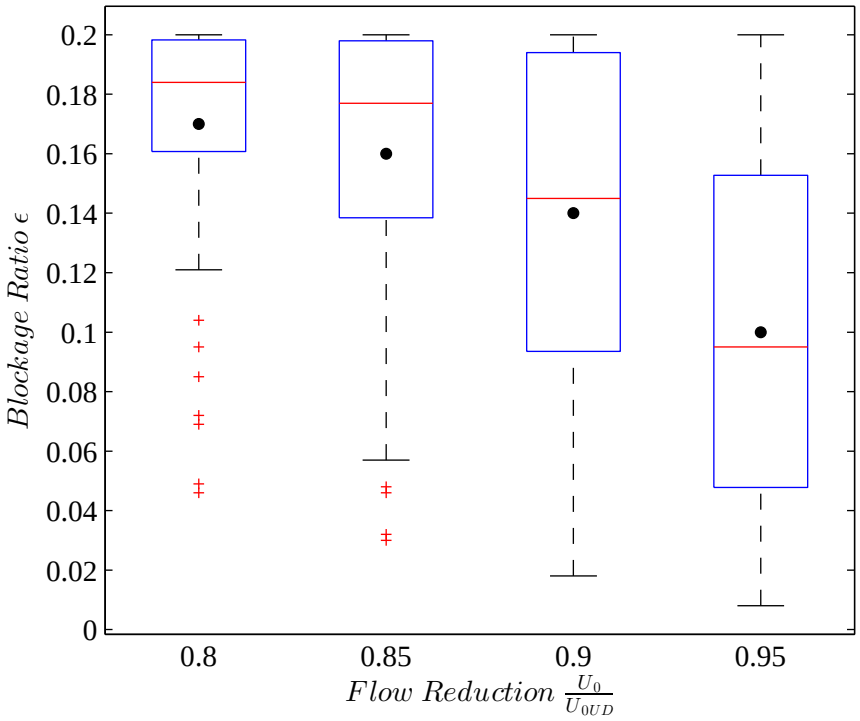


Figure 5.8: Range of uniform blockage ratios from farm configurations produced for 5%, 10%, 15% and 20% reductions in flow velocities for all the ocean channels meeting the cross-sectional area, depth and length requirements and for turbine blade areas of $400\,m^2$.

of contention. Combining this result with the farm lengths represented by the number of rows they are comprised of generally gives tidal farms of relatively small sizes in comparison to the sizes of the channels they are to be implanted in.

Figure 5.9 presents the ranges of powers per turbine required for the farm configurations corresponding to the 5%, 10%, 15% and 20% reductions in flow velocities, and for turbine blade areas of $400\,m^2$. The Seagen turbine used here as a model-turbine rates at $1.2\,MW$ [22]. The turbines currently being developed or tested have capacities ranging approximately from $25\,kW$, Kobold plant, to $1.5\,MW$, next phase of the Seagen turbine [32]. Considering this interval to form the range of acceptable turbine capacities, a substantial number of channels including ones with high potentials fall outside the adequate bracket. Few channels require turbine rating below $25\,kW$. They number 1, 3, 4 and 5 for reductions in flow velocities of 5%, 10%, 15% and 20% respectively. These channels rank towards the lower end of the upper tidal current potential limit spectrum and therefore account for very little of any country's potential tidal resource.

A more substantial number of channels, inclusive of ones of noticeable potential im-

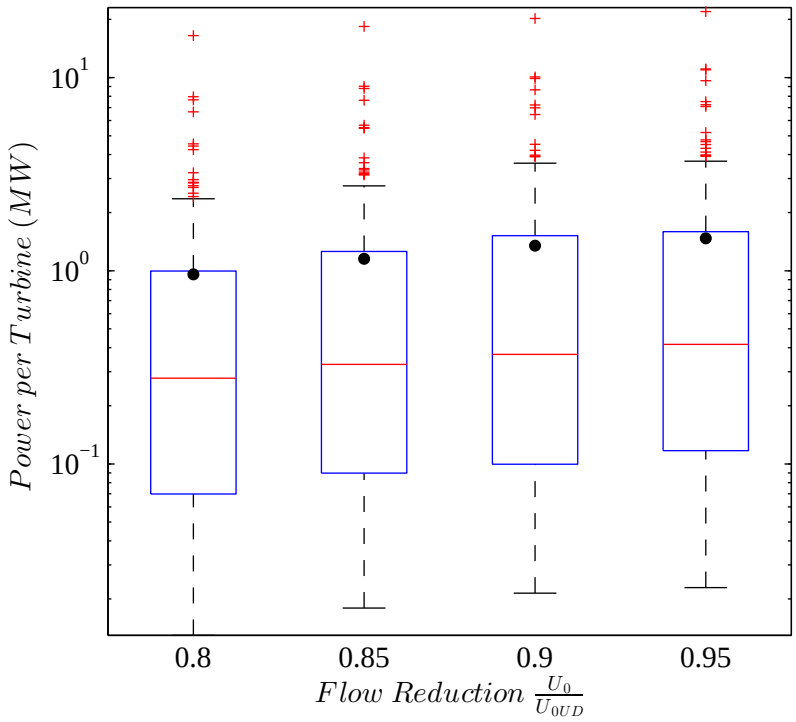


Figure 5.9: Range of powers per turbine from farm configurations produced for 5%, 10%, 15% and 20% reductions in flow velocities and a uniform blockage ratio below 0.2 for all the ocean channels meeting the cross-sectional area, depth and length requirements and for turbine blade areas of $400\,m^2$.

portance, require turbines of capacities exceeding $1.5\,MW$ in the farm configuration chosen. They amount 36, 35, 29 and 27 and represent 27%, 26%, 21% and 20% of the 136 channels included here for reductions in flow velocities of 5%, 10%, 15% and 20% respectively. This issue could be resolved simply, by adding more rows to the farms of concerns, as the current configuration aims to achieve a minimum possible number of rows, or by introducing limits regarding individual turbine power in the V10 model. Realisable resource estimations are now produced for each of the country included in this thesis, but solely based on their ocean channels.

## 5.3 Realisable Power Estimations

The realisable power estimates are produced using the V10 model [56]. The pool of sites used in this section corresponds to the 136 ocean channels selected as described in Section

5.1. Four sets of resource estimations are produced in accordance with the four chosen flow reductions of 0.95, 0.9, 0.85 and 0.8. The farm configuration displaying uniform blockage ratios below 20% is used because it produces better yields than the one targeting a 20% blockage ratio and it allows for all the channels to be taken into account at all flow reductions. Mixing and electro-mechanical losses are taken into account as detailed in Section 5.1, but the drag from support structures is not. The resource estimations are organised by country and discussed in comparison with the ones made in Chapter 4 using potentials as well as existing relevant studies. The uncertainties on the realisable powers have been ignored because they would be very difficult to gauge meaningfully considering the data originate from third party sources in which no error estimation exists. Therefore, the results presented here must be taken with caution as their quality is relative to the quality of the input data. The results for all the countries and individual sites are presented in Appendix D. The UK and Ireland are, as was done in Chapter 3, treated separately because their databases, as opposed to the other countries' databases, are believed to be whole. Table 5.2 presents a summary of the potentials, as well as the realisable outputs at a uniform blockage ratio below 20% for flow reduction of 0.95, 0.9, 0.85 and 0.8 for each of the 11 countries included in this thesis.

### 5.3.1 The UK

Appendix D includes the realisable power estimates for 35 ocean channels located in the UK, having lost *N Ronaldsay Firth*, *Burra Sound*, *Hoy Sound*, *Copinsay Pass*, *Gunna Sound*, *Corran Narrows*, *Loch Leven Narrows* and *Staple Sound* to the newly introduced cross-sectional area and depth limits. The realisable tidal resource for the UK adds up to approximately $7.5\,GW$, $13\,GW$, $18\,GW$ and $23\,GW$ at flow reductions of 0.95, 0.9, 0.85 and 0.8 respectively without any input from lagoon channels, which represent 3% of the estimated UK's tidal current potential.

The newly introduced $15\,m$ depth-limit matches the minimum depth used in the 2011 Black & Veatch report. The cut-off point pertaining to the channels' cross-sectional area is not directly related to the other limit introduced in the 2011 Black & Veatch report establishing a threshold for the mean annualised power density of $1.5\,kW\,m^{-2}$. The number of sites used is slightly different varying from 35 in this study to 30 in the 2011 Black & Veatch one, but all of them are ocean channels [3]. The realisable tidal resource after applying the SIF comes down to $2.5\,GW$, $1.6\,GW$ for the 2004 and 2005 Black & Veatch reports respectively [4, 5]. Two levels of realisable resource estimates are offered in the 2011 Black & Veatch report representing what are being called the 'Technical Resource' and the 'Practical Resource'. The realisable resource introduced here is most closely related to their practical

resource. The 2011 report also offers a series of realisable resource estimations across a range of statistically derived uncertainty quantifications of P10, P50 and P90. The corresponding 2011 Black & Veatch UK practical tidal resource amounts 1.2 $GW$, 2.4 $GW$ and 3.4 $GW$ respectively. These values are very low in comparison to the ones produced here with the largest one only reaching 45% of the realisable resource estimation for reductions in flow velocities of 5%.

The proportion of the tidal current potential originating from ocean channels that can be extracted varies greatly with the flow reduction chosen giving 20%, 36%, 50% and 64% for reductions in flow velocities of 5%, 10%, 15% and 20% respectively. The corresponding proportion of the overall tidal current potential attains 20%, 35%, 49% and 62% respectively. The small difference can be explained by the relatively low importance of the lagoon channels' contribution to the overall resource in the UK. The principle, previously highlighted, of concentration of the resource within a few of the sites is once again observed here, as regardless of the flow reduction used, the top 10 sites contribute to 96% of the UK's realisable tidal resource. The top 3 channels, the *English Channel*, *St George's Channel - Carmel Head* and *North Channel - The Rhins*, each offer at least 1 $GW$ of realisable tidal power potential at all the flow reductions considered.

### 5.3.2 Ireland

Appendix D includes the realisable power estimates for 12 ocean channels located in Ireland, having lost *Clare Is*, 13 $m$ deep, to the depth limit. Three sites located or in connection with Northern Ireland, *North Channel - The Rhins*, *West Islay*, and *North Channel - Kintyre Peninsula*, have been included in the UK resource estimation and excluded from this section. The realisable tidal resource is estimated to amount approximately 51 $MW$, 94 $MW$, 130 $MW$, and 170 $MW$ for reductions in flow velocities of 5%, 10%, 15% and 20% respectively. These values represent only 10%, 18%, 25% and 32% of the overall tidal current potential in Ireland, but 18%, 32%, 46% and 58% of the ocean-channel tidal current potential. The strong difference can be explained by the significant contribution to the overall tidal current potential made by the lagoon channels in Ireland, providing as much as 45% of it. Their absence from the realisable power estimates is strongly felt. Similarly to the UK, most of the tidal resource comes from a small number of sites, with 7 sites concentrating 96% of it. *West Arklow Bank* makes the most significant contribution with at least 58% of the overall realisable resource at all the flow reductions considered.

### 5.3.3 Other Countries

The choice of flow reduction has a significant impact on the final proportion of the potential resource which can be extracted. For most of the countries, a substantial proportion of the ocean-channel tidal current potential can be achieved at a flow reduction of 0.8. As was observed in the tidal current potential estimations in Chapter 3, it appears that the resource in each country is concentrated amongst a small cluster of sites.

**Canada** Only 41 of the 64 ocean channels meet the minimum depth and cross-sectional area thresholds. realisable power estimations for these sites can be found in Appendix D. Estimates of $26\,GW$, $43\,GW$, $57\,GW$ and $70\,GW$ for the realisable powers at 5%, 10%, 15% and 20% reductions in flow velocities were produced here. These values represent 24%, 39%, 52% and 65% of the overall tidal current potential and 25%, 42%, 56% and 70% of the ocean-derived tidal potential. As observed previously, the top 10 channels concentrate 96% of the realisable tidal resource, with the top 5 channels, all located in the Hudson Strait, contributing to more than $2\,GW$ each at all the flow reductions used.

**Norway** Appendix D includes the realisable power estimates for 20 ocean channels located in Norway, the country having lost 30 sites to the cross-sectional area and depth limits. The realisable tidal resource reaches $64\,MW$, $110\,MW$, $160\,MW$ and $200\,MW$ for 5%, 10%, 15% and 20% reductions in flow speeds respectively. These values equate to 15%, 26%, 37% and 46% of the overall tidal potential, which corresponds to the ocean-derived potential as there is no lagoon channel represented in the data for Norway. These percentages are markedly lower than what can be found for other countries in terms of the proportions of the ocean-channel potentials reached. This can be explained by the substantial loss incurred of 60% of the original sites. The top 10 channels contribute to between 92% and 93% of the overall resource, the top 12 to at least 96%. The leading channel, *Moskenstraumen*, alone, contributes to between 44% and 45% of Norway's overall realisable tidal resource at all the flow reductions considered.

**New Zealand** Appendix D includes the realisable power estimates for the 4 ocean channels located in New Zealand and taken into account in this study. Estimates of $4.5\,GW$, $7.2\,GW$, $9.5\,GW$ and $11\,GW$ for the realisable powers at 5%, 10%, 15% and 20% reductions in flow velocities were produced here. These values represent 28%, 45%, 59% and 69% of the ocean-derived tidal current potential, which is approximately equivalent to their proportions of the overall tidal current potential contribution as *Kaipara Harbour*'s participation is

relatively negligible in comparison to that of the ocean channels. Most of the tidal resource comes from one site, *Cook Strait*, which alone concentrates at least 97% of the realisable tidal resource from the ocean channels at all the flow reductions used.

**Australia** Appendix D includes the realisable power estimates for the 2 ocean channels located in Australia and taken into account in this study. The realisable tidal resource reaches $700\,MW$, $1300\,MW$, $1800\,MW$ and $2400\,MW$ for 5%, 10%, 15% and 20% reductions in flow speeds respectively. These values represent 17%, 31%, 43% and 56% of the ocean-derived tidal current potential, but only 2%, 3%, 4% and 6% of the overall tidal current potential. The difference comes from the presence of the top lagoon channel in Australia, *King Sound*, which alone accounts for $34\,GW$ of the overall tidal current potential and most of the country's tidal resource. Although the contribution of *Banks Strait* is very small in comparison to *King Sound,* it is significantly higher than that of the other Australian ocean channel, *Adolphus Channel*. It accounts for 94% of the ocean-channel realisable tidal resource at all the flow reductions considered.

**The USA** Appendix D includes the realisable power estimates for 17 ocean channels located in the USA, having lost 7 of them to the newly introduced cross-sectional area and depth limits. The ocean-channel realisable tidal resource for the USA adds up to approximately $100\,MW$, $180\,MW$, $250\,MW$ and $330\,MW$ at flow reductions of 0.95, 0.9, 0.85 and 0.8 respectively. The proportion of the tidal current potential originating from ocean channels that can be achieved varies from 15%, 28%, 39% and 50% for reductions in flow velocities of 5%, 10%, 15% and 20% respectively. The corresponding proportion of the overall tidal current potential attains only 1%, 1%, 2% and 2% respectively. The large difference observed here can be explained by the domination in terms of contribution of one of the lagoon channel, *Cook Inlet*, which makes the ocean channels' participation look relatively negligible. Three channels, *Adak Strait*, *Avatanak Strait* and *Umnak Pass*, located in Alaska, offer even contributions amounting each to approximately 20% of the ocean-channel realisable resource at all the flow reductions used.

**Singapore, Chile, Japan and Italy** Japan, Singapore and Italy each only have one channel represented here and realisable powers for these channels can be found in Appendix D. For the *Naruto Strait,* in Japan, the realisable tidal resource attains $0.72\,MW$, $1.3\,MW$, $1.7\,MW$ and $2.2\,MW$ for 5%, 10%, 15% and 20% reductions in flow speeds respectively. The corresponding values for the *Singapore Strait* and the *Strait of Messina,* Italy, reach $1.2\,GW$,

2.2 $GW$, 3.2 $GW$ and 4.2 $GW$ and 4.1 $MW$, 7.1 $MW$, 9.9 $MW$ and 12 $MW$ respectively.

Appendix D includes the realisable power estimates for the 3 ocean channels located in Chile and taken into account in this study. The realisable tidal resource reaches 1.0 $GW$, 1.1 $GW$, 1.6 $GW$ and 2.0 $GW$ for 5%, 10%, 15% and 20% reductions in flow speeds respectively. These values equate to 20%, 37%, 49% and 61% of the tidal current potential, which corresponds to the ocean-derived tidal potential as there is no lagoon channel represented in the data for Chile. One of the sites, *Chacao Channel*, accounts for at least 58% of the realisable tidal resource at all the flow reductions used.

Table 5.2: Upper limit of the tidal current potential resource, as well as the realisable outputs at 0.95, 0.9, 0.85 and 0.8 flow reduction and at a uniform blockage ratio below 20% for the 11 countries included in this study. Country codes can be found in the Nomenclature. Note that realisable outputs only include a reduced pool of ocean channels.

| **Country Code** | **Upper Limit of Potential** | **Realisable Output At 0.95 Flow Reduction** | **Realisable Output At 0.9 Flow Reduction** | **Realisable Output At 0.85 Flow Reduction** | **Realisable Output At 0.8 Flow Reduction** |
|---|---|---|---|---|---|
| UK | $37\,GW \pm 6\,GW$ | $7.5\,GW$ | $13\,GW$ | $18\,GW$ | $23\,GW$ |
| IR | $530\,MW \pm 80\,MW$ | $51\,MW$ | $94\,MW$ | $130\,MW$ | $170\,MW$ |
| CA | $110\,GW \pm 17\,GW$ | $26\,GW$ | $43\,GW$ | $57\,GW$ | $70\,GW$ |
| NW | $440\,MW \pm 66\,MW$ | $64\,MW$ | $110\,MW$ | $160\,MW$ | $200\,MW$ |
| NZ | $16\,GW \pm 2.4\,GW$ | $4.5\,GW$ | $7.2\,GW$ | $9.5\,GW$ | $11\,GW$ |
| OZ | $42\,GW \pm 6.3\,GW$ | $700\,MW$ | $1300\,MW$ | $1800\,MW$ | $2400\,MW$ |
| US | $19\,GW \pm 3\,GW$ | $100\,MW$ | $180\,MW$ | $250\,MW$ | $330\,MW$ |
| SG | $7.7\,GW \pm 1.2\,GW$, | $1.2\,GW$ | $2.2\,GW$ | $3.2\,GW$ | $4.2\,GW$ |
| CH | $4.9\,GW \pm 0.7\,GW$ | $1.0\,GW$ | $1.1\,GW$ | $1.6\,GW$ | $2.0\,GW$ |
| JP | $2.2\,GW \pm 0.3\,GW$ | $0.72\,MW$ | $1.3\,MW$ | $1.7\,MW$ | $2.2\,MW$ |
| IT | $20\,MW \pm 3\,MW$ | $4.1\,MW$ | $7.1\,MW$ | $9.9\,MW$ | $12\,MW$ |

## 5.4 Conclusion

The V10 model was used in this Chapter with a new set of constraints relative to the depth, cross-sectional area and length for the ocean channels included in the thesis database. 70 ocean channels were consequently excluded. None of the lagoon channels were included in the calculations pertaining to the current Chapter.

Two farm configurations, which limit the blockage ratio of each of their row to a maximum of 20%, were investigated. The farm configuration displaying a uniform blockage ratio was found to produce slightly better yield than the one targeting a 20% blockage ratio for most of its rows, probably because, contrary to the other configuration, it allowed for the inclusion of all the channels considered. It was therefore kept for later use. Its particulars were examined. The farm sizes obtained from its usage were relatively small compared to the sizes of the channels in which the farms would be implanted. This result carries positive bearing as it ensues less negative impact on the environment and easier accommodation for the other waterway users. Additionally, a blockage ratio of 20% represents no barrier to the possible extraction of substantial fractions of the available potentials. On the other hand, the large numbers of Seagen-like turbines needed to fill the partial rows and the high power ratings required for these turbines at highly promising sites, was thought to be of concern. The production of bigger and more powerful turbines to be able to exploit these sites of noticeable importance is likely to become a necessity.

The realisable powers for a uniform blockage ratio of maximum 20% and at flow reductions of 0.95, 0.9, 0.85 and 0.8 for the 11 countries included here can be found summarised in Table 5.2. As discussed previously, the results presented in the table show that, for most countries, a large portion of the available potential can be realised within these constraints. The countries for which lagoon channels contribute a substantial amount to the overall potential end up with poor outcomes in this section, because of the absence of their main contributors.

# Chapter 6

# Conclusions and Recommendations

This chapter summarises the key objectives and major findings of this thesis. Recommendations for future work will also be discussed in order to help improve the quality of tidal site assessments to come. The main objectives of this thesis were to:

- Produce tidal resource potential estimates for each of the countries represented here and compare the results obtained with other existing appropriate resource studies.
- Research the existence of patterns using an authentic broad database of channels.
- Produce realisable tidal resource estimations for each of the countries represented here and compare the results obtained with other existing resource studies and upper tidal current potential limits as appropriate.

## 6.1 Conclusions

This thesis used a database of 206 ocean and 33 lagoon channels. The channels were chosen as authentic and therefore representing naturally occurring geometries and physical characteristics. Three ocean-channel assessment methods and three lagoon-channel assessment methods were applied to produce the potentials of all of the sites included. Comparisons between the GC05 and V11 models as well as the Lagoon-GC05 and Lagoon-V11 models ascertain the applicability of the V11 and Lagoon-V11 assessment methods to preliminary resource assessments, with a relative deviation of at most, as expected, about 15%. Comparisons between the V11 and KE Flux models as well as the Lagoon-V11 and KE Flux models confirmed the lack of validity of the KE Flux method for tidal resource assessments. No pattern of behaviour for the KE Flux model in relation to any of the others could be identified

and great variations exist with regards to the quality of its assessment results, rendering moot the usefulness of any such result.

Existing differences in the sources used for the input data led to a verification of their applicability in the context of a common study. No significant inconsistencies were discovered and countries' potentials proceeded to be calculated using the V11 and Lagoon-V11 models. The assessments were based on relatively complete databases for the UK and Ireland, whereas these were only partial for the other countries included in the study. Overall potentials of $37\,GW\ \pm 6\,GW$ and $530\,MW\ \pm 80\,MW$ were obtained for the UK and Ireland respectively. These results are in par with what has been previously found in other studies for the UK, but well below previous estimates for Ireland. Canada was found to have the most promising cluster of sites and the largest tidal current resource with $110\,GW\ \pm 17\,GW$, which comes up to more than double the value of a previously made resource estimation. Norway's results were relatively low, $440\,MW\ \pm 66\,MW$, in comparison to past studies where the tidal resource was estimated to reach $4.7\,GW$. Resource estimations for New Zealand and Australia produced significantly high values with regards to their low numbers of sites with $16\,GW\ \pm 2.4\,GW$ and $42\,GW\ \pm 6.3\,GW$ respectively. Australia's channel pool includes the highest ranking lagoon channel, whose contribution accounts for 81% of the overall resource of the country, as calculated here. The overall potential for the USA amounted to about $19\,GW\ \pm 3\,GW$ and those of Singapore, Chile, Japan and Italy, which include very few sites each, to $7.7\,GW\ \pm 1.2\,GW$, $4.9\,GW\ \pm 0.7\,GW$ , $2.2\,GW\ \pm 0.3\,GW$ and $20\,MW\ \pm 3\,MW$ respectively.

A number of dimensionless quantities to be used as discriminatory parameters were extracted directly from the V11 and Lagoon-V11 equations, including $\alpha$, $\lambda_0$ and $\lambda_{peak}$ and $\alpha*$, $\beta_L$, $\lambda_0$ and $\lambda_{peak}$ for ocean and lagoon channels respectively. Other dimensionless parameters, comprising $\frac{v}{\sqrt{gh}}$, $\omega\sqrt{\frac{h}{g}}$, $\frac{L}{h}$, $\frac{w}{h}$, $C_D$ for ocean channels and with the addition of $\frac{\eta_{01}}{h}$ for lagoon channels, were determined through the non-dimensionalisations of the V11 and Lagoon-V11 equations. Tests were conducted between the discriminatory parameters and the potentials calculated using V11 and Lagoon-V11, but no pattern was found. Possible relationships between the discriminatory parameters and the quality of the KE Flux results were also investigated. The quality of the ocean channel estimates was found to be related to the discriminatory parameter $\frac{L}{h}$ and that of the lagoon channel estimates to the discriminatory parameter $\beta_L$.

A study of the flow reductions at peak power potentials showed a spread of values of 0.56 to 0.59 and 0.56 to 0.71 for ocean and lagoon channels respectively. Tests conducted between the flow reductions at peak power potentials and the discriminatory parameters revealed a

pattern in relation to the Froude number for the ocean channels. The introduction of flow reduction limitations reduces the power potential available at each site. The greater gain obained with regards to the power potential of a given channel is made when decreasing the allowed flow reduction from the highest value considered 0.95 to 0.9 or 0.85. Significant improvements in the tidal resource potentially available can be made, for both ocean and lagoon channels, with relatively small changes in the flow reduction at its higher end. Tests were conducted between the discriminatory parameters and the power efficiencies at a flow reduction of 0.9. Patterns were found in relation to the Froude number for both ocean and lagoon channels.

A sensitivity study relative to the input variables was conducted and the mean peak velocity, $v$, as well as the average tidal elevation in the ocean, $\eta_{01}$, were determined to be the variables with the most significant impact on potentials. The effects of these two pieces of data on the potential calculations are noteworthy and the quality of their measurements is largely affecting the quality of the overall resource estimations. Tests were conducted between the discriminatory parameters and the relative change in potentials when a 10% increase in each of the input variables, individually, is applied. These tests exposed existing trends for both ocean and lagoon channels in relation to the Froude number.

A comparison was made between two farm configurations for ocean channels using the V10 model: a farm configuration with a targeted blockage ratio of 20% and a farm configuration displaying a uniform blockage ratio of maximum 20%. The second configuration was found to produce the best power yields and have the advantage of allowing the inclusion of all the channels that can be considered. Its particulars in relation to the ocean channels studied were examined. They showed that optimal farm sizes, at reasonable flow reductions and blockage ratios, were relatively small in comparison to their channel of deployment. The large numbers of Seagen-like turbines required, particularly in promising sites, was thought to be a concern and to mean that larger designs of turbines should be considered. A constant blockage ratio of at most 20% was showed to represent no barrier to optimal tidal energy extraction at flow reductions ranging from 0.8 to 0.95. Finally, the power rating of currently available tidal turbines was found to be too small to accommodate a number of sites of noticeable potential importance.

Realisable resource estimates were produced for all the countries included in this study. These resource estimates were based on a smaller pool of channels than the one used to calculate the potentials, adding up to 136 channels. Only ocean channels were included. The reasons for having a reduced number of channels are explained in Section 5.3. The results are presented in Table 6.1. These results were obtained with the same farm configuration for all

Table 6.1: Realisable resource estimates for the 11 countries included in this study for reductions in flow velocities of 5%, 10%, 15% and 20%.

| Country Name | Realisable Resource Estimates for Reduction in Flow Velocities of 5% | 10% | 15% | 20% |
|---|---|---|---|---|
| United Kingdom | 7.5 *GW* | 13 *GW* | 18 *GW* | 23 *GW* |
| Ireland | 51 *MW* | 94 *MW* | 130 *MW* | 170 *MW* |
| Canada | 26 *GW* | 43 *GW* | 57 *GW* | 70 *GW* |
| Norway | 64 *MW* | 110 *MW* | 160 *MW* | 200 *MW* |
| New Zealand | 4.5 *GW* | 7.2 *GW* | 9.5 *GW* | 11 *GW* |
| Australia | 0.7 *GW* | 1.3 *GW* | 1.8 *GW* | 2.4 *GW* |
| USA | 100 *MW* | 180 *MW* | 250 *MW* | 330 *MW* |
| Japan | 0.72 *MW* | 1.3 *MW* | 1.7 *MW* | 2.2 *MW* |
| Singapore | 1.2 *GW* | 2.2 *GW* | 3.2 *GW* | 4.2 *GW* |
| Italy | 4.1 *MW* | 7.1 *MW* | 9.9 *MW* | 12 *MW* |
| Chile | 1.0 *GW* | 1.1 *GW* | 1.6 *GW* | 2.0 *GW* |

channels: turbines deployed to form a uniform blockage ratios below 20%. These results can be used for comparison with other studies, but should be looked upon as representing a low threshold for the realisable resource estimate of a given country. Indeed, for some countries the missing lagoon channels have a significant impact on the overall value obtained; for other countries, the realisable resource estimates are based on a small non-exhaustive number of channels.

## 6.2 Recommendations

The sensitivity study relative to the input variables has shown that the quality of the data measurements has a significant impact on the quality of the tidal resource estimations produced, particularly with regards to the mean peak velocity, $v$, for ocean channels and the average tidal elevation in the ocean, $\eta_{01}$, for lagoon channels. Projects focused on gathering accurate data for the purpose of channel power potential estimations would prove extremely useful to improve assessment results. With a concentration of the resource within a small cluster of sites, for most countries, the number of channels that would warrant accurate data collections can be limited without markedly affecting the overall resource.

It would also be valuable to ensure the data collected are accompanied by good estim-

ations of their uncertainties. This would in turn allow for meaningful error margins to be given with any country's resource estimation. The inclusion of lagoon-type channels in the realisable country's resource assessments would also definitely be of interest, particularly for countries in which lagoon channels represent a substantial proportion of the overall resource, such as Australia.

The V10 model enables one to include the drag from support structures and adjust a good range of parameters. Including all these parameters and incorporating a channel by channel tuning of the options available would help improve the quality of the realisable power estimates.

Finally, the effects on the quality of the power potential assessments of using the GC05, Lagoon-GC05, V11 or Lagoon-V11 one-dimensional models on wide channels with significant variations in their flow velocities in the across-flow direction are largely unknown. It would be interesting to be able to gauge these effects in relation to the channels concerned.

# Bibliography

[1] Ahmadian, R. and Falconer, R. A. (2012). Assessment of array shape of tidal stream turbines on hydro-environmental impacts and power output. *Renewable Energy*, *44*, 318–327.

[2] Bahaj, A. S. (2013). Marine current energy conversion : the dawn of a new era in electricity production. , (January).

[3] Black & Veatch (2011). UK Tidal Current Resource & Economics. Technical Report July.

[4] Black & Veatch Consulting (2004). Uk, Europe and Global Tidal Stream Energy Resource Assessment. Technical report.

[5] Black and Veatch (2005). UK Tidal Stream Energy Resource Assessment - Phase II. Technical Report 0, Carbon Trust.

[6] Blanchfield, J., Garrett, C., Wild, P., and Rowe, a. (2008). The extractable power from a channel linking a bay to the open ocean. *Proceedings of the Institution of Mechanical Engineers, Part A: Journal of Power and Energy*, *222*(3), 289–297.

[7] Blanchfield, J. B. (2007). *The Extractable Power from Tidal Streams, including a Case Study for Haida Gwaii*. Ph. D. thesis, University of Victoria.

[8] Block, E. (2008). Tidal power: an update. *Renewable Energy Focus*, *9*(6), 58–61.

[9] Blunden, L. S. and Bahaj, A. S. (2007). Tidal energy resource assessment for tidal stream generators. *Proceedings of the Institution of Mechanical Engineers, Part A: Journal of Power and Energy*, *221*(2), 137–146.

[10] Bryden, I., Grinsted, T., and Melville, G. (2004). Assessing the potential of a simple tidal channel to deliver useful energy. *Applied Ocean Research*, *26*(5), 198–204.

[11] C G Justuc, W R Hargraves, A. Y. (1976). Nationwide Assessment of Potential Output from Wind-Powered Generators. *Journal of Applied Meteorology*, *15*(7).

[12] Council of The European Union (2007). Presidency Conclusions - Brussels European Council - 8/7 March 2007 - 7224/07.

[13] CSIRO (2012). Ocean renewable energy: 2015-2050 - An analysis of ocean energy in Australia. Technical Report July.

[14] Dangar, P. B., Kaware, S. H., and Katti, P. K. (2011). Site Matching Of Offshore Wind Turbines - A Case Study. *Wind Energy Applications*, (1), 4098–4105.

[15] Demirbas, A. (2009). Global Renewable Energy Projections. *Energy Sources, Part B: Economics, Planning, and Policy*, *4*(2), 212–224.

[16] Destouni, G. and Frank, H. (2010). Renewable Energy. *Ambio*, *39*(S1), 18–21.

[17] Douglas, C. a., Harrison, G. P., and Chick, J. P. (2008). Life cycle assessment of the Seagen marine current turbine. *Proceedings of the Institution of Mechanical Engineers, Part M: Journal of Engineering for the Maritime Environment*, *222*(1), 1–12.

[18] El-geziry, T. M., Bryden, I. G., and Meng, S. J. C. (2009). Environmental impact assessment for tidal energy schemes: an exemplar case study of the Strait of Messina. *Journal of Marine Engineering and Technology*, (A13), 39–48.

[19] Electricity Commission, Energy Efficiency and Conservation Authority, and Greater Wellington Regional Council (2008). Development of Marine Energy in New Zealand. Technical Report June.

[20] Errazuriz & Asociados Ingenieros and The University of Edinburgh (2012). Marine Energy Development - Taking Steps for Developing the Chilean Resource. Technical report.

[21] Fairley, I., Evans, P., Wooldridge, C., Willis, M., and Masters, I. (2013). Evaluation of tidal stream resource in a potential array area via direct measurements. *Renewable Energy*, *57*, 70–78.

[22] Fraenkel, P. (2010). Practical tidal turbine design considerations : a review of technical alternatives and key design decisions leading to the development of the SeaGen 1 . 2MW tidal turbine. , (October), 1–19.

[23] Fraenkel, P. L. (2002). Power from marine currents. *Proceedings of the Institution of Mechanical Engineers, Part A: Journal of Power and Energy*, *216*(1), 1–14.

[24] Garrett, C. and Cummins, P. (2004). Generating Power from Tidal Currents. *Journal of Waterway, Port, Coastal, and Ocean Engineering*, *130*(3), 114–118.

[25] Garrett, C. and Cummins, P. (2005). The power potential of tidal currents in channels. *Proceedings of the Royal Society A: Mathematical, Physical and Engineering Sciences*, *461*(2060), 2563–2572.

[26] Garrett, C. and Cummins, P. (2007). The efficiency of a turbine in a tidal channel. *Journal of Fluid Mechanics*, *588*(September 2007).

[27] Garrett, C. and Cummins, P. (2008). Limits to tidal current power. *Renewable Energy*, *33*(11), 2485–2490.

[28] Georgia Tech Research Corporation (2011). Assessment of Energy Production Potential from Tidal Streams in the United States. Technical report.

[29] Grabbe, M. r. (2013). *Hydro-Kinetic Energy Conversion - Resource and Technology*.

[30] Grabbe, M. r., Lalander, E., Lundin, S., and Leijon, M. (2009). A review of the tidal current energy resource in Norway. *Renewable and Sustainable Energy Reviews*, *13*(8), 1898–1909.

[31] Gross, R., Leach, M., and Bauen, A. (2003). Progress in renewable energy. *Environment international*, *29*(1), 105–22.

[32] IEA Energy Technology Network (2010). Marine Energy. Technical Report November.

[33] International Energy Agency (2012). World Energy Outlook 2012. Technical report.

[34] Jäger-Waldau, A., Szabó, M., Scarlat, N., and Monforti-Ferrario, F. (2011). Renewable electricity in Europe. *Renewable and Sustainable Energy Reviews*, *15*(8), 3703–3716.

[35] Jangamshetti, S. H. and Rau, V. G. (2001). Optimum siting of wind turbine generators. *IEEE Transactions on Energy Conservation*, *16*(1), 8–13.

[36] Karsten, R. H., McMillan, J. M., Lickley, M. J., and Haynes, R. D. (2008). Assessment of tidal current energy in the Minas Passage, Bay of Fundy. *Proceedings of the Institution of Mechanical Engineers, Part A: Journal of Power and Energy*, *222*(5), 493–507.

[37] Khan, J. and Bhuyan, G. S. (2009). Ocean Energy: Global Technology Development Status. Technical report.

[38] Kim, K.-P., Ahmed, M. R., and Lee, Y.-H. (2012). Efficiency improvement of a tidal current turbine utilizing a larger area of channel. *Renewable Energy*, *48*, 557–564.

[39] Lehr, U., Nitsch, J., Kratzat, M., Lutz, C., and Edler, D. (2008). Renewable energy and employment in Germany. *Energy Policy*, *36*(1), 108–117.

[40] Li, Y. and Calisal, S. M. (2010). Estimating Power Output from a Tidal Current Turbine Farm with First-order Approximation of Hydrodynamic Interaction between Turbines. *International Journal of Green Energy*, *7*(2), 153–163.

[41] Li, Y., Lence, B. J., and Calisal, S. M. (2011). An integrated model for estimating energy cost of a tidal current turbine farm. *Energy Conversion and Management*, *52*(3), 1677–1687.

[42] Neill, S. P., Litt, E. J., Couch, S. J., and Davies, A. G. (2009). The impact of tidal stream turbines on large-scale sediment dynamics. *Renewable Energy*, *34*(12), 2803–2812.

[43] O Rourke, F., Boyle, F., and Reynolds, A. (2010). Tidal energy update 2009. *Applied Energy*, *87*(2), 398–409.

[44] O'Rourke, F., Boyle, F., and Reynolds, A. (2010). Tidal current energy resource assessment in Ireland: Current status and future update. *Renewable and Sustainable Energy Reviews*, *14*(9), 3206–3212.

[45] Plew, D. R. and Stevens, C. L. (2013). Numerical modelling of the effect of turbines on currents in a tidal channel - Tory Channel, New Zealand. *Renewable Energy*, *57*, 269–282.

[46] RenewableUK (2012). Marine Energy in the UK - State of the Industry Report 2012. Technical Report March.

[47] Romão da Silva Melo, R. and da Silveira Neto, A. (2012). Integral analysis of rotors of a wind generator. *Renewable and Sustainable Energy Reviews*, *16*(7), 4809–4817.

[48] Rourke, F. O., Boyle, F., and Reynolds, A. (2009). Renewable energy resources and technologies applicable to Ireland. *Renewable and Sustainable Energy Reviews*, *13*(8), 1975–1984.

[49] Rourke, F. O., Boyle, F., and Reynolds, A. (2010). Marine current energy devices: Current status and possible future applications in Ireland. *Renewable and Sustainable Energy Reviews*, *14*(3), 1026–1036.

[50] Schleicher-Tappeser, R. (2012). How renewables will change electricity markets in the next five years. *Energy Policy*, *48*, 64–75.

[51] Stevens, C., Sutton, P., Smith, M., and Dickson, R. (2008). Tidal flows in Te Aumiti (French Pass), South Island, New Zealand. *New Zealand Journal of Marine and Freshwater Research*, *42*(4), 451–464.

[52] Sustainable Energy Ireland (2004). Tidal & Current Energy Resources in Ireland. Technical report.

[53] Sutherland, G., Foreman, M., and Garrett, C. (2007). Tidal current energy assessment for Johnstone Strait, Vancouver Island. *Proceedings of the Institution of Mechanical Engineers, Part A: Journal of Power and Energy*, *221*(2), 147–157.

[54] Tarbotton, M. and Larson, M. (2006). Canada Ocean Energy Atlas (Phase 1) - Potential Tidal Current Energy Resources - Analysis Background.

[55] TNS Opinion & Social (2010). Special Eurobarometer 324 - Europeans and Nuclear Safety. Technical report, European Commission.

[56] Vennell, R. (2010). Tuning turbines in a tidal channel. *Journal of Fluid Mechanics*, *663*, 253–267.

[57] Vennell, R. (2011a). Estimating the power potential of tidal currents and the impact of power extraction on flow speeds. *Renewable Energy*, *36*(12), 3558–3565.

[58] Vennell, R. (2011b). Tuning tidal turbines in-concert to maximise farm efficiency. *Journal of Fluid Mechanics*, *671*, 587–604.

[59] Vennell, R. (2012a). Realizing the potential of tidal currents and the efficiency of turbine farms in a channel. *Renewable Energy*, *47*, 95–102.

[60] Vennell, R. (2012b). The energetics of large tidal turbine arrays. *Renewable Energy*, *48*, 210–219.

[61] Vennell, R. (2013). Exceeding the Betz limit with tidal turbines. *Renewable Energy*, *55*, 277–285.

[62] Walkington, I. and Burrows, R. (2009). Modelling tidal stream power potential. *Applied Ocean Research*, *31*(4), 239–245.

# Appendix A

# Data Tables for Ocean and Lagoon Channels

Tables A.1 and A.2 present the input data used to calculate the power potentials of all the ocean and lagoon channels included in this study respectively. In both tables, data are organised by country in alphabetical order.

Table A.1: Physical characteristics of all the ocean channels included in this study, organised in alphabetical order by country and comprising the site names, the widths $w$, the depths $h$, the lengths $L$ and the velocities $v$, with all data displayed in SI units. Country codes can be found in the Nomenclature.

| Country | Site Name | $w\ (m)$ | $h\ (m)$ | $L\ (m)$ | $v\ (m\,s^{-1})$ |
|---|---|---|---|---|---|
| OZ | Adolphus Channel | 6445 | 17 | 14260 | 1.8 |
| | Banks Strait | 16112 | 45 | 22039 | 2.6 |
| CA | Active Pass | 561 | 20 | 1222 | 4.1 |
| | Algernine Narrows | 2000 | 59 | 8593 | 5.1 |
| | Arran Rapids | 271 | 22 | 1370 | 6.2 |
| | Beaver Passage | 810 | 100 | 12038 | 2.1 |
| | Bellot Strait | 1000 | 16 | 25743 | 4.1 |
| | Cache Pt Channel | 6000 | 10 | 13520 | 2.6 |
| | Current Passage 1 | 1398 | 100 | 4186 | 2.6 |
| | Current Passage 2 | 1502 | 80 | 3074 | 3.1 |
| | Dent Rapids | 420 | 45 | 796 | 4.9 |
| | Discovery Pass. S. | 1459 | 42 | 7241 | 3.6 |

| Country | Site Name | $w\ (m)$ | $h\ (m)$ | $L\ (m)$ | $v\ (ms^{-1})$ |
|---|---|---|---|---|---|
| | Dodd Narrows | 91 | 9 | 611 | 4.4 |
| | Draney Narrows | 139 | 8 | 907 | 4.6 |
| | Egg Island | 750 | 25 | 3297 | 3.6 |
| | Gabriola Pass. | 137 | 8 | 2130 | 4.5 |
| | Gillard Passage 1 | 237 | 16 | 815 | 5.9 |
| | Gillard Passage 2 | 393 | 10 | 444 | 4.6 |
| | Gran Manan Channel | 5446 | 80 | 23891 | 1.2 |
| | Gray Strait | 6000 | 550 | 5741 | 3.1 |
| | Greene Pt Rap. 1 | 440 | 25 | 1722 | 3.6 |
| | Hawkins Narrows | 55 | 3 | 685 | 4.1 |
| | Head Harbour Passage 1 | 890 | 65 | 3797 | 2.6 |
| | Hidden Inlet | 142 | 3 | 945 | 4.6 |
| | Hole-in-the-Wall 1 | 189 | 8 | 778 | 5.5 |
| | Kildidt Narrows | 75 | 2 | 1611 | 6.2 |
| | Koksoak Entrance | 2000 | 40 | 6334 | 3.1 |
| | Labrador Narrows | 1500 | 100 | 6593 | 3.1 |
| | Lacy/Lawson Is | 2750 | 80 | 6186 | 3.6 |
| | Lower Rapids 1 | 371 | 8 | 1130 | 3.6 |
| | Lubec Narrows | 180 | 3 | 1074 | 3.6 |
| | McLelan Strait | 200 | 8 | 3926 | 3.6 |
| | Mill - Baffin Is | 26125 | 229 | 5482 | 4.1 |
| | Mill - Salisbury Is | 32054 | 204 | 7001 | 4.1 |
| | N Boundary Passage | 5158 | 140 | 1648 | 2.1 |
| | Nahwitti Bar 1 | 2993 | 9 | 3148 | 2.8 |
| | Nakertok Narrows | 1100 | 6 | 3185 | 4.6 |
| | Nakwakto Rapids | 434 | 10 | 1778 | 7.7 |
| | Nettilling Fiord | 1700 | 5 | 12779 | 4.1 |
| | Nitinat Narrows | 61 | 20 | 111 | 4.1 |
| | Nottingham Is - Ungava | 64098 | 228 | 3593 | 4.1 |

| Country | Site Name | $w\ (m)$ | $h\ (m)$ | $L\ (m)$ | $v\ (ms^{-1})$ |
|---|---|---|---|---|---|
| | Old Sow | 625 | 60 | 426 | 3.1 |
| | Otter Passage | 620 | 50 | 6649 | 3.1 |
| | Outer Narrows | 210 | 17 | 1111 | 4.4 |
| | Passage de Ile aux Coudres | 1700 | 30 | 15927 | 2.8 |
| | Petit Passage | 335 | 18 | 4111 | 3.6 |
| | Placentia Gut | 80 | 3 | 370 | 4.6 |
| | Pointe Amour | 1500 | 35 | 81858 | 2.3 |
| | Porcher Narrows | 120 | 10 | 1741 | 3.6 |
| | Porlier Pass | 339 | 15 | 1556 | 4.4 |
| | Quatsino Narrows | 207 | 18 | 2630 | 4.4 |
| | Race Passage | 884 | 20 | 1685 | 3.3 |
| | Reversing Falls | 90 | 15 | 333 | 6.2 |
| | Riviere Arnaud (Payne) Entrance | 2300 | 9 | 5482 | 4.6 |
| | Riviere George Entrance | 3000 | 35 | 15186 | 4.1 |
| | Salisbury - Notthingham Is | 22146 | 147 | 11668 | 4.1 |
| | Scott Channel | 9970 | 22 | 5074 | 1.5 |
| | Sechelt Rapids 2 | 261 | 8 | 1648 | 7.8 |
| | Seymour Narrows | 769 | 41 | 3019 | 7.7 |
| | Smoky Narrows | 1500 | 55 | 2630 | 6.2 |
| | South Pender Is | 1985 | 100 | 4223 | 2.1 |
| | Stuart Narrows | 261 | 7 | 852 | 3.3 |
| | Upper rapids 2 | 242 | 18 | 500 | 4.6 |
| | Weyton Passage | 1535 | 75 | 3093 | 3.1 |
| | Whirlpool Rapids | 321 | 28 | 1593 | 3.6 |
| | Yuculta Rapids | 539 | 20 | 3148 | 5.1 |
| CH | Chacao Channel | 2408 | 82 | 18150 | 5.0 |
| | Chiloé Island 1 | 7149 | 130 | 14446 | 1.3 |
| | Chiloé Island 2 | 6093 | 110 | 23520 | 1.2 |
| IR | Blasket Sound | 1463 | 17 | 2037 | 1.0 |
| | Clare Is | 4148 | 13 | 5445 | 0.6 |
| | Dursey Sound | 148 | 18 | 870 | 2.1 |

| Country | Site Name | $w\ (m)$ | $h\ (m)$ | $L\ (m)$ | $v\ (ms^{-1})$ |
|---|---|---|---|---|---|
| | Foul Sound | 1741 | 34 | 3445 | 0.8 |
| | Gascanane Sound | 1222 | 15 | 685 | 1.5 |
| | Gregory's Sound | 1648 | 34 | 3574 | 1.0 |
| | Inishshark | 1019 | 22 | 3334 | 1.3 |
| | Inishtrahull Sound | 5334 | 50 | 1296 | 2.1 |
| | Rusk Channel | 1167 | 15 | 6371 | 0.8 |
| | Scariff Deenish Is | 574 | 40 | 889 | 0.8 |
| | Tuskar Rock | 5686 | 28 | 1685 | 1.3 |
| | West Arklow Bank | 8945 | 23 | 23150 | 1.0 |
| | West Mullet | 3445 | 21 | 10001 | 1.0 |
| IT | Strait of Messina | 3056 | 70 | 519 | 2.3 |
| JP | Kanmon Strait | 1500 | 14 | 27780 | 5.0 |
| | Naruto Strait | 556 | 50 | 963 | 2.0 |
| NZ | Cook Strait | 25002 | 150 | 100008 | 1.1 |
| | Foveaux Strait | 10742 | 20 | 37040 | 1.3 |
| | French Pass | 148 | 65 | 722 | 2.5 |
| | Tory Channel | 852 | 55 | 7760 | 1.0 |
| NW | Akterøya - Aslakøya | 100 | 7 | 370 | 2.1 |
| | Ballstadstraumen | 350 | 15 | 1611 | 1.5 |
| | Brasøysundet | 70 | 6 | 105564 | 2.6 |
| | Burøysund | 100 | 5 | 741 | 1.0 |
| | Engsundet | 150 | 9 | 278 | 3.1 |
| | Gimsøystraumen | 450 | 12 | 1759 | 2.3 |
| | Gjøssøysundet | 250 | 5 | 1148 | 2.1 |
| | Godfjorden | 400 | 7 | 630 | 1.5 |
| | Graddstraumen | 300 | 5 | 815 | 3.1 |
| | Grøtøysundet Troms | 1100 | 35 | 2834 | 2.1 |
| | Grovfjorden | 50 | 5 | 1278 | 2.1 |
| | Hamsundpollen | 50 | 5 | 148 | 1.5 |
| | Havøysundet | 50 | 6 | 1593 | 1.5 |
| | Inner Andamsfjorden | 300 | 12 | 1204 | 1.0 |
| | Kågsundet | 500 | 100 | 4334 | 1.0 |

| Country | Site Name | $w\ (m)$ | $h\ (m)$ | $L\ (m)$ | $v\ (ms^{-1})$ |
|---|---|---|---|---|---|
| | Kaldvågsstraumen | 100 | 7 | 1111 | 3.1 |
| | Kamøysundet - Lilla Kamøya | 50 | 6 | 389 | 4.1 |
| | Kjellingsundet | 400 | 5 | 315 | 2.1 |
| | Kjerringvikstraumen | 100 | 9 | 815 | 2.6 |
| | Kjøfjorden | 200 | 15 | 1130 | 1.0 |
| | Kråkøya | 400 | 50 | 1408 | 2.1 |
| | Kvalsundet | 600 | 45 | 3445 | 1.8 |
| | Kvalsundet Troms | 770 | 15 | 1796 | 3.1 |
| | Lauksundet | 400 | 12 | 1519 | 1.0 |
| | Magerøysundet | 1100 | 40 | 5334 | 2.1 |
| | Måsøysundet | 2500 | 40 | 2204 | 1.5 |
| | Maursundet | 800 | 32 | 7964 | 1.0 |
| | Meistervik | 100 | 6 | 778 | 2.1 |
| | Mjøsundet | 200 | 22 | 370 | 1.0 |
| | Moskenstraumen | 4000 | 45 | 2296 | 3.1 |
| | Nærøysundet | 200 | 40 | 1648 | 2.3 |
| | Nappstraumen | 1000 | 17 | 2926 | 1.0 |
| | Nesnakroken | 1600 | 9 | 3241 | 1.0 |
| | Øyhellsundet | 350 | 3 | 1241 | 2.1 |
| | Reinøyspira | 200 | 27 | 2482 | 1.0 |
| | Remmastraumen | 12 | 3 | 704 | 2.1 |
| | Rystraumen | 480 | 30 | 1130 | 3.1 |
| | Saltstraumen | 130 | 25 | 315 | 4.4 |
| | Sandtorgstraumen | 600 | 10 | 1945 | 2.1 |
| | Sørsalten | 40 | 4 | 704 | 3.3 |
| | Sørsundet | 200 | 3 | 296 | 2.1 |
| | Spannbogstraumen | 100 | 7 | 3297 | 1.5 |
| | Steikarviksundet | 300 | 6 | 1759 | 1.0 |
| | Store Vågsøysundet | 1000 | 40 | 1148 | 2.1 |
| | Støtt strait | 150 | 5 | 926 | 3.1 |
| | Toftsundet | 200 | 15 | 1037 | 2.1 |
| | Trangstraumen | 200 | 12 | 2445 | 2.1 |
| | Trollsundet | 1000 | 19 | 4148 | 3.1 |

| Country | Site Name | $w\ (m)$ | $h\ (m)$ | $L\ (m)$ | $v\ (ms^{-1})$ |
|---|---|---|---|---|---|
| | Tromsøysundet | 200 | 8 | 1408 | 1.5 |
| | Vesterstraumen | 130 | 3 | 648 | 3.1 |
| SG | Singapore Strait | 9630 | 17 | 67042 | 3.0 |
| UK | Bardsey Island | 2463 | 38 | 2963 | 2.8 |
| | Big Russel | 4315 | 30 | 4278 | 1.9 |
| | Bluemull Sound | 630 | 32 | 4315 | 2.6 |
| | Burra Sound | 259 | 9 | 945 | 1.9 |
| | Cantik Sound | 1037 | 16 | 982 | 1.8 |
| | Copinsay Pass | 1278 | 8 | 1926 | 1.5 |
| | Corran Narrows | 204 | 13 | 407 | 1.7 |
| | Dover Strait | 28706 | 30 | 13705 | 1.1 |
| | English Channel | 91859 | 50 | 49263 | 1.5 |
| | Eynhallow Sound | 500 | 22 | 2834 | 1.2 |
| | Gulf of Corryvreckan | 963 | 80 | 2908 | 4.4 |
| | Gunna Sound | 796 | 9 | 1389 | 1.3 |
| | Hoy Sound | 444 | 12 | 945 | 3.5 |
| | Jack Sound | 315 | 17 | 963 | 3.3 |
| | Kyle Rhea | 185 | 19 | 3611 | 3.3 |
| | Loch Leven Narrows | 111 | 4 | 852 | 2.6 |
| | N Ronaldsay Firth | 2241 | 14 | 6686 | 1.8 |
| | North Carna | 389 | 35 | 611 | 1.3 |
| | North Channel - Kintyre Peninsula | 19261 | 110 | 10371 | 1.4 |
| | North Channel - The Rhins | 30373 | 100 | 45930 | 0.9 |
| | North East Jersey | 5019 | 25 | 8704 | 1.6 |
| | North Isle of Man | 25558 | 30 | 25558 | 1.4 |
| | Pentland Firth Deep | 8704 | 60 | 30188 | 2.1 |
| | Pentland Firth Shallow | 1667 | 28 | 6093 | 2.6 |
| | Race of Alderney | 8927 | 32 | 5371 | 1.9 |
| | Ramsey Sound | 870 | 29 | 2778 | 3.1 |
| | Sanda Sound | 1871 | 30 | 3093 | 2.3 |

| Country | Site Name | $w\ (m)$ | $h\ (m)$ | $L\ (m)$ | $v\ (ms^{-1})$ |
|---|---|---|---|---|---|
| | Severn Estuary | 10186 | 16 | 44078 | 1.3 |
| | Sound of Eigg | 3741 | 35 | 4852 | 2.1 |
| | Sound of Handa | 482 | 21 | 1074 | 1.3 |
| | Sound of Islay | 1259 | 21 | 17038 | 2.3 |
| | Sound of Mull | 1704 | 30 | 1296 | 1.1 |
| | South Canna | 8186 | 27 | 1389 | 1.8 |
| | St George's Channel - Carmel Head | 86859 | 55 | 24261 | 1.2 |
| | St George's Channel - St David's Head | 68339 | 70 | 10927 | 0.7 |
| | Staple Sound | 945 | 12 | 1093 | 2.1 |
| | Switha Sound | 926 | 25 | 1593 | 1.5 |
| | The Swinge | 1352 | 17 | 3426 | 2.4 |
| | West Islay | 54634 | 45 | 25187 | 1.1 |
| | West Luing | 1796 | 22 | 815 | 3.1 |
| | Westray Firth | 3111 | 27 | 5982 | 1.9 |
| | Yell Sound - West Channel | 648 | 23 | 1926 | 2.1 |
| US | Adak Strait | 11482 | 29 | 8038 | 1.1 |
| | Akutan - Akun Is | 630 | 6 | 463 | 1.9 |
| | Akutan Pass | 4352 | 21 | 2296 | 1.4 |
| | Atka - Amlia Is | 1000 | 16 | 907 | 1.9 |
| | Avatanak Strait | 5889 | 38 | 11668 | 1.1 |
| | Chugul - Tagalak Is | 2074 | 12 | 1296 | 1.4 |
| | Derbin Strait | 1722 | 37 | 4037 | 1.4 |
| | Fenimore - Ikiginak Is | 5223 | 21 | 1389 | 1.4 |
| | Florida Keys | 2278 | 10 | 1056.00 | 1.4 |
| | Igitkin - Chugul Is | 1426 | 25 | 1370 | 1.1 |

| Country | Site Name | $w\ (m)$ | $h\ (m)$ | $L\ (m)$ | $v\ (ms^{-1})$ |
|---|---|---|---|---|---|
| | Igitkin - Great Sitkin Is | 4074 | 30 | 1111 | 1.1 |
| | Little Tanaga - Kagalaska Is 1 | 1167 | 17 | 833 | 1.4 |
| | Little Tanaga - Kagalaska Is 2 | 1037 | 33 | 611 | 1.4 |
| | Muskeget - Chappaquiddick Is | 11297 | 12 | 2222 | 1.9 |
| | Muskeget - Tuckernuck Is | 2093 | 4 | 1204 | 1.9 |
| | N of Whale Is | 982 | 6 | 1148 | 1.7 |
| | Oglodak - Atka Is | 6538 | 21 | 1389 | 1.4 |
| | S of Whale Is | 852 | 15 | 4611 | 1.9 |
| | Sundstrom - Sitkinak Is | 4260 | 13 | 3760 | 1.4 |
| | Tanaga - Kanaga Is | 7223 | 22 | 7852 | 1.1 |
| | Ugamak Strait | 5093 | 30 | 5241 | 1.1 |
| | Umnak Pass | 5815 | 38 | 10001 | 1.2 |
| | Unalga Pass | 2722 | 22 | 2296 | 1.9 |
| | Vineyard Sound | 5389 | 40 | 3222 | 1.2 |

The following table, Table A.2, includes information regarding the physical characteristics of the lagoon channels included in this study organised in alphabetical order by country as aforementioned.

Table A.2: Physical characteristics of all the lagoon channels included in this study, organised in alphabetical order by country and comprising the site names, the widths $w$, the depths $h$, the lengths $L$ the lagoon surface areas $A_L$ and the tidal elevations $\eta_{01}$ with all data displayed in SI units except the lagoon surface areas expressed in $km^2$. Country codes can be found in the Nomenclature.

| Country | Site Name | $w\ (m)$ | $h\ (m)$ | $L\ (m)$ | $A_L\ (km^2)$ | $\eta_{01}\ (m)$ |
|---|---|---|---|---|---|---|
| OZ | Broad Sound | 22965 | 12 | 14260 | 1040 | 3.2 |
| | King Sound | 12594 | 65 | 20557 | 4191 | 4.6 |
| CA | Minas Basin | 4376 | 56 | 12038 | 1000 | 4.7 |
| IR | Bertraghboy Bay | 389 | 15 | 630 | 38 | 1.4 |
| | Bull's Mouth | 3000 | 5 | 2963 | 13 | 1.3 |
| | Dingle Harbour | 111 | 5 | 500 | 265 | 1.2 |
| | Greatman's Bay | 741 | 8 | 3723 | 327 | 1.5 |
| | Kilkieran Bay | 1463 | 10 | 1074 | 12 | 1.5 |
| | Lough Foyle | 1037 | 16 | 1204 | 41 | 0.7 |
| | River Shannon | 3130 | 20 | 1852 | 160 | 1.4 |
| | Youghal | 315 | 5 | 1463 | 3 | 1.4 |
| NZ | Kaipara Harbour | 2500 | 25 | 15001 | 580 | 1.1 |
| UK | Cromarty Firth | 926 | 32 | 2667 | 62 | 1.3 |
| | Firth of Forth | 982 | 40 | 1278 | 62 | 1.8 |
| | Firth of Tay | 1000 | 9 | 3760 | 79 | 1.7 |
| | Inverness Firth | 1130 | 30 | 759 | 70 | 1.4 |
| | Loch Carron | 333 | 12 | 2204 | 14 | 1.7 |
| | Loch Sligachan | 148 | 4 | 259 | 2 | 1.5 |
| | Menai Strait | 241 | 14 | 1796 | 13 | 1.6 |
| | Morecambe Bay | 1685 | 37 | 5408 | 4 | 3.2 |
| | Plymouth Sound | 278 | 22 | 352 | 16 | 1.7 |
| | Poole Harbour | 278 | 14 | 148 | 22 | 0.5 |
| | Strangford Lough | 463 | 30 | 8482 | 101 | 1.7 |
| | The Wash | 6704 | 21 | 8982 | 345 | 2.4 |
| US | Cobscook Bay | 870 | 14 | 5019 | 58 | 3.3 |
| | Cook Inlet | 13890 | 34 | 10927 | 3623 | 3.7 |
| | Cooper River | 907 | 7 | 2797 | 186 | 0.9 |
| | Delaware Bay | 15927 | 9 | 7038 | 2102 | 1.0 |

| Country | Site Name | $w\ (m)$ | $h\ (m)$ | $L\ (m)$ | $A_L\ (km^2)$ | $\eta_{01}\ (m)$ |
|---|---|---|---|---|---|---|
| | Grays Harbor | 1574 | 8 | 8112 | 147 | 1.3 |
| | Hague Channel | 7686 | 17 | 8278 | 554 | 2.3 |
| | North Edisto River | 519 | 12 | 4945 | 86 | 1.1 |
| | Satilla River | 1037 | 7 | 4482 | 152 | 1.2 |
| | Taku inlet | 2648 | 10 | 5797 | 85 | 2.2 |

# Appendix B

# Key for Channel Identification

Tables B.1 and B.2 present the key used to respectively identify ocean and lagoon channels in some of the figures found in Section 3.3.

Table B.1: Key for the identification of the ocean channels as represented on some of the figures in Section 3.3.

| **Range of Potential Upper Limit** | **Colour** | **Number** | **Site Name** |
|---|---|---|---|
| $> 10\,GW$ | Brown | 1 | Nottingham Is - Ungava |
| | | 2 | Mill - Salisbury Is |
| | | 3 | Salisbury - Notthingham Is |
| | | 4 | Mill - Baffin Is |
| | | 5 | English Channel |
| | | 6 | Cook Strait |
| $> 1\,GW\ \&\ < 10\,GW$ | Red | 1 | Singapore Strait |
| | | 2 | Gray Strait |
| | | 3 | St George's Channel - Carmel Head |
| | | 4 | North Channel - The Rhins |
| | | 5 | Banks Strait |
| | | 6 | Chacao Channel |
| | | 7 | West Islay |
| | | 8 | Pentland Firth Deep |
| | | 9 | Kanmon Strait |
| | | 10 | Riviere George Entrance |

| Range of Potential Upper Limit | Colour | Number | Site Name |
|---|---|---|---|
| | | 11 | North Channel - Kintyre Peninsula |
| | | 12 | North Isle of Man |
| | | 13 | Algernine Narrows |
| $> 100\,MW$ & $< 1\,GW$ | Orange | 1 | St George's Channel - St David's Head |
| | | 2 | Pointe Amour |
| | | 3 | Chiloé Island 1 |
| | | 4 | Bellot Strait |
| | | 5 | Chiloé Island 2 |
| | | 6 | Nettilling Fiord |
| | | 7 | Lacy/Lawson Is |
| | | 8 | Cache Pt Channel |
| | | 9 | Severn Estuary |
| | | 10 | Riviere Arnaud (Payne) Entrance |
| | | 11 | Foveaux Strait |
| | | 12 | Seymour Narrows |
| | | 13 | Dover Strait |
| | | 14 | Gran Manan Channel |
| | | 15 | Smoky Narrows |
| | | 16 | Passage de Ile aux Coudres |
| | | 17 | Labrador Narrows |
| | | 18 | Adolphus Channel |
| | | 19 | Discovery Pass. S. |
| | | 20 | Koksoak Entrance |
| | | 21 | Race of Alderney |
| | | 22 | West Arklow Bank |
| | | 23 | N Boundary Passage |
| | | 24 | Moskenstraumen |
| | | 25 | Gulf of Corryvreckan |
| | | 26 | Nakwakto Rapids |
| | | 27 | Nakertok Narrows |
| | | 28 | Beaver Passage |
| | | 29 | Sound of Islay |
| | | 30 | Current Passage 1 |

| Range of Potential Upper Limit | Colour | Number | Site Name |
|---|---|---|---|
| | | 31 | Current Passage 2 |
| | | 32 | Weyton Passage |
| | | 33 | South Pender Is |
| | | 34 | North East Jersey |
| | | 35 | Adak Strait |
| | | 36 | Scott Channel |
| | | 37 | Umnak Pass |
| | | 38 | Avatanak Strait |
| | | 39 | Sound of Eigg |
| $> 50\,MW$ & $< 100\,MW$ | Yellow | 1 | Yuculta Rapids |
| | | 2 | Bardsey Island |
| | | 3 | Nahwitti Bar 1 |
| | | 4 | Pentland Firth Shallow |
| | | 5 | Sechelt Rapids 2 |
| | | 6 | Muskeget - Chappaquiddick Is |
| | | 7 | Otter Passage |
| | | 8 | Big Russel |
| | | 9 | Westray Firth |
| | | 10 | Trollsundet |
| | | 11 | Tanaga - Kanaga Is |
| | | 12 | Egg Island |
| | | 13 | Brasøysundet |
| $> 20\,MW$ & $< 50\,MW$ | Green | 1 | Inishtrahull Sound |
| | | 2 | Head Harbour Passage 1 |
| | | 3 | N Ronaldsay Firth |
| | | 4 | Sanda Sound |
| | | 5 | South Canna |
| | | 6 | Arran Rapids |
| | | 7 | Magerøysundet |
| | | 8 | Ramsey Sound |
| | | 9 | Vineyard Sound |
| | | 10 | Ugamak Strait |
| | | 11 | The Swinge |

| Range of Potential Upper Limit | Colour | Number | Site Name |
|---|---|---|---|
| | | 12 | Petit Passage |
| | | 13 | West Mullet |
| | | 14 | Bluemull Sound |
| | | 15 | Race Passage |
| | | 16 | Unalga Pass |
| | | 17 | Sundstrom - Sitkinak Is |
| | | 18 | Active Pass |
| $> 10\,MW$ & $< 20\,MW$ | Turquoise | 1 | West Luing |
| | | 2 | Quatsino Narrows |
| | | 3 | Strait of Messina |
| | | 4 | Dent Rapids |
| | | 5 | Porlier Pass |
| | | 6 | Kvalsundet Troms |
| | | 7 | Måsøysundet |
| | | 8 | Grøtøysundet Troms |
| | | 9 | Gillard Passage 1 |
| | | 10 | Derbin Strait |
| | | 11 | Akutan Pass |
| | | 12 | Greene Pt Rap. 1 |
| | | 13 | McLelan Strait |
| | | 14 | Tuskar Rock |
| | | 15 | Oglodak - Atka Is |
| | | 16 | S of Whale Is |
| | | 17 | Tory Channel |
| | | 18 | Kildidt Narrows |
| | | 19 | Fenimore - Ikiginak Is |
| | | 20 | Whirlpool Rapids |
| | | 21 | Gabriola Pass. |
| | | 22 | Kyle Rhea |
| | | 23 | Hole-in-the-Wall 1 |
| | | 24 | Kvalsundet |
| $> 1\,MW$ & $< 10\,MW$ | Blue | 1 | Outer Narrows |
| | | 2 | Lower Rapids 1 |

| Range of Potential Upper Limit | Colour | Number | Site Name |
|---|---|---|---|
| | | 3 | Rystraumen |
| | | 4 | Kågsundet |
| | | 5 | Hoy Sound |
| | | 6 | Gillard Passage 2 |
| | | 7 | Muskeget - Tuckernuck Is |
| | | 8 | Maursundet |
| | | 9 | Store Vågsøysundet |
| | | 10 | Gregory's Sound |
| | | 11 | Yell Sound - West Channel |
| | | 12 | Hidden Inlet |
| | | 13 | Old Sow |
| | | 14 | Igitkin - Great Sitkin Is |
| | | 15 | Draney Narrows |
| | | 16 | Upper rapids 2 |
| | | 17 | Jack Sound |
| | | 18 | Inishshark |
| | | 19 | Sandtorgstraumen |
| | | 20 | Gimsøystraumen |
| | | 21 | Clare Is |
| | | 22 | Porcher Narrows |
| | | 23 | Kråkøya |
| | | 24 | Staple Sound |
| | | 25 | Copinsay Pass |
| | | 26 | Foul Sound |
| | | 27 | Lubec Narrows |
| | | 28 | Naruto Strait |
| | | 29 | Chugul - Tagalak Is |
| | | 30 | Stuart Narrows |
| | | 31 | Switha Sound |
| | | 32 | Florida Keys |
| | | 33 | Graddstraumen |
| | | 34 | Reversing Falls |
| | | 35 | Atka - Amlia Is |

| Range of Potential Upper Limit | Colour | Number | Site Name |
|---|---|---|---|
| | | 36 | Cantik Sound |
| | | 37 | Nesnakroken |
| | | 38 | Nærøysundet |
| | | 39 | Sound of Mull |
| | | 40 | Rusk Channel |
| | | 41 | N of Whale Is |
| | | 42 | Blasket Sound |
| | | 43 | Igitkin - Chugul Is |
| | | 44 | Nappstraumen |
| | | 45 | Dodd Narrows |
| | | 46 | Trangstraumen |
| | | 47 | Støtt strait |
| | | 48 | Øyhellsundet |
| | | 49 | Gascanane Sound |
| | | 50 | Saltstraumen |
| | | 51 | Eynhallow Sound |
| | | 52 | French Pass |
| | | 53 | Little Tanaga - Kagalaska Is 1 |
| | | 54 | Little Tanaga - Kagalaska Is 2 |
| | | 55 | Kaldvågsstraumen |
| | | 56 | Placentia Gut |
| | | 57 | Hawkins Narrows |
| | | 58 | Gunna Sound |
| | | 59 | Gjøssøysundet |
| | | 60 | Vesterstraumen |
| | | 61 | Ballstadstraumen |
| $< 1\,MW$ | Violet | 1 | Akutan - Akun Is |
| | | 2 | Toftsundet |
| | | 3 | Burra Sound |
| | | 4 | Sound of Handa |
| | | 5 | Loch Leven Narrows |
| | | 6 | Kjerringvikstraumen |
| | | 7 | Kamøysundet—Lilla Kamøya |

| Range of Potential Upper Limit | Colour | Number | Site Name |
|---|---|---|---|
| | | 8 | Dursey Sound |
| | | 9 | Engsundet |
| | | 10 | Spannbogstraumen |
| | | 11 | Reinøyspira |
| | | 12 | Kjellingsundet |
| | | 13 | North Carna |
| | | 14 | Tromsøysundet |
| | | 15 | Sørsalten |
| | | 16 | Godfjorden |
| | | 17 | Scariff Deenish Is |
| | | 18 | Lauksundet |
| | | 19 | Meistervik |
| | | 20 | Steikarviksundet |
| | | 21 | Grovfjorden |
| | | 22 | Sørsundet |
| | | 23 | Inner Andamsfjorden |
| | | 24 | Nitinat Narrows |
| | | 25 | Corran Narrows |
| | | 26 | Kjøfjorden |
| | | 27 | Akterøya—Aslakøya |
| | | 28 | Havøysundet |
| | | 29 | Mjøsundet |
| | | 30 | Burøysund |
| | | 31 | Remmastraumen |
| | | 32 | Hamsundpollen |

Table B.2: Key for the identification of the lagoon channels as represented on some of the figures in Section 3.3.

| **Range of Potential Upper Limit** | **Colour** | **Letter** | **Site Name** |
|---|---|---|---|
| $> 10\,GW$ | Brown | a | King Sound |
| | | b | Cook Inlet |
| $> 1\,GW$ & $< 10\,GW$ | Red | a | Minas Basin |
| | | b | Broad Sound |
| $> 100\,MW$ & $< 1\,GW$ | Orange | a | Hague Channel |
| | | b | The Wash |
| | | c | Delaware Bay |
| | | d | Kaipara Harbour |
| | | e | Cobscook Bay |
| | | f | Taku inlet |
| | | g | River Shannon |
| | | h | Strangford Lough |
| $> 50\,MW$ & $< 100\,MW$ | Yellow | a | Firth of Tay |
| | | b | Firth of Forth |
| | | c | Greatman's Bay |
| | | d | Grays Harbor |
| | | e | Inverness Firth |
| $> 20\,MW$ & $< 50\,MW$ | Green | a | Satilla River |
| | | b | Cromarty Firth |
| | | c | North Edisto River |
| | | d | Cooper River |
| | | e | Bertraghboy Bay |
| $> 10\,MW$ & $< 20\,MW$ | Turquoise | a | Plymouth Sound |
| | | b | Morecambe Bay |
| | | c | Loch Carron |
| | | d | Menai Strait |
| $> 1\,MW$ & $< 10\,MW$ | Blue | a | Dingle Harbour |
| | | b | Kilkieran Bay |
| | | c | Lough Foyle |
| | | d | Bull's Mouth |

| Range of Potential Upper Limit | Colour | Letter | Site Name |
|---|---|---|---|
| | | e | Poole Harbour |
| | | f | Youghal |
| | | g | Loch Sligachan |

# Appendix C

# Upper Limits of the Tidal Current Potentials of Ocean and Lagoon Channels

Tables C.1 and C.2 present the upper limits of the tidal current power potentials for each of the ocean and lagoon channels included in this study respectively. The tables also include the contribution to the country's resource of a given channel as well as the cumulative contribution from a channel and all its precessing ones. Overall potential resources are also given for each country. Data are organised by country from highest to lowest potentials in the order in which the countries are mentioned in Section 3.5.

Table C.1: Estimation of the upper tidal current potential limit for each of the ocean channels and for each of the countries included in this study. Country codes can be found in the Nomenclature.

| Country Rank | Overall Rank | Site Name | Upper Limit of Potential ($MW$) | Resource Contribution | Cumulative Contribution |
|---|---|---|---|---|---|
| **UK** | | | | | |
| 1 | 5 | English Channel | 16000 | 45% | 45% |
| 2 | 9 | St George's Channel - Carmel Head | 5500 | 15% | 60% |
| 3 | 10 | North Channel - The Rhins | 4000 | 11% | 71% |
| 4 | 13 | West Islay | 2400 | 6.7% | 77% |
| 5 | 14 | Pentland Firth Deep | 2300 | 6.2% | 83% |
| 6 | 17 | North Channel - Kintyre Peninsula | 1500 | 4.1% | 87% |
| 7 | 18 | North Isle of Man | 1300 | 3.5% | 91% |
| 8 | 20 | St George's Channel - St David's Head | 960 | 2.6% | 94% |
| 9 | 28 | Severn Estuary | 550 | 1.5% | 95% |
| 10 | 32 | Dover Strait | 460 | 1.2% | 96% |
| 11 | 40 | Race of Alderney | 200 | 0.56% | 97% |
| 12 | 44 | Gulf of Corryvreckan | 160 | 0.43% | 97% |
| 13 | 48 | Sound of Islay | 130 | 0.36% | 98% |
| 14 | 53 | North East Jersey | 110 | 0.31% | 98% |
| 15 | 58 | Sound of Eigg | 100 | 0.28% | 98% |
| 16 | 60 | Bardsey Island | 93 | 0.26% | 98% |

| Country Rank | Overall Rank | Site Name | Upper Limit of Potential (*MW*) | Resource Contribution | Cumulative Contribution |
|---|---|---|---|---|---|
| 17 | 62 | Pentland Firth Shallow | 90 | 0.24% | 99% |
| 18 | 66 | Big Russel | 73 | 0.2% | 99% |
| 19 | 67 | Westray Firth | 70 | 0.19% | 99% |
| 20 | 75 | N Ronaldsay Firth | 41 | 0.11% | 99% |
| 21 | 76 | Sanda Sound | 40 | 0.11% | 99% |
| 22 | 77 | South Canna | 40 | 0.11% | 100% |
| 23 | 80 | Ramsey Sound | 35 | 0.096% | 100% |
| 24 | 83 | The Swinge | 31 | 0.085% | 100% |
| 25 | 86 | Bluemull Sound | 25 | 0.069% | 100% |
| 26 | 91 | West Luing | 20 | 0.054% | 100% |
| 27 | 112 | Kyle Rhea | 11 | 0.031% | 100% |
| 28 | 119 | Hoy Sound | 7.5 | 0.021% | 100% |
| 29 | 125 | Yell Sound - West Channel | 5.7 | 0.016% | 100% |
| 30 | 131 | Jack Sound | 5 | 0.014% | 100% |
| 31 | 138 | Staple Sound | 4 | 0.011% | 100% |
| 32 | 139 | Copinsay Pass | 4 | 0.011% | 100% |
| 33 | 145 | Switha Sound | 3.4 | 0.0092% | 100% |
| 34 | 150 | Cantik Sound | 2.9 | 0.0079% | 100% |
| 35 | 153 | Sound of Mull | 2.4 | 0.0067% | 100% |
| 36 | 165 | Eynhallow Sound | 1.5 | 0.0041% | 100% |

| Country Rank | Overall Rank | Site Name | Upper Limit of Potential (*MW*) | Resource Contribution | Cumulative Contribution |
|---|---|---|---|---|---|
| 37 | 172 | Gunna Sound | 1.1 | 0.003% | 100% |
| 38 | 178 | Burra Sound | 0.77 | 0.0021% | 100% |
| 39 | 179 | Sound of Handa | 0.69 | 0.0019% | 100% |
| 40 | 180 | Loch Leven Narrows | 0.68 | 0.0019% | 100% |
| 41 | 188 | North Carna | 0.46 | 0.0013% | 100% |
| 42 | 200 | Corran Narrows | 0.18 | 0.00050% | 100% |
| | | **UK TOTAL** | **36000** | | |
| **IR** | | | | | |
| 1 | 41 | West Arklow Bank | 170 | 59% | 59% |
| 2 | 73 | Inishtrahull Sound | 50 | 17% | 76% |
| 3 | 85 | West Mullet | 27 | 9.3% | 86% |
| 4 | 104 | Tuskar Rock | 15 | 5.3% | 91% |
| 5 | 124 | Gregory's Sound | 6.9 | 2.4% | 93% |
| 6 | 132 | Inishshark | 4.7 | 1.6% | 95% |
| 7 | 135 | Clare Is | 4.3 | 1.5% | 96% |
| 8 | 140 | Foul Sound | 3.9 | 1.3% | 98% |
| 9 | 154 | Rusk Channel | 2.4 | 0.81% | 98% |
| 10 | 156 | Blasket Sound | 2 | 0.70% | 99% |
| 11 | 163 | Gascanane Sound | 1.5 | 0.52% | 100% |
| 12 | 183 | Dursey Sound | 0.54 | 0.19% | 100% |

| Country Rank | Overall Rank | Site Name | Upper Limit of Potential (*MW*) | Resource Contribution | Cumulative Contribution |
|---|---|---|---|---|---|
| 13 | 192 | Scariff Deenish Is | 0.39 | 0.13% | 100% |
| | | **IR TOTAL** | **290** | | |
| **CA** | | | | | |
| 1 | 1 | Nottingham Is - Ungava | 29000 | 26% | 26% |
| 2 | 2 | Mill - Salisbury Is | 25000 | 23% | 49% |
| 3 | 3 | Salisbury - Notthingham Is | 21000 | 19% | 68% |
| 4 | 4 | Mill - Baffin Is | 18000 | 16% | 84% |
| 5 | 8 | Gray Strait | 6200 | 5.6% | 90% |
| 6 | 16 | Riviere George Entrance | 1500 | 1.4% | 91% |
| 7 | 19 | Algernine Narrows | 1200 | 1.1% | 92% |
| 8 | 21 | Pointe Amour | 910 | 0.83% | 93% |
| 9 | 23 | Bellot Strait | 780 | 0.71% | 94% |
| 10 | 25 | Nettilling Fiord | 640 | 0.58% | 94% |
| 11 | 26 | Lacy/Lawson Is | 610 | 0.56% | 95% |
| 12 | 27 | Cache Pt Channel | 600 | 0.54% | 95% |
| 13 | 29 | Riviere Arnaud (Payne) Entrance | 530 | 0.48% | 96% |
| 14 | 31 | Seymour Narrows | 470 | 0.43% | 96% |
| 15 | 33 | Gran Manan Channel | 450 | 0.41% | 97% |
| 16 | 34 | Smoky Narrows | 450 | 0.41% | 97% |
| 17 | 35 | Passage de Ile aux Coudres | 310 | 0.29% | 98% |

| Country Rank | Overall Rank | Site Name | Upper Limit of Potential (*MW*) | Resource Contribution | Cumulative Contribution |
|---|---|---|---|---|---|
| 18 | 36 | Labrador Narrows | 310 | 0.28% | 98% |
| 19 | 38 | Discovery Pass. S. | 260 | 0.24% | 98% |
| 20 | 39 | Koksoak Entrance | 210 | 0.19% | 98% |
| 21 | 42 | N Boundary Passage | 160 | 0.15% | 98% |
| 22 | 45 | Nakwakto Rapids | 150 | 0.14% | 99% |
| 23 | 46 | Nakertok Narrows | 150 | 0.13% | 99% |
| 24 | 47 | Beaver Passage | 130 | 0.12% | 99% |
| 25 | 49 | Current Passage 1 | 120 | 0.11% | 99% |
| 26 | 50 | Current Passage 2 | 120 | 0.11% | 99% |
| 27 | 51 | Weyton Passage | 120 | 0.10% | 99% |
| 28 | 52 | South Pender Is | 110 | 0.10% | 99% |
| 29 | 55 | Scott Channel | 110 | 0.099% | 99% |
| 30 | 59 | Yuculta Rapids | 100 | 0.091% | 99% |
| 31 | 61 | Nahwitti Bar 1 | 91 | 0.083% | 99% |
| 32 | 63 | Sechelt Rapids 2 | 87 | 0.079% | 100% |
| 33 | 65 | Otter Passage | 76 | 0.069% | 100% |
| 34 | 71 | Egg Island | 53 | 0.048% | 100% |
| 35 | 74 | Head Harbour Passage 1 | 49 | 0.045% | 100% |
| 36 | 78 | Arran Rapids | 38 | 0.034% | 100% |
| 37 | 84 | Petit Passage | 28 | 0.026% | 100% |

| Country Rank | Overall Rank | Site Name | Upper Limit of Potential (*MW*) | Resource Contribution | Cumulative Contribution |
|---|---|---|---|---|---|
| 38 | 87 | Race Passage | 25 | 0.023% | 100% |
| 39 | 90 | Active Pass | 21 | 0.019% | 100% |
| 40 | 92 | Quatsino Narrows | 20 | 0.018% | 100% |
| 41 | 94 | Dent Rapids | 19 | 0.017% | 100% |
| 42 | 95 | Porlier Pass | 19 | 0.017% | 100% |
| 43 | 99 | Gillard Passage 1 | 17 | 0.015% | 100% |
| 44 | 102 | Greene Pt Rap. 1 | 16 | 0.015% | 100% |
| 45 | 103 | McLelan Strait | 16 | 0.014% | 100% |
| 46 | 108 | Kildidt Narrows | 12 | 0.011% | 100% |
| 47 | 110 | Whirlpool Rapids | 11 | 0.010% | 100% |
| 48 | 111 | Gabriola Pass. | 11 | 0.010% | 100% |
| 49 | 113 | Hole-in-the-Wall 1 | 10 | 0.0095% | 100% |
| 50 | 115 | Outer Narrows | 8.4 | 0.0077% | 100% |
| 51 | 116 | Lower Rapids 1 | 8.3 | 0.0075% | 100% |
| 52 | 120 | Gillard Passage 2 | 7.3 | 0.0067% | 100% |
| 53 | 126 | Hidden Inlet | 5.6 | 0.0051% | 100% |
| 54 | 127 | Old Sow | 5.5 | 0.005% | 100% |
| 55 | 129 | Draney Narrows | 5.3 | 0.0048% | 100% |
| 56 | 130 | Upper rapids 2 | 5.2 | 0.0047% | 100% |
| 57 | 136 | Porcher Narrows | 4.2 | 0.0038% | 100% |

| Country Rank | Overall Rank | Site Name | Upper Limit of Potential (*MW*) | Resource Contribution | Cumulative Contribution |
|---|---|---|---|---|---|
| 58 | 141 | Lubec Narrows | 3.8 | 0.0034% | 100% |
| 59 | 144 | Stuart Narrows | 3.5 | 0.0032% | 100% |
| 60 | 148 | Reversing Falls | 3 | 0.0027% | 100% |
| 61 | 159 | Dodd Narrows | 2 | 0.0018% | 100% |
| 62 | 170 | Placentia Gut | 1.2 | 0.0011% | 100% |
| 63 | 171 | Hawkins Narrows | 1.1 | 0.0010% | 100% |
| 64 | 199 | Nitinat Narrows | 0.21 | 0.00019% | 100% |
| | | **CA TOTAL** | **110000** | | |
| **NW** | | | | | |
| 1 | 43 | Moskenstraumen | 160 | 36% | 36% |
| 2 | 69 | Trollsundet | 55 | 13% | 49% |
| 3 | 72 | Brasøysundet | 53 | 12% | 61% |
| 4 | 79 | Magerøysundet | 36 | 8.2% | 69% |
| 5 | 96 | Kvalsundet Troms | 18 | 4.1% | 73% |
| 6 | 97 | Måsøysundet | 18 | 4.0% | 77% |
| 7 | 98 | Grøtøysundet Troms | 17 | 4.0% | 81% |
| 8 | 114 | Kvalsundet | 10 | 2.3% | 84% |
| 9 | 117 | Rystraumen | 8 | 1.8% | 85% |
| 10 | 118 | Kågsundet | 7.6 | 1.7% | 87% |
| 11 | 122 | Maursundet | 7.1 | 1.6% | 89% |

| Country Rank | Overall Rank | Site Name | Upper Limit of Potential ($MW$) | Resource Contribution | Cumulative Contribution |
|---|---|---|---|---|---|
| 12 | 123 | Store Vågsøysundet | 7 | 1.6% | 90% |
| 13 | 133 | Sandtorgstraumen | 4.5 | 1.0% | 91% |
| 14 | 134 | Gimsøystraumen | 4.3 | 0.99% | 92% |
| 15 | 137 | Kråkøya | 4.1 | 0.93% | 93% |
| 16 | 147 | Graddstraumen | 3 | 0.69% | 94% |
| 17 | 151 | Nesnakroken | 2.7 | 0.63% | 95% |
| 18 | 152 | Nærøysundet | 2.6 | 0.60% | 95% |
| 19 | 158 | Nappstraumen | 2 | 0.46% | 96% |
| 20 | 160 | Trangstraumen | 1.9 | 0.44% | 96% |
| 21 | 161 | Støtt strait | 1.7 | 0.39% | 97% |
| 22 | 162 | Øyhellsundet | 1.6 | 0.36% | 97% |
| 23 | 164 | Saltstraumen | 1.5 | 0.35% | 97% |
| 24 | 169 | Kaldvågsstraumen | 1.4 | 0.32% | 98% |
| 25 | 173 | Gjøssøysundet | 1.1 | 0.24% | 98% |
| 26 | 174 | Vesterstraumen | 1 | 0.24% | 98% |
| 27 | 175 | Ballstadstraumen | 1 | 0.23% | 98% |
| 28 | 177 | Toftsundet | 0.84 | 0.19% | 99% |
| 29 | 181 | Kjerringvikstraumen | 0.59 | 0.14% | 99% |
| 30 | 182 | Kamøysundet—Lilla Kamøya | 0.57 | 0.13% | 99% |
| 31 | 184 | Engsundet | 0.52 | 0.12% | 99% |

| Country Rank | Overall Rank | Site Name | Upper Limit of Potential (*MW*) | Resource Contribution | Cumulative Contribution |
|---|---|---|---|---|---|
| 32 | 185 | Spannbogstraumen | 0.52 | 0.12% | 99% |
| 33 | 186 | Reinøyspira | 0.48 | 0.11% | 99% |
| 34 | 187 | Kjellingsundet | 0.47 | 0.11% | 99% |
| 35 | 189 | Tromsøysundet | 0.45 | 0.10% | 99% |
| 36 | 190 | Sørsalten | 0.44 | 0.10% | 99% |
| 37 | 191 | Godfjorden | 0.4 | 0.092% | 100% |
| 38 | 193 | Lauksundet | 0.35 | 0.080% | 100% |
| 39 | 194 | Meistervik | 0.29 | 0.066% | 100% |
| 40 | 195 | Steikarviksundet | 0.26 | 0.059% | 100% |
| 41 | 196 | Grovfjorden | 0.24 | 0.054% | 100% |
| 42 | 197 | Sørsundet | 0.22 | 0.050% | 100% |
| 43 | 198 | Inner Andamsfjorden | 0.21 | 0.048% | 100% |
| 44 | 201 | Kjøfjorden | 0.15 | 0.033% | 100% |
| 45 | 202 | Akterøya—Aslakøya | 0.14 | 0.032% | 100% |
| 46 | 203 | Havøysundet | 0.13 | 0.029% | 100% |
| 47 | 204 | Mjøsundet | 0.061 | 0.014% | 100% |
| 48 | 205 | Burøysund | 0.036 | 0.0081% | 100% |
| 49 | 206 | Remmastraumen | 0.031 | 0.0071% | 100% |
| 50 | 207 | Hamsundpollen | 0.012 | 0.0026% | 100% |
| | | **NW TOTAL** | **440** | | |

| Country Rank | Overall Rank | Site Name | Upper Limit of Potential (*MW*) | Resource Contribution | Cumulative Contribution |
|---|---|---|---|---|---|
| **NZ** | | | | | |
| 1 | 6 | Cook Strait | 15000 | 97% | 97% |
| 2 | 30 | Foveaux Strait | 490 | 3.1% | 100% |
| 3 | 107 | Tory Channel | 12 | 0.079% | 100% |
| 4 | 166 | French Pass | 1.5 | 0.0094% | 100% |
| | | **NZ TOTAL** | **16000** | | |
| **OZ** | | | | | |
| 1 | 11 | Banks Strait | 3900 | 94% | 94% |
| 2 | 37 | Adolphus Channel | 270 | 6.3% | 100% |
| | | **OZ TOTAL** | **4200** | | |
| **US** | | | | | |
| 1 | 54 | Adak Strait | 110 | 16% | 16% |
| 2 | 56 | Umnak Pass | 100 | 16% | 32% |
| 3 | 57 | Avatanak Strait | 100 | 16% | 48% |
| 4 | 64 | Muskeget - Chappaquiddick Is | 78 | 12% | 60% |
| 5 | 70 | Tanaga - Kanaga Is | 54 | 8.2% | 68% |
| 6 | 81 | Vineyard Sound | 33 | 4.9% | 73% |
| 7 | 82 | Ugamak Strait | 32 | 4.9% | 78% |
| 8 | 88 | Unalga Pass | 23 | 3.5% | 81% |
| 9 | 89 | Sundstrom - Sitkinak Is | 22 | 3.3% | 84% |

| Country Rank | Overall Rank | Site Name | Upper Limit of Potential (*MW*) | Resource Contribution | Cumulative Contribution |
|---|---|---|---|---|---|
| 10 | 100 | Derbin Strait | 17 | 2.6% | 87% |
| 11 | 101 | Akutan Pass | 16 | 2.5% | 89% |
| 12 | 105 | Oglodak - Atka Is | 15 | 2.3% | 92% |
| 13 | 106 | S of Whale Is | 13 | 1.9% | 94% |
| 14 | 109 | Fenimore - Ikiginak Is | 12 | 1.8% | 95% |
| 15 | 121 | Muskeget - Tuckernuck Is | 7.3 | 1.1% | 96% |
| 16 | 128 | Igitkin - Great Sitkin Is | 5.5 | 0.83% | 97% |
| 17 | 143 | Chugul - Tagalak Is | 3.6 | 0.54% | 98% |
| 18 | 146 | Florida Keys | 3.1 | 0.46% | 98% |
| 19 | 149 | Atka - Amlia Is | 3 | 0.45% | 99% |
| 20 | 155 | N of Whale Is | 2.4 | 0.36% | 99% |
| 21 | 157 | Igitkin -Chugul Is | 2 | 0.31% | 99% |
| 22 | 167 | Little Tanaga - Kagalaska Is 1 | 1.4 | 0.22% | 100% |
| 23 | 168 | Little Tanaga - Kagalaska Is 2 | 1.4 | 0.21% | 100% |
| 24 | 176 | Akutan - Akun Is | 0.86 | 0.13% | 100% |
| | | **US TOTAL** | **660** | | |
| **SG** | | | | | |
| 1 | 7 | Singapore Strait | 7700 | 52% | 52% |
| | | **SG TOTAL** | **7700** | | |
| **CH** | | | | | |

| Country Rank | Overall Rank | Site Name | Upper Limit of Potential (*MW*) | Resource Contribution | Cumulative Contribution |
|---|---|---|---|---|---|
| 1 | 12 | Chacao Channel | 3400 | 23% | 75% |
| 2 | 22 | Chiloé Island 1 | 790 | 5.4% | 95% |
| 3 | 24 | Chiloé Island 2 | 730 | 4.9% | 100% |
| | | **CH TOTAL** | **4900** | | |
| **JP** | | | | | |
| 1 | 15 | Kanmon Strait | 2200 | 15% | 90% |
| 2 | 142 | Naruto Strait, | 3.6 | 0.025% | 100% |
| | | **JP TOTAL** | **2200** | | |
| **IT** | | | | | |
| 1 | 93 | Strait of Messina | 20 | 0.13% | 100% |
| | | **IT TOTAL** | **20** | | |

Table C.2: Estimation of the upper tidal current potential limit for each of the lagoon channels and for each of the countries with lagoon-type channels included in this study. Country codes can be found in the Nomenclature.

| Country Rank | Overall Rank | Site Name | Upper Limit of Potential (*MW*) | Resource Contribution | Cumulative Contribution |
|---|---|---|---|---|---|
| **UK** | | | | | |
| 1 | 6 | The Wash | 720 | 65% | 65% |
| 2 | 12 | Strangford Lough | 100 | 9.1% | 74% |
| 3 | 13 | Firth of Tay | 73 | 6.6% | 80% |
| 4 | 14 | Firth of Forth | 71 | 6.4% | 87% |
| 5 | 17 | Inverness Firth | 50 | 4.5% | 91% |
| 6 | 19 | Cromarty Firth | 39 | 3.5% | 95% |
| 7 | 23 | Plymouth Sound | 16 | 1.4% | 96% |
| 8 | 24 | Morecambe Bay | 16 | 1.4% | 97% |
| 9 | 25 | Loch Carron | 13 | 1.2% | 99% |
| 10 | 26 | Menai Strait | 11 | 1.0% | 100% |
| 11 | 31 | Poole Harbour | 2.2 | 0.20% | 100% |
| 12 | 33 | Loch Sligachan | 1.7 | 0.15% | 100% |
| | | **UK TOTAL** | **1100** | | |
| **IR** | | | | | |
| 1 | 11 | River Shannon | 110 | 47% | 47% |
| 2 | 15 | Greatman's Bay | 66 | 28% | 74% |
| 3 | 22 | Bertraghboy Bay | 26 | 11% | 85% |

| | | | | | |
|---|---|---|---|---|---|
| 4 | 27 | Dingle Harbour | 9.6 | 4.0% | 89% |
| 5 | 28 | Kilkieran Bay | 9.4 | 3.9% | 93% |
| 6 | 29 | Lough Foyle | 7.1 | 3.0% | 96% |
| 7 | 30 | Bull's Mouth | 7 | 2.9% | 99% |
| 8 | 32 | Youghal | 1.8 | 0.74% | 100% |
| | | **IR TOTAL** | **240** | | |
| **CA** | | | | | |
| 1 | 3 | Minas Basin | 8200 | 100% | 100% |
| | | **CA TOTAL** | **8200** | | |
| **NZ** | | | | | |
| 1 | 8 | Kaipara Harbour | 240 | 100% | 100% |
| | | **NZ TOTAL** | **240** | | |
| **OZ** | | | | | |
| 1 | 1 | King Sound | 34000 | 91% | 91% |
| 2 | 4 | Broad Sound | 3500 | 9.5% | 100% |
| | | **OZ TOTAL** | **38000** | | |
| **US** | | | | | |
| 1 | 2 | Cook Inlet | 16000 | 89% | 89% |
| 2 | 5 | Hague Channel | 990 | 5.4% | 94% |
| 3 | 7 | Delaware Bay | 560 | 3.0% | 97% |
| 4 | 9 | Cobscook Bay | 210 | 1.1% | 98% |

| | | | | | |
|---|---|---|---|---|---|
| 5 | 10 | Taku inlet | 140 | 0.79% | 99% |
| 6 | 16 | Grays Harbor | 64 | 0.35% | 99% |
| 7 | 18 | Satilla River | 45 | 0.24% | 100% |
| 8 | 20 | North Edisto River | 32 | 0.17% | 100% |
| 9 | 21 | Cooper River | 29 | 0.16% | 100% |
| | | **US TOTAL** | **18000** | | |

# Appendix D

# Realisable Power Estimates for Ocean Channels

Table D.1 presents the realisable power estimates at 0.95, 0.9, 0.85 and 0.8 flow reductions for each of the ocean channels meeting the cross-sectional area, depth and length requirements. The table also includes the overall realisable resource estimates for each country at each of the flow reductions considered. Data are organised by country from highest to lowest potentials in the order in which the countries are mentioned in Section 5.3.

Table D.1: Estimation of the realisable tidal resource available for each of the ocean channels meeting the minimum cross-sectional area, depth and length requirements and for each of the countries included in this study at 0.95, 0.9, 0.85 and 0.8 flow reductions. Country codes can be found in the Nomenclature.

| **Site Name** | **Realisable Power (*MW*) at 0.95 Flow Reduction** | **Realisable Power (*MW*) at 0.9 Flow Reduction** | **Realisable Power (*MW*) at 0.85 Flow Reduction** | **Realisable Power (*MW*) at 0.8 Flow Reduction** |
|---|---|---|---|---|
| **UK** | | | | |
| English Channel | 3100 | 5600 | 7900 | 10000 |
| St George's Channel - Carmel Head | 1100 | 2100 | 2800 | 3500 |
| North Channel - The Rhins | 1100 | 1800 | 2400 | 2900 |
| West Islay | 510 | 890 | 1200 | 1500 |
| Pentland Firth Deep | 420 | 760 | 1100 | 1400 |
| North Channel - Kintyre Peninsula | 390 | 640 | 860 | 1000 |
| North Isle of Man | 200 | 390 | 570 | 730 |
| St George's Channel - St David's Head | 260 | 430 | 560 | 680 |
| Severn Estuary | 87 | 160 | 240 | 300 |
| Dover Strait | 85 | 150 | 220 | 270 |
| Race of Alderney | 35 | 64 | 92 | 120 |
| Gulf of Corryvreckan | 29 | 52 | 72 | 91 |
| Sound of Islay | 21 | 37 | 56 | 71 |

| Site Name | Realisable Power ($MW$) at 0.95 Flow Reduction | Realisable Power ($MW$) at 0.9 Flow Reduction | Realisable Power ($MW$) at 0.85 Flow Reduction | Realisable Power ($MW$) at 0.8 Flow Reduction |
|---|---|---|---|---|
| North East Jersey | 18 | 35 | 49 | 64 |
| Sound of Eigg | 18 | 31 | 45 | 58 |
| Bardsey Island | 16 | 29 | 41 | 53 |
| Pentland Firth Shallow | 15 | 27 | 39 | 50 |
| Big Russel | 13 | 22 | 32 | 42 |
| Westray Firth | 12 | 22 | 31 | 39 |
| South Canna | 7.1 | 13 | 18 | 22 |
| Sanda Sound | 6.9 | 12 | 18 | 22 |
| Ramsey Sound | 6.1 | 11 | 15 | 20 |
| The Swinge | 5.2 | 9.2 | 13 | 17 |
| Bluemull Sound | 4.3 | 7.7 | 11 | 14 |
| West Luing | 3.5 | 6.4 | 8.9 | 11 |
| Kyle Rhea | 1.9 | 3.3 | 4.8 | 6.2 |
| Yell Sound - West Channel | 0.99 | 1.8 | 2.5 | 3.2 |
| Jack Sound | 0.87 | 1.6 | 2.2 | 2.8 |
| Switha Sound | 0.60 | 1.1 | 1.5 | 1.9 |
| Cantik Sound | 0.51 | 0.91 | 1.3 | 1.6 |
| Sound of Mull | 0.49 | 0.85 | 1.2 | 1.5 |

| Site Name | Realisable Power ($MW$) at 0.95 Flow Reduction | Realisable Power ($MW$) at 0.9 Flow Reduction | Realisable Power ($MW$) at 0.85 Flow Reduction | Realisable Power ($MW$) at 0.8 Flow Reduction |
|---|---|---|---|---|
| Eynhallow Sound | 0.27 | 0.47 | 0.68 | 0.87 |
| Sound of Handa | 0.12 | 0.22 | 0.31 | 0.39 |
| North Carna | 0.093 | 0.16 | 0.22 | 0.28 |
| **UK TOTAL** | **7500** | **13000** | **18000** | **23000** |
| **IR** | | | | |
| West Arklow Bank | 30 | 56 | 80 | 100 |
| Inishtrahull Sound | 9.7 | 17 | 24 | 30 |
| West Mullet | 4.6 | 8.5 | 12 | 15 |
| Tuskar Rock | 2.9 | 5.1 | 7.0 | 9.1 |
| Gregory's Sound | 1.4 | 2.4 | 3.4 | 4.2 |
| Inishshark | 0.81 | 1.5 | 2.1 | 2.7 |
| Foul Sound | 0.84 | 1.5 | 2.0 | 2.5 |
| Rusk Channel | 0.41 | 0.75 | 1.1 | 1.4 |
| Blasket Sound | 0.36 | 0.64 | 0.92 | 1.2 |
| Gascanane Sound | 0.27 | 0.49 | 0.68 | 0.86 |
| Dursey Sound | 0.095 | 0.17 | 0.24 | 0.31 |
| Scariff Deenish Is | 0.096 | 0.16 | 0.21 | 0.26 |
| **IR TOTAL** | **51** | **94** | **130** | **170** |

| Site Name | Realisable Power ($MW$) at 0.95 Flow Reduction | Realisable Power ($MW$) at 0.9 Flow Reduction | Realisable Power ($MW$) at 0.85 Flow Reduction | Realisable Power ($MW$) at 0.8 Flow Reduction |
|---|---|---|---|---|
| **CA** | | | | |
| Nottingham Is - Ungava | 7300 | 12000 | 16000 | 19000 |
| Mill - Salisbury Is | 5900 | 9800 | 13000 | 17000 |
| Mill - Baffin Is | 4500 | 7300 | 9900 | 12000 |
| Salisbury - Notthingham Is | 4300 | 7600 | 10000 | 13000 |
| Gray Strait | 2000 | 3100 | 3900 | 4700 |
| Riviere George Entrance | 240 | 460 | 660 | 850 |
| Algernine Narrows | 210 | 370 | 540 | 700 |
| Pointe Amour | 150 | 270 | 390 | 510 |
| Bellot Strait | 110 | 220 | 330 | 420 |
| Lacy/Lawson Is | 110 | 200 | 290 | 360 |
| Gran Manan Channel | 110 | 190 | 250 | 310 |
| Seymour Narrows | 81 | 150 | 210 | 260 |
| Smoky Narrows | 79 | 140 | 200 | 250 |
| Labrador Narrows | 62 | 110 | 150 | 190 |
| Passage de Ile aux Coudres | 52 | 94 | 130 | 180 |
| Discovery Pass. S. | 44 | 79 | 110 | 150 |
| N Boundary Passage | 44 | 71 | 93 | 110 |

| Site Name | Realisable Power ($MW$) at 0.95 Flow Reduction | Realisable Power ($MW$) at 0.9 Flow Reduction | Realisable Power ($MW$) at 0.85 Flow Reduction | Realisable Power ($MW$) at 0.8 Flow Reduction |
|---|---|---|---|---|
| Koksoak Entrance | 35 | 63 | 91 | 120 |
| Beaver Passage | 30 | 51 | 70 | 87 |
| Current Passage 1 | 27 | 46 | 64 | 79 |
| South Pender Is | 27 | 44 | 61 | 75 |
| Current Passage 2 | 23 | 41 | 56 | 71 |
| Weyton Passage | 22 | 39 | 54 | 69 |
| Scott Channel | 18 | 33 | 48 | 61 |
| Yuculta Rapids | 17 | 30 | 44 | 56 |
| Otter Passage | 13 | 23 | 34 | 43 |
| Head Harbour Passage 1 | 9.4 | 17 | 22 | 29 |
| Egg Island | 9.1 | 16 | 23 | 30 |
| Arran Rapids | 6.4 | 12 | 17 | 21 |
| Petit Passage | 4.7 | 8.0 | 12 | 15 |
| Race Passage | 4.3 | 7.8 | 11 | 14 |
| Active Pass | 3.7 | 6.6 | 9.2 | 12 |
| Dent Rapids | 3.4 | 6.2 | 8.7 | 11 |
| Quatsino Narrows | 3.3 | 6.0 | 8.6 | 11 |
| Porlier Pass | 3.2 | 5.8 | 8.1 | 11 |

| Site Name | Realisable Power (*MW*) at 0.95 Flow Reduction | Realisable Power (*MW*) at 0.9 Flow Reduction | Realisable Power (*MW*) at 0.85 Flow Reduction | Realisable Power (*MW*) at 0.8 Flow Reduction |
|---|---|---|---|---|
| Gillard Passage 1 | 2.9 | 5.3 | 7.5 | 9.5 |
| Greene Pt Rap. 1 | 2.8 | 5.1 | 7.2 | 9.1 |
| Whirlpool Rapids | 2.0 | 3.5 | 5.0 | 6.3 |
| Outer Narrows | 1.4 | 2.6 | 3.7 | 4.7 |
| Old Sow | 0.98 | 1.9 | 2.6 | 3.3 |
| Upper rapids 2 | 0.88 | 1.7 | 2.3 | 2.9 |
| **CA TOTAL** | **26000** | **43000** | **57000** | **71000** |
| **NW** | | | | |
| Moskenstraumen | 28 | 51 | 72 | 90 |
| Trollsundet | 9.2 | 16 | 24 | 30 |
| Magerøysundet | 6.4 | 11 | 16 | 20 |
| Kvalsundet Troms | 3.0 | 5.5 | 7.7 | 10 |
| Måsøysundet | 3.4 | 6.0 | 8.2 | 10 |
| Grøtøysundet Troms | 3.1 | 5.5 | 7.7 | 10 |
| Kvalsundet | 1.9 | 3.4 | 4.8 | 6.1 |
| Kågsundet | 2.2 | 3.5 | 4.5 | 5.5 |
| Rystraumen | 1.4 | 2.5 | 3.6 | 4.5 |
| Maursundet | 1.4 | 2.4 | 3.4 | 4.3 |

| Site Name | Realisable Power ($MW$) at 0.95 Flow Reduction | Realisable Power ($MW$) at 0.9 Flow Reduction | Realisable Power ($MW$) at 0.85 Flow Reduction | Realisable Power ($MW$) at 0.8 Flow Reduction |
|---|---|---|---|---|
| Store Vågsøysundet | 1.3 | 2.3 | 3.3 | 4.1 |
| Kråkøya | 0.80 | 1.4 | 1.9 | 2.4 |
| Nærøysundet | 0.48 | 0.86 | 1.2 | 1.5 |
| Nappstraumen | 0.34 | 0.64 | 0.90 | 1.2 |
| Saltstraumen | 0.27 | 0.49 | 0.69 | 0.88 |
| Ballstadstraumen | 0.18 | 0.32 | 0.44 | 0.58 |
| Toftsundet | 0.15 | 0.26 | 0.37 | 0.47 |
| Reinøyspira | 0.09 | 0.16 | 0.22 | 0.28 |
| Kjøfjorden | 0.025 | 0.046 | 0.064 | 0.083 |
| Mjøsundet | 0.011 | 0.021 | 0.029 | 0.036 |
| **NW TOTAL** | **64** | **110** | **160** | **200** |
| **NZ** | | | | |
| Cook Strait | 4400 | 7100 | 9300 | 11000 |
| Foveaux Strait | 74 | 150 | 220 | 280 |
| Tory Channel | 2.9 | 4.9 | 6.7 | 8.3 |
| French Pass | 0.29 | 0.53 | 0.73 | 0.90 |
| **NZ TOTAL** | **4500** | **7300** | **9500** | **11000** |
| **OZ** | | | | |

| Site Name | Realisable Power (*MW*) at 0.95 Flow Reduction | Realisable Power (*MW*) at 0.9 Flow Reduction | Realisable Power (*MW*) at 0.85 Flow Reduction | Realisable Power (*MW*) at 0.8 Flow Reduction |
|---|---|---|---|---|
| Banks Strait | 660 | 1200 | 1700 | 2200 |
| Adolphus Channel | 42 | 80 | 110 | 150 |
| **OZ TOTAL** | **700** | **1300** | **1800** | **2400** |
| **US** | | | | |
| Adak Strait | 20 | 36 | 50 | 65 |
| Avatanak Strait | 20 | 36 | 51 | 64 |
| Umnak Pass | 20 | 36 | 50 | 64 |
| Tanaga - Kanaga Is | 9.4 | 17 | 24 | 31 |
| Vineyard Sound | 6.6 | 12 | 16 | 20 |
| Ugamak Strait | 5.9 | 11 | 15 | 19 |
| Unalga Pass | 3.9 | 7.0 | 10 | 13 |
| Derbin Strait | 3.2 | 5.7 | 7.9 | 10 |
| Akutan Pass | 2.9 | 5.1 | 7.3 | 9.1 |
| Oglodak - Atka Is | 2.7 | 4.7 | 6.6 | 8.5 |
| S of Whale Is | 2.1 | 3.8 | 5.5 | 7.1 |
| Fenimore - Ikiginak Is | 2.1 | 3.8 | 5.3 | 6.8 |
| Igitkin - Great Sitkin Is | 1.1 | 1.9 | 2.6 | 3.3 |
| Atka - Amlia Is | 0.52 | 0.94 | 1.3 | 1.7 |

| Site Name | Realisable Power (*MW*) at 0.95 Flow Reduction | Realisable Power (*MW*) at 0.9 Flow Reduction | Realisable Power (*MW*) at 0.85 Flow Reduction | Realisable Power (*MW*) at 0.8 Flow Reduction |
|---|---|---|---|---|
| Igitkin - Chugul Is | 0.39 | 0.68 | 0.94 | 1.2 |
| Little Tanaga - Kagalaska Is 2 | 0.27 | 0.48 | 0.67 | 0.84 |
| Little Tanaga - Kagalaska Is 1 | 0.26 | 0.46 | 0.64 | 0.81 |
| **US TOTAL** | **100** | **180** | **250** | **330** |
| **SG** | | | | |
| Singapore Strait | 1200 | 2200 | 3200 | 4200 |
| **SG TOTAL** | **1200** | **2200** | **3200** | **4200** |
| **CH** | | | | |
| Chacao Channel | 570 | 1100 | 1500 | 1900 |
| Chiloé Island 1 | 220 | 360 | 470 | 570 |
| Chiloé Island 2 | 190 | 330 | 430 | 520 |
| **CH TOTAL** | **1000** | **1800** | **2400** | **3000** |
| **JP** | | | | |
| Naruto Strait | 0.72 | 1.3 | 1.7 | 2.2 |
| **JP TOTAL** | **0.72** | **1.3** | **1.7** | **2.2** |
| **IT** | | | | |
| Strait of Messina | 4.1 | 7.1 | 9.9 | 12 |
| **IT TOTAL** | **4.1** | **7.1** | **9.9** | **12** |

# Appendix E

# Channels' Geographical Coordinates

Tables E.1 and E.2 present the geographical coordinates, given as latitude and longitude in decimal degrees, of all the ocean and lagoon channels included in this study respectively. In both tables, data are organised by country in alphabetical order. In both tables, the precision of the coordinates given varies with the size of the channel being considered.

Table E.1: Geographical coordinates of the ocean channels included in this study.

| Country | Site Name | Latitude | Longitude |
|---|---|---|---|
| OZ | Adolphus Channel | -10.7° | 142.6° |
| | Banks Strait | -40.7° | 148.0° |
| CA | Active Pass | 48.86° | -123.30° |
| | Algernine Narrows | 58.79° | -69.56° |
| | Arran Rapids | 50.42° | -125.13° |
| | Beaver Passage | 53.73° | -130.35° |
| | Bellot Strait | 71.99° | -94.8° |
| | Cache Pt Channel | 68.60° | -113.5° |
| | Current Passage 1 | 50.40° | -125.86° |
| | Current Passage 2 | 50.38° | -125.87° |
| | Dent Rapids | 50.40° | -125.20° |
| | Discovery Pass. S. | 50.01° | -125.20° |
| | Dodd Narrows | 49.13° | -123.81° |
| | Draney Narrows | 51.47° | -127.55° |
| | Egg Island | 68.54° | -97.40° |
| | Gabriola Pass. | 49.13° | -123.70° |

| Country | Site Name | Latitude | Longitude |
|---|---|---|---|
| | Gillard Passage 1 | 50.39° | -125.15° |
| | Gillard Passage 2 | 50.39° | -125.14° |
| | Gran Manan Channel | 44.74° | -66.92° |
| | Gray Strait | 60.9° | -64.7° |
| | Greene Pt Rap. 1 | 50.44° | -125.50° |
| | Hawkins Narrows | 53.40° | -129.41° |
| | Head Harbour Passage 1 | 44.94° | -66.92° |
| | Hidden Inlet | 54.95° | -130.33° |
| | Hole-in-the-Wall 1 | 50.29° | -125.20° |
| | Kildidt Narrows | 51.88° | -128.10° |
| | Koksoak Entrance | 58.52° | -68.16° |
| | Labrador Narrows | 69.71° | -82.5° |
| | Lacy/Lawson Is | 60.58° | -64.62° |
| | Lower Rapids 1 | 50.30° | -125.25° |
| | Lubec Narrows | 44.85° | -66.97° |
| | McLelan Strait | 60.340° | -64.62° |
| | Mill - Baffin Is | 64.1° | -77.4° |
| | Mill - Salisbury Is | 63.8° | -77.5° |
| | N Boundary Passage | 48.79° | -123.01° |
| | Nahwitti Bar 1 | 50.88° | -127.97° |
| | Nakertok Narrows | 60.00° | -70.28° |
| | Nakwakto Rapids | 51.09° | -127.50° |
| | Nettilling Fiord | 66.71° | -72.9° |
| | Nitinat Narrows | 48.671° | -124.852° |
| | Nottingham Is - Ungava | 62.8° | -77.82° |
| | Old Sow | 44.921° | -66.988° |
| | Otter Passage | 53.13° | -129.73° |
| | Outer Narrows | 51.08° | -127.62° |

| Country | Site Name | Latitude | Longitude |
|---|---|---|---|
| | Passage de Ile aux Coudres | 47.42° | -70.40° |
| | Petit Passage | 44.39° | -66.21° |
| | Placentia Gut | 47.249° | -53.963° |
| | Pointe Amour | 51.5° | -56.4° |
| | Porcher Narrows | 53.89° | -130.46° |
| | Porlier Pass | 40.01° | -123.58° |
| | Quatsino Narrows | 50.54° | -127.56° |
| | Race Passage | 48.305° | -123.53° |
| | Reversing Falls | 45.26° | -66.08° |
| | Riviere Arnaud (Payne) Entrance | 59.98° | -69.82° |
| | Riviere George Entrance | 58.78° | -66.12° |
| | Salisbury - Notthingham Is | 63.4° | -77.3° |
| | Scott Channel | 50.78° | -128.49° |
| | Sechelt Rapids 2 | 49.73° | -123.89° |
| | Seymour Narrows | 50.14° | -125.35° |
| | Smoky Narrows | 58.920° | -69.24° |
| | South Pender Is | 48.71° | -123.21° |
| | Stuart Narrows | 50.89° | -126.94° |
| | Upper rapids 2 | 50.30° | -125.23° |
| | Weyton Passage | 50.58° | -126.81° |
| | Whirlpool Rapids | 50.45° | -125.76° |
| | Yuculta Rapids | 50.37° | -125.14° |
| CH | Chacao Channel | -41.77° | -73.55° |
| | Chiloé Island 1 | -42.64° | -73.14° |
| | Chiloé Island 2 | -42.7° | -72.88° |
| IR | Blasket Sound | 52.11° | -10.48° |
| | Clare Is | 53.78° | -9.91° |
| | Dursey Sound | 51.609° | -10.158° |
| | Foul Sound | 53.06° | -9.55° |
| | Gascanane Sound | 51.452° | -9.45° |
| | Gregory's Sound | 53.09° | -9.61° |

| Country | Site Name | Latitude | Longitude |
|---|---|---|---|
| | Inishshark | 53.61° | -10.26° |
| | Inishtrahull Sound | 55.40° | -7.27° |
| | Rusk Channel | 52.50° | -6.18° |
| | Scariff Deenish Is | 51.734° | -10.231° |
| | Tuskar Rock | 52.21° | -6.25° |
| | West Arklow Bank | 52.80° | -6.02° |
| | West Mullet | 54.11° | -10.18° |
| IT | Strait of Messina | 38.24° | 15.62° |
| JP | Kanmon Strait | 33.94° | 131.0° |
| | Naruto Strait | 34.23° | 134.64° |
| NZ | Cook Strait | -41.1° | 174.5° |
| | Foveaux Strait | -46.6° | 168.4° |
| | French Pass | -40.92° | 173.83° |
| | Tory Channel | -41.24° | 174.18° |
| NW | Akterøya - Aslakøya | 68.008° | 15.107° |
| | Ballstadstraumen | 68.557° | 16.31° |
| | Brasøysundet | 65.91° | 12.167° |
| | Burøysund | 70.224° | 19.734° |
| | Engsundet | 67.980° | 15.384° |
| | Gimsøystraumen | 68.26° | 14.26° |
| | Gjøssøysundet | 69.988° | 18.50° |
| | Godfjorden | 68.752° | 15.83° |
| | Graddstraumen | 67.23° | 15.00° |
| | Grøtøysundet Troms | 70.138° | 18.82° |
| | Grovfjorden | 68.672° | 17.113° |
| | Hamsundpollen | 68.123° | 15.497° |
| | Havøysundet | 70.993° | 24.66° |
| | Inner Andamsfjorden | 70.088° | 18.84° |
| | Kågsundet | 70.041° | 20.76° |
| | Kaldvågsstraumen | 68.029° | 15.80° |
| | Kamøysundet - Lilla Kamøya | 70.846° | 23.064° |

| Country | Site Name | Latitude | Longitude |
|---|---|---|---|
| | Kjellingsundet | 67.078° | 14.304° |
| | Kjerringvikstraumen | 68.292° | 16.48° |
| | Kjøfjorden | 69.81° | 29.75° |
| | Kråkøya | 64.885° | 11.30° |
| | Kvalsundet | 70.506° | 23.93° |
| | Kvalsundet Troms | 69.81° | 19.01° |
| | Lauksundet | 70.117° | 20.768° |
| | Magerøysundet | 70.94° | 25.48° |
| | Måsøysundet | 70.98° | 24.98° |
| | Maursundet | 69.93° | 20.92° |
| | Meistervik | 69.321° | 18.936° |
| | Mjøsundet | 68.888° | 17.460° |
| | Moskenstraumen | 67.79° | 12.82° |
| | Nærøysundet | 64.846° | 11.21° |
| | Nappstraumen | 68.14° | 13.47° |
| | Nesnakroken | 66.19° | 12.99° |
| | Øyhellsundet | 68.29° | 14.86° |
| | Reinøyspira | 70.880° | 24.26° |
| | Remmastraumen | 64.884° | 11.571° |
| | Rystraumen | 69.555° | 18.73° |
| | Saltstraumen | 67.231° | 14.61° |
| | Sandtorgstraumen | 68.563° | 16.51° |
| | Sørsalten | 64.851° | 11.30° |
| | Sørsundet | 68.124° | 15.403° |
| | Spannbogstraumen | 68.50° | 16.46° |
| | Steikarviksundet | 70.263° | 19.18° |
| | Store Vågsøysundet | 69.83° | 18.648° |
| | Støtt strait | 66.92° | 13.437° |
| | Toftsundet | 65.46° | 12.12° |
| | Trangstraumen | 68.40° | 15.11° |
| | Trollsundet | 71.039° | 23.99° |
| | Tromsøysundet | 69.651° | 18.97° |
| | Vesterstraumen | 68.457° | 15.50° |
| SG | Singapore Strait | 1.26° | 104.0° |

| Country | Site Name | Latitude | Longitude |
|---|---|---|---|
| UK | Bardsey Island | 52.77° | -4.77° |
| | Big Russel | 49.45° | -2.40° |
| | Bluemull Sound | 60.70° | -0.98° |
| | Burra Sound | 58.931° | -3.31° |
| | Cantik Sound | 58.795° | -3.12° |
| | Copinsay Pass | 58.91° | -2.70° |
| | Corran Narrows | 56.720° | -5.239° |
| | Dover Strait | 51.0° | 1.4° |
| | English Channel | 50.1° | -1.6° |
| | Eynhallow Sound | 59.12° | -3.06° |
| | Gulf of Corryvreckan | 56.153° | -5.72° |
| | Gunna Sound | 56.55° | -6.73° |
| | Hoy Sound | 58.945° | -3.29° |
| | Jack Sound | 51.734° | -5.257° |
| | Kyle Rhea | 57.23° | -5.65° |
| | Loch Leven Narrows | 56.68° | -5.18° |
| | N Ronaldsay Firth | 59.32° | -2.42° |
| | North Carna | 56.673° | -5.884° |
| | North Channel - Kintyre Peninsula | 55.2° | -5.9° |
| | North Channel - The Rhins | 54.7° | -5.3° |
| | North East Jersey | 49.25° | -1.98° |
| | North Isle of Man | 54.5° | -4.6° |
| | Pentland Firth Deep | 58.70° | -3.11° |
| | Pentland Firth Shallow | 58.66° | -3.12° |
| | Race of Alderney | 49.72° | -2.05° |
| | Ramsey Sound | 51.87° | -5.32° |
| | Sanda Sound | 55.29° | -5.59° |
| | Severn Estuary | 51.3° | -3.3° |
| | Sound of Eigg | 56.86° | -6.21° |
| | Sound of Handa | 58.370° | -5.17° |

| Country | Site Name | Latitude | Longitude |
|---|---|---|---|
| | Sound of Islay | 55.84° | -6.09° |
| | Sound of Mull | 56.49° | -5.71° |
| | South Canna | 57.00° | -6.62° |
| | St George's Channel - Carmel Head | 53.4° | -5.3° |
| | St George's Channel - St David's Head | 52.0° | -5.9° |
| | Staple Sound | 55.62° | -1.62° |
| | Switha Sound | 58.809° | -3.09° |
| | The Swinge | 49.72° | -2.28° |
| | West Islay | 55.4° | -6.7° |
| | West Luing | 56.253° | -5.67° |
| | Westray Firth | 59.16° | -2.84° |
| | Yell Sound - West Channel | 60.46° | -1.17° |
| US | Adak Strait | 51.81° | -177.00° |
| | Akutan - Akun Is | 54.135° | -165.652° |
| | Akutan Pass | 54.02° | -166.04° |
| | Atka - Amlia Is | 52.128° | -174.06° |
| | Avatanak Strait | 54.12° | -165.41° |
| | Chugul - Tagalak Is | 51.94° | -175.76° |
| | Derbin Strait | 54.08° | -165.22° |
| | Fenimore - Ikiginak Is | 51.97° | -175.53° |
| | Florida Keys | 24.69° | -81.17° |
| | Igitkin - Chugul Is | 51.95° | -175.87° |
| | Igitkin - Great Sitkin Is | 51.98° | -175.99° |
| | Little Tanaga - Kagalaska Is 1 | 51.814° | -176.25° |

| Country | Site Name | Latitude | Longitude |
|---|---|---|---|
| | Little Tanaga - Kagalaska Is 2 | 51.816° | -176.23° |
| | Muskeget - Chappaquiddick Is | 41.35° | -70.37° |
| | Muskeget - Tuckernuck Is | 41.32° | -70.28° |
| | N of Whale Is | 57.98° | -152.80° |
| | Oglodak - Atka Is | 51.99° | -175.37° |
| | S of Whale Is | 57.92° | -152.82° |
| | Sundstrom - Sitkinak Is | 56.64° | -154.08° |
| | Tanaga - Kanaga Is | 51.72° | -177.71° |
| | Ugamak Strait | 54.17° | -164.88° |
| | Umnak Pass | 53.35° | -167.8° |
| | Unalga Pass | 53.94° | -166.19° |
| | Vineyard Sound | 41.51° | -70.62° |

Table E.2: Geographical coordinates of the lagoon channels included in this study.

| **Country** | **Site Name** | **Latitude** | **Longitude** |
|---|---|---|---|
| OZ | Broad Sound | -22.05° | 149.76° |
| | King Sound | -16.3° | 123.8° |
| CA | Minas Basin | 45.3° | -64.4° |
| IR | Bertraghboy Bay | 53.373° | -9.89° |
| | Bull's Mouth | 54.03° | -9.93° |
| | Dingle Harbour | 52.121° | -10.261° |
| | Greatman's Bay | 53.25° | -9.63° |
| | Kilkieran Bay | 53.30° | -9.71° |
| | Lough Foyle | 55.20° | -6.96° |

| Country | Site Name | Latitude | Longitude |
|---|---|---|---|
| | River Shannon | 52.57° | -9.67° |
| | Youghal | 51.948° | -7.839° |
| NZ | Kaipara Harbour | -36.43° | 174.13° |
| UK | Cromarty Firth | 57.68° | -4.00° |
| | Firth of Forth | 56.000° | -3.40° |
| | Firth of Tay | 56.45° | -2.73° |
| | Inverness Firth | 57.58° | -4.08° |
| | Loch Carron | 57.354° | -5.57° |
| | Loch Sligachan | 57.315° | -6.103° |
| | Menai Strait | 53.125° | -4.32° |
| | Morecambe Bay | 53.93° | -3.11° |
| | Plymouth Sound | 50.359° | -4.170° |
| | Poole Harbour | 50.680° | -1.948° |
| | Strangford Lough | 54.37° | -5.55° |
| | The Wash | 53.01° | 0.43° |
| US | Cobscook Bay | 44.90° | -67.04° |
| | Cook Inlet | 60.71° | -151.5° |
| | Cooper River | 32.75° | -79.86° |
| | Delaware Bay | 38.87° | -75.08° |
| | Grays Harbor | 46.93° | -124.10° |
| | Hague Channel | 56.01° | -160.69° |
| | North Edisto River | 32.55° | -80.17° |
| | Satilla River | 30.98° | -81.41° |
| | Taku inlet | 58.23° | -134.09° |